University of Alberta

Melt Miscibility Studies of Polyethylene Blends by MD and SEM

By

Zhengang Fan

A thesis submitted to the Faculty of Graduate Studies and Research in partial fulfillment of the requirements for the degree of **Doctor of Philosophy**

in

Chemical Engineering

Department of Chemical and Materials Engineering

Edmonton, Alberta

Fall, 2001

National Library of Canada
Acquisitions and Bibliographic Services
395 Wellington Street
Ottawa ON K1A 0N4
Canada

Bibliothèque nationale du Canada
Acquisitions et services bibliographiques
395, rue Wellington
Ottawa ON K1A 0N4
Canada

Your file Votre référence

Our file Notre référence

The author has granted a non-exclusive licence allowing the National Library of Canada to reproduce, loan, distribute or sell copies of this thesis in microform, paper or electronic formats.

L'auteur a accordé une licence non exclusive permettant à la Bibliothèque nationale du Canada de reproduire, prêter, distribuer ou vendre des copies de cette thèse sous la forme de microfiche/film, de reproduction sur papier ou sur format électronique.

The author retains ownership of the copyright in this thesis. Neither the thesis nor substantial extracts from it may be printed or otherwise reproduced without the author's permission.

L'auteur conserve la propriété du droit d'auteur qui protège cette thèse. Ni la thèse ni des extraits substantiels de celle-ci ne doivent être imprimés ou autrement reproduits sans son autorisation.

0-612-68928-X

Canada

University of Alberta

Library Release Form

Name of Author: **Zhengang Fan**

Title of Thesis: **Melt Miscibility Studies of Polyethylene Blends by MD and SEM**

Degree: **Doctor of Philosophy**

Year this Degree Granted: 2001

Permission is hereby granted to the University of Alberta Library to reproduce single copies of this thesis and to lend or sell such copies for private, scholarly or scientific research purposes only.

The author reserves all other publication and other rights in association with the copyright in the thesis, and except as herein before provided, neither the thesis nor any substantial portion thereof may be printed or otherwise reproduced in any material form whatever without the author's prior written permission.

Zhengang Fan

Zhengang Fan
14, 10615-107 Street
Edmonton, AB
Canada T5H 2Y8

Date: August 21, 2001

University of Alberta

Faculty of Graduate Studies and Research

The undersigned certify that they have read, and recommend to the Faculty of Graduate Studies and Research for acceptance, a thesis entitled **Melt Miscibility Studies of Polyethylene Blends by MD and SEM** submitted by **Zhengang Fan** in partial fulfillment of the requirements for the degree of **Doctor of Philosophy** in **Chemical Engineering**.

M. C. Williams
Dr. M. C. Williams

Dr. P. Y. K. Choi

Dr. W. McCaffrey

Dr. S. Bergens

Dr. J. J. de Pablo (external examiner)

Date: August 2, 2001

This thesis is dedicated to my parents.

ABSTRACT

The effects of molecular structure difference of polyethylene molecules on the melt phase behavior of polyethylene blends were studied using molecular simulations. In particular, molecular dynamics (MD) was applied to compute Hildebrand solubility parameters (δ) of models of high-density polyethylene (HDPE) and low-density polyethylene (LDPE) as well as linear low-density polyethylene (LLDPE) with different branching characteristics at five elevated temperatures. The Flory-Huggins interaction parameters (χ) between different constituent models for the blends of interest were then calculated using the resulting δ values. Effects such as branch content as well as branch length of branched polyethylenes including LDPE and LLDPE on the miscibility with HDPE were my major concerns in this study. More complex blends of LDPE and LLDPE with different branching characteristics from both of them were also studied. It turns out that the branch content is a major factor in controlling the phase behavior of blends of HDPE and branched polyethylene. The present data also suggest that the molecular interaction of non-CH_2 (i.e., CH and CH_3) groups is the major reason that leads to phase separation of polyethylene blends. In addition, long chain branching in LDPE also plays an important role in determining its melt miscibility with HDPE and LLDPE. The level of branch content of LLDPE above which the blends of HDPE/LLDPE are immiscible and segregate in the melt was found to be around 40-50 branches/1,000 backbone carbon atoms at the chosen simulation temperatures. However, the

corresponding branch content cut-off value of LDPE to segregate in its blends with HDPE was found to be around 25-30 branches/1,000 long chain carbons at the chosen simulation temperatures. For the LDPE/LLDPE blends, it is found that when the branch content of LDPE is higher than 30 branches/1,000 long chain carbons, phase separation may occur between LDPE and LLDPE components. In addition to the fact that branch content plays a leading role in determining the phase behavior of polyethylene blends, the present results of my studies suggest that the long chain branching may also have significant influence on the miscibility of polyethylene blends.

Applications of scanning electron microscopy technique to the melt miscibility study of polyethylene blends were also explored in the thesis. Some interesting results were observed.

ACKNOWLEDGEMENTS

I would like to thank the University of Alberta Ph.D. Scholarship Program, Nova Chemicals, and the Natural Sciences and Engineering Research Council of Canada (NSERC) for the financial support of the thesis work.

From deep of my heart, I wish to express my special gratitude to my supervisor, Dr. M. C. Williams for his constructive and patient guidance and persistent encouragement both in the whole thesis work and in daily life.

Thanks also go to Dr. P. Y. K. Choi, as a co-supervisor, who provided me necessary computational resources and some guidance for the computational work of the thesis.

Dr. W. McCaffrey and Dr. U.T. Sundararaj are also gratefully thanked for their constructive suggestions and advice for the thesis work.

Helpful discussions with Dr. S. Goyal, Dr. K. Ho and Dr. C. Russell, from Nova Chemicals, are sincerely appreciated.

My sincere thanks are also due to Ms. T. Barker for her help in my SEM experiments, and to Mr. B. Barton for installing and maintaining the Cerius2 program for my computational work of the thesis.

Table of Contents

Chapter 1 Introduction 1

1.1 Organizations and Scope of the Thesis 1

1.2 Fundamentals of Polyethylene Polymers 2

1.3 Polyethylene Blends and the Miscibility of Polyethylene Blends 4

Chapter 2 Miscibility Studies of Polyethylene Blends- a Literature Review 8

Chapter 3 Polymer Mixtures 33

3.1 Thermodynamics of Mixtures 33

3.2 Theories of Characterizing Phase Behavior of Mixtures 35

3.2.1 Ideal Solution 35

3.2.2 Regular Solution 35

3.2.3 Polymer Systems 36

3.3.1 The Solubility Parameter Approach 37

3.3.2 Determination of Hildebrand Solubility Parameters 49

3.3.3 Flory-Huggins Interaction Parameter 41

Chapter 4 Molecular Dynamics Simulation 45

4.1 Fundamentals of Statistical Thermodynamics and Computer Simulations 45

4.2 Force-Field 51

4.3 Nosé Formalism for NVT Canonical Ensemble Dynamics 56

4.4 MD Simulations for Condensed State 58

4.5 Model Construction 60

4.6 Comparison of DREIDING and COMPASS Force-fields 65

4.7 Molecular Weight Effect 69

4.8 Pressures in MD Simulations 72

Chapter 5 MD Simulation Results on Polyethylene Blends 75

5.1 Introduction 75

5.2 HDPE/LLDPE Blend Systems 76

5.2.1 HDPE and Butene-based LLDPE Systems 77

5.2.1.1 Molecular Models 77

5.2.1.2 Results and Discussion 78

5.2.1.3 Standard Deviation 86

5.2.1.4 Trans/Gauche Ratio 87

5.2.1.5 Pressure 90

5.2.2 HDPE with Hexene- and Octene-Based LLDPE Blend Systems 93

5.2.2.1 Molecular Models 93

5.2.2.2 Results and Discussion 100

5.2.2.3 Trans/Gauche Ratio 108

5.3 HDPE/LDPE Blend Systems 111

5.3.1 Introduction 111

5.3.2 Molecular Models 112

5.3.3 Results and Discussion 114

5.3.4 Trans/Gauche Ratio 119

5.4 LDPE/LLDPE Blend Systems 121

5.4.1 Introduction 121

5.4.2 Results and Discussion 121

Chapter 6 Scanning Electron Microscopy 135

6.1 Introduction 135

6.2 The Working Principle of SEM 136

6.3 Introduction to Morphological Studies of Polyolefin Blends via SEM 138

6.4 The Procedure of SEM Examinations in the Thesis Work 144

6.4.1 Melt-Blending 144

6.4.2 The SEM Examinations 145

Chapter 7 SEM Observations of Polyethylene Blends 146

7.1 Composition Effect on the Morphology of HDPE/LDPE, HDPE/LLDPE and LLDPE/LDPE Blends 146

7.1.1 Materials and Experiments 146

7.1.2 Results and Discussion 158

7.2 Tracer Studies on the Phase Behavior of Polyethylene Blends 156

7.2.1HDPE/LDPE Blends- A Special Case 156

7.2.1.1 Materials 156

7.2.1.2 Variations in Sample Preparation Methods 157

7.2.1.3 Results and Discussion 162

7.2.2 Tracer Studies of Blends of Polystyrene and LDPE 164

7.2.3 Concluding Remarks on Tracer Studies 168

7.3 More Words on SEM Studies of the Phase Behavior of Polyethylene Blends 169

Chapter 8 Final Words 170

8.1 Summary and Comments 170

8.1.1 Theoretical Work 170

8.1.2 Experimental Work 174

8.2 Future Work 176

References 178

List of Tables

Table 4-1 Lennard-Jones Parameters for van der Waals Potential 55

Table 4-2 Computed Hildebrand Solubility Parameters, $(MPa)^{1/2}$, Using COMPASS and DREIDING Force-Fields for Model Blends of HDPE and LLDPE 68

Table 4-3 Effect of Molecular Weight on the Computed Hildebrand Solubility Parameters of HDPE 69

Table 5-1 Characteristics of the Models Used in the Simulations 78

Table 5-2 Experimental Densities of all Polyethylenes at Different Temperatures 79

Table 5-3 Computed Hildebrand Solubility Parameters, δ, of the Models, $(MPa)^{1/2}$ 80

Table 5-4 Simulated Trans/Gauche Ratios for HDPE and BLLDPE 87

Table 5-5 Pressures Simulated on HDPE/BLLDPE Systems, (MPa) 91

Table 5-6 Pressures Simulated Using COMPASS, (MPa) 92

Table 5-7 Characteristics of the Models Used in the Study 94

Table 5-8 Computed Hildebrand Solubility Parameters, δ, of the Models, $(MPa)^{1/2}$ 96

Table 5-8A The Comparison of δ Values of Polyethylene Melts at 166 °C, Measured by P-V-T Method and Computed by MD Simulations, $(MPa)^{1/2}$ 97

Table 5-9 Simulated Trans/Gauche Ratios for HDPE, HLLDPE and OLLDPE 102

Table 5-10 Characteristics of the Models Used in the Simulations 106

Table 5-11 Computed Hildebrand Solubility Parameters, δ, $(MPa)^{1/2}$ for HDPE/LDPE Model Systems 109

Table 5-12 Simulated Trans/Gauche Ratios for HDPE and LDPE 114

Table 5-13 Pressures Simulated on HDPE and LDPE Systems, (MPa) 114

Table 7-1 Characteristics of PE Samples from Nova Chemicals 146

Table 7-2 The Annotation of Blend Samples 147

Table 7-3 Characteristics of PE Samples from Nova Chemicals 157

Table 7-4 Sample Annotation 158

List of Figures

Figure 4-1 Primary Cell and Image Cells under Periodic Boundary Conditions 59

Figure 4-2 An Amorphous HDPE Molecular Model in Condensed State, Generated as an Initial Structure in the MD Simulations 62

Figure 4-3 A Total Energy MD Simulation Profile for an HLLDPE Model 64

Figure 4-4 A Total Energy MD Simulation Profile for an LDPE Model 64

Figure 4-5 Effect of Molecular Weight on the Computed Hildebrand Solubility Parameters of HDPE 70

Figure 5-1 Computed δ of HDPE and Butene-based LLDPE vs. Temperature 81

Figure 5-2 Calculated χ vs. Temperature for Blends of HDPE/BLLDPE 82

Figure 5-3 Calculated χ vs. Branch Content of BLLDPE for Blends of HDPE/BLLDPE 85

Figure 5-3A A Dihedral Distribution Profile for an HLLDPE Simulation Run 88

Figure 5-4 Trans/Gauche Ratio vs. Branch Content of BLLDPE 89

Figure 5-5 Temperature Dependence of χ for Blends of HDPE/HLLDPE 98

Figure 5-6 Branch Content Dependence of χ for Blends of HDPE/HLLDPE 99

Figure 5-7 Temperature Dependence of χ for Blends of HDPE/OLLDPE 100

Figure 5-8 Branch Content Dependence of χ for Blends of HDPE/OLLDPE 101

Figure 5-9 Trans/Gauche Ratios for HLLDPE at the Simulation Temperatures 103

Figure 5-10 Trans/Gauche Ratios for OLLDPE at the Simulation Temperatures 104

Figure 5-11 Temperature Dependence of χ for HDPE/LDPE Blends 110

Figure 5-12 Computed χ vs. Branch content of LDPE for HDPE/LDPE Blends 112

Figure 5-13 χ vs. T for Blends of HLLDPE/LDPE-with-10-branches 117

Figure 5-14 χ vs.HLLDPE Branch Content for HLLDPE/LDPE-with-10-branches 118

Figure 5-15 χ vs. T for Blends of OLLDPE/LDPE-with-10-branches 119

Figure 5-16 χ vs.OLLDPE Branch Content for OLLDPE/LDPE-with-10-branches 120

Figure 5-17 χ vs. T for Blends of HLLDPE/LDPE-with-20-branches 121

Figure 5-18 χ vs.HLLDPE Branch Content for HLLDPE/LDPE-with-20-branches 122

Figure 5-19 χ vs. T for Blends of OLLDPE/LDPE-with-20-branches 123

Figure 5-20 χ vs.OLLDPE Branch Content for OLLDPE/LDPE-with-20-branches 124

Figure 5-21 χ vs. T for Blends of HLLDPE/LDPE-with-30-branches 126

Figure 5-22 χ vs.HLLDPE Branch Content for HLLDPE/LDPE-with-30-branches 127

Figure 5-23 χ vs. T for Blends of OLLDPE/LDPE-with-30-branches 128

Figure 5-24 χ vs.OLLDPE Branch Content for OLLDPE/LDPE-with-30-branches 129

Figure 5-25 χ vs. T for Blends of HLLDPE/LDPE-with-40-branches 130

Figure 5-26 χ vs.HLLDPE Branch Content for HLLDPE/LDPE-with-40-branches 131

Figure 5-27 χ vs. T for Blends of OLLDPE/LDPE-with-40-branches 132

Figure 5-28 χ vs.OLLDPE Branch Content for OLLDPE/LDPE-with-40-branches 133

Figure 7-1 SEM Picture of Pure LDPE, Sample 1 150

Figure 7-2 25%HDPE in LDPE, Sample 2 150

Figure 7-3 50%HDPE in LDPE, Sample 3 151

Figure 7-4 75%HDPE in LDPE, Sample 4 151

Figure 7-5 Pure HDPE, Sample 5 152

Figure 7-6 Pure LLDPE, Sample 6 152

Figure 7-7 25%HDPE in LLDPE, Sample 7 153

Figure 7-8 50%HDPE in LLDPE, Sample 8 153

Figure 7-9 75%HDPE in LLDPE, Sample 9 154

Figure 7-10 25%LLDPE in LDPE, Sample 10 154

Figure 7-11 50%LLDPE in LDPE, Sample 11 155

Figure 7-12 75%LLDPE in LDPE, Sample 12 155

Figure 7-13 SEM Picture of Sample B 159

Figure 7-14 SEM Picture of Sample C 160

Figure 7-15 SEM Picture of Sample A 160

Figure 7-16 SEM Picture of Sample D 161

Figure 7-17 SEM Picture of Sample E 161

Figure 7-18 20% PS in LDPE, quenched into liquid nitrogen immediately after blending 166

Figure 7-19 20% PS in LDPE, quenched into liquid nitrogen after annealing at 160 °C for one hour 166

Figure 7-20 20% PS in LDPE with PS initially mixed with 10% tracer 167

Figure 7-21 20% PS in LDPE with LDPE initially mixed with 10% tracer 167

Nomenclature

A	Helmholtz free energy, kJ/mol
D_{hb}	Hydrogen bond energy well depth, kJ/mol
D_o	van der Waals energy well depth, kJ/mol
e	Total interaction energy of all molecules on mixing, kJ/mol
E	Total potential energy of a system, kJ/mol
E_A	Total interaction energy for bond angle bending, kJ/mol
E_b	Total bonded interaction energy, kJ/mol
E_{elec}	Total energy for electrostatic interaction, kJ/mol
E_{hb}	Total interaction energy for hydrogen bond, kJ/mol
e_{ij}	Total interaction energy between molecules i and j, kJ/mol
E_{INV}	Total interaction energy for four-body central inversion, kJ/mol
E_{nb}	Total non-bonded interaction energy, kJ/mol
E_S	Total interaction energy for bond stretching, kJ/mol
E_T	Total interaction energy for torsion angle rotation, kJ/mol
E_{vdw}	Total interaction energy for van der Waals, kJ/mol
ΔE_v	Total vaporization energy of a material, kJ/mol
$\mathbf{F}$	Force in Newton's equation of motion in the form of a vector, N
ΔG_{mix}	Gibbs free energy change on mixing, kJ/mol
ΔH_{mix}	Enthalpy change on mixing, kJ/mol
H	Hamiltonian operator
i	species (or component) i, or integer number

j	species (or component) j
k_B	Boltzmann constant, kJ/mol/K
K_A	A constant in Equation 4-9, mol/kJ
K_{INV}	A constant in Equation 4-11, mol/kJ
K_S	A constant in Equation 4-8, mol Å/kJ
K_T	A constant in Equation 4-10, mol/kJ
N_1	Number of molecules of the solvent for mixtures of small molecules, or for solvent-polymer mixtures; number of the segment of polymer one for polymer-polymer mixtures
N_2	Number of molecules of component two for mixtures of small molecules; number of the segments of polymer two for polymer-solvent and/or polymer-polymer mixtures
p	Momentum in the form of a vector, kgm/s
P	Pressure, N/m^2
Q	Canonical partition function for an NVT ensemble
q	Position coordinate in the form of a vector, m
R	Stretched bond length, or van der Waals bond length, Å
R_{DA}	Distance between atoms of hydrogen bonding donor and acceptor, Å
R_{hb}	Hydrogen bond length, Å
R_o	Equilibrium bond length, or equilibrium van der Waals bond length, Å
S	Entropy of a system, kJ/mol/K
ΔS_{mix}	Entropy change on mixing, kJ/mol/K
T	Absolute temperature, K

U Internal energy of a system, kJ/mol

$(\partial U/\partial V)_T$ Partial derivative of internal energy with respect to volume at fixed temperature, $N/m^2/mol$

V Total volume of a material, m^3

V_s Molar volume of the solvent for polymer-solvent mixtures or the molar volume of the smaller polymer segment for polymer-polymer mixtures, m^3/mol

x_i Molar fractions of component i of a mixture

Z Any thermodynamic property in Equation 4-2

z Coordination number in the lattice model, i.e., each site of the lattice has z neighboring sites

Greek Symbols

α Thermal expansion coefficient, K^{-1}

β Compressibility, m^3/kJ

χ_{12} Flory-Huggins interaction parameter between component one and two, dimensionless

δ Hildebrand solubility parameter, $(MPa)^{1/2}$

ε_o Equilibrium van der Waals energy well depth for united atom model, kJ/mol

ϕ_i Molar volume fraction of component i

ϕ_o Equilibrium torsion angle

ϕ Torsional angle

μ_i Chemical potential for species i, kJ/mol

Π	Internal pressure, MPa
θ	Instantaneous bond angle
θ_o	Equilibrium bond angle
θ_{DHA}	Bond angle between atoms of hydrogen bonding donor, hydrogen and the hydrogen bonding acceptor
σ_o	Equilibrium van der Waals bond length for united atom model, Å
$\sum_i$	Sign of sum over i
ψ	Wave function in Equation 4-1; plane angle in Equation 4-11
Ψ_o	Equilibrium plane angle and defined as zero for a planar molecule

Chapter 1

Introduction

1.1 Organization and Scope of the Thesis

The major goal of this thesis work is to predict and characterize the phase behavior of various types of polyethylene blends by using MD simulations and SEM techniques. The thesis is arranged in four parts. The first part contains Chapters 1 and 2. Chapter 1 provides general information about the background of polyethylene polymers and miscibility issues in the polyethylene field, while chapter 2 provides a detailed literature review on the miscibility studies of polyethylene blends. Part Two includes chapters 3-5 that discuss the theoretical background of the molecular dynamics (MD) simulation technique and the results of MD simulations of polyethylene blend systems. Chapter 3 introduces the thermodynamics of polymer mixtures. In particular, the Hildebrand solubility parameter and Flory-Huggins interaction parameter theories are introduced as the background thermodynamic support of the MD work. Chapter 4 introduces statistical thermodynamics and molecular dynamics simulations. The methodologies (the adoption of the energy potential form and parameters) used in the MD simulations are justified and solidified. Chapter 5 presents and discusses the results of the MD simulations on the miscibility of polyethylene blends, constituting a major part of the thesis. Part Three

contains chapter 6 and chapter 7, discussing the background of the SEM technique for morphological studies of polymer blends, and the observed morphologies of polyethylene blends. Chapter 8 constitutes Part Four that summarizes the thesis work and discusses the future work.

1.2 Fundamentals of Polyethylene Polymers

Polyethylene (PE) polymers are chain molecules with wide range of molecular weight distributions and a variety of configurations. The basic structure of PE is the repeat-unit, $—(CH_2—CH_2)_n—$, which is made by polymerizing the monomer, ethylene, under certain conditions. In commercial PEs, the number of repeat-units, n, can be from around 400 to above 50,000. While the basic structure of polyethylene molecules, i.e. the repeat-unit, is the same in all molecules, they can be assembled differently; for example, branches can be present on the main chain (called the backbone). There may be short-branches (1-7 carbons) or long branches (more than 8 carbons) depending on the polymerization process and conditions (e.g., temperature and pressure). A polyethylene molecule without branches is called linear polyethylene (LPE) while a PE molecule with branches is called branched polyethylene (BPE).

PE is a semi-crystalline polymer whose properties are greatly influenced by its crystallinity and relative amounts of amorphous phases. The thickness of the lamella, the basic crystalline unit, is about 5 to 15 nm. Between lamellae, there are amorphous regions that are PE molecules passing through the amorphous regions from one lamella to another. When polyethylene molecules are crystallized from the melt,

spherulites are formed, which are built up by lamellae (aggregated into spherical clusters) in various ways depending on the kinetics of crystallization process. While the crystalline phase provides mechanical strength until the melting temperature is exceeded, the amorphous phase provides flexibility and high impact strength. Mechanical properties are strongly influenced by the size of spherulites.

LPE has a density ranging from 0.960 to 0.970 g/cm^3 with crystallinity of 70-90%, and has a melting point as high as 135 °C, and is usually called high-density polyethylene (HDPE). However, BPE can differ considerably. One type, produced by a high-pressure free-radical polymerization process (122-303 MPa; 130-350 °C), leading to randomly branched structures that include both short and long branches is called low-density polyethylene (LDPE) and was the first commercial polyethylene product. Because of the interference of branches on the main chain, LDPE has smaller thickness of laminar structure, leading to lower melting points (105-115 °C) and densities (around 0.910-0.935) g/cm^3 with crystallinities (40-60%), compared with HDPE values. Usually, commercial LDPE products contain about 15-30 branches per thousand carbons. It has been verified that the density of an ideal polyethylene crystal is 1.00 g/cm^3 while the density of the amorphous phase is believed to be about 0.855 g/cm^3. Therefore, the density of PE generally falls between the density values of the crystalline phase and amorphous phase.

With the advent of modern catalyst techniques, a special type of branched polyethylene molecules with only short-branches on linear backbones can be produced by copolymerizing ethylene and an α-olefin (which can be 1-butene, 1-hexene or 1-octene, etc.) at atmosphere pressure, called linear low-density

polyethylene (LLDPE) with melting points around 122 °C. The densities of LLDPE can be as low as 0.915 g/cm^3 and as high as 0.958 g/cm^3 with a crystallinity of about 25-75 %. These new catalysts are now known as Ziegler-Natta type of catalysts discovered by Ziegler and Natta and co-workers in the early 1950s. With current technology, LLDPE can be produced at 2 MPa of pressure and 100 °C of temperature. No doubt that the latter technology is at much lower cost than that of the "high pressure" free radical process for producing LDPE. For more general information about polyethylenes and background of polymers, see the references [Flory, 1953; Mark et al., 1985; Rudin, 1999].

1.3 Polyethylene Blends and the Miscibility of the Components

As aforementioned, various PEs exhibit different characteristics and properties. Therefore, different types of polyethylenes are often blended together to meet various kinds of requirements of processing and final product properties. Thus, miscibility studies of polyethylene blends in the liquid state have both industrial and scientific significance. The polyethylene melt processing industry is concerned about the miscibility of the components because miscibility affects the melt rheology. The melt rheology, in turn, will affect the solid state morphology and final product properties. In addition, it is important from a purely scientific viewpoint to understand the miscibility of the components in the liquid state based on fundamental thermodynamics. Furthermore, if polyethylene blends are immiscible, such a multi-phase liquid system develops a morphology during flow which, in turn, modifies the melt rheology.

In fact, the phase behavior of polyethylene blends in the melt has already drawn a great deal of research attention [Hill et al., 1988-1999; Alamo et al., 1994-1997; Plans et al., 1991; Martínez-Salazar et al., 1991; Graessley et al., 1994;1995; Fan et al., 1997; Choi, 2000]. For example, it has been found that the branch content of LLDPE molecules is the controlling factor that determines the phase behavior of HDPE/LLDPE blends [Hill et al., 1993; Barham et al., 1993; Hill and Barham, 1994; Alamo et al., 1997; Morgan et al., 1999; Choi, 2000]. However, different views have been expressed in the literature about the cut-off values of the branch content for HDPE/LLDPE blends above which the components segregate and become immiscible and about the domain size scale that could be detected [Barham et al., 1993; Morgan et al., 1999; Barham et al., 1988]. In the cases of HDPE/LDPE and LDPE/LLDPE blends, there is also some basic disagreement about the general question of miscibility of blend components, some researchers reporting liquid-liquid phase separation [Barham et al.,1993; Hill et al., 1988-1996], while others report complete melt homogeneity [Alamo et al., 1994; 1997; Agamalian et al., 1999]. Despite a great deal of effort that has been made for the last couple decades to understand and to characterize the melt phase behavior of polyethylene blends, it is still a controversial topic and needs to be explored further. A detailed literature review on these issues will be given in the following chapter.

In the most basic approach, miscibility can be addressed in terms of the Hildebrand solubility parameters (δ) of pure components. However, for polymer melts, it is impossible to measure δ directly through the energy (heat, enthalpy, etc.) of evaporation, as for small-molecule liquids, because polymers cannot be vaporized.

In practice, indirect methods have been used instead. Once δ values are determined experimentally or theoretically, Flory-Huggins interaction parameters (χ) for a binary mixture can then be calculated from the resulting δ values and used to judge the miscibility of the constituents of the mixture so long as the interaction energy of the components follows the geometric mean assumption.

With the advent of molecular simulation techniques and computer technology, MD simulation has become more and more popular in the study of phase behavior of polymer blends [Colbourn, 1994; Londono et al., 1998; Maranas et al., 1998; Luettmer-Strthmann and Lipson, 1999]. In particular, strategies based on MD simulation have been developed [Kavassalis et al., 1996] to compute δ for non-ionic surfactants and polymers such as polypropylene and polyethylene over a wide range of temperatures. However, the application of such strategies has not been seen in the literature of solubility characteristics of different types of polyethylenes as far as I know.

Although theories involving δ or χ can be quite useful in determining the phase behavior of polymer mixtures from a thermodynamic viewpoint, they predict nothing about the domain size of a multi-phase system. Therefore, microscopy techniques are needed to get the most direct evidence of the blend morphology if immiscibilty applies to the systems being studied. In the literature, successful application of scanning electron microscopy technique has been reported to study immiscible polymer blend systems as will be reviewed in chapter 6. I am encouraged to use SEM to explore the visual evidence of the phase behavior in the important blends of dissimilar polyethylenes provided that the blends are phase-separated.

In this thesis, I am going to present the use of the MD simulation technique for computing the δ of various PEs and the resultant χ parameters for mixtures of different PE components. As suggested in my MD simulation work, branch content of branched PEs is the controlling factor in determining the phase behavior of HDPE/LLDPE blends. However, long-chain branching also plays an important role in the miscibility issue of PE blends. In addition, exploratory work on the morphological studies of polyethylene blends by using SEM will also be presented.

Chapter 2

Miscibility Studies of Polyethylene Blends

—a Literature Review

Extensive miscibility studies of polyethylene blends have been seen in the literature for the past two decades. Early studies were mainly focused on blends in the solid state (i.e., the characteristics of the crystallization processes of the components). However, more recent concerns of phase behavior of polyethylene blends have been concentrated on the liquid state prior to crystallization. As mentioned in chapter one, different polyethylenes, i.e., linear and branched, were often blended together to increase the stiffness of LDPE and toughness and flexibility of linear polyethylene, mainly, HDPE, in the early stage of the polyethylene industry. It was believed that the blends of different types of polyethylene would form homogeneous crystals due to their similar chemical compositions, i.e., CH_2 group. However, many of studies have shown that for certain kinds of blends, there are at least two melting peaks in thermographs based on thermal analysis techniques, which indicates that different families of crystals exist in the blends. These studies have implied that some branched and linear polyethylenes do not co-crystallize and they phase-separate upon or before the crystallization process. Later on, researchers started

to explore the reason for this phenomenon and the relationship between the solid-state morphology and its previous liquid-state morphology for polyethylene blends. Therefore, the studies have been extended to the recent concerns about the melt miscibility of the components of the blends. A second issue involves co-crystallization effects when the melt blend freezes and how these effects influence morphology in the final solid state. While the first issue is relevant to blend preparation and melt processing, the second issue affects the physical properties of the products. Thus research on these issues has both academic and industrial significance.

Polyethylene is a semicrystalline polymer and thus has amorphous and crystalline regions in the solid state that can be interpreted as different phases no matter if different polyethylenes co-crystallize or not. Therefore, difficulties arise when blends of two semicrystalline polymers are being studied for their phase behavior in the solid state. However, if only the crystalline phase is concerned without considering amorphous part when the miscibility issue is raised for blends of semicrystalline polymers, the issue becomes simpler.

Datta and Birley [1982] did an extensive study on the compatibility of components in the solid state for HDPE/LDPE and HDPE/LLDPE blends based on differential scanning calorimetry (DSC) thermal analysis, X-ray diffraction and mechanical property measurements. The weight average molecular weights of the polyethylenes they used were as follows: LDPE 129,800 with M_w/M_n=7.3, HDPE 232,400 with M_w/M_n=19.2, LLDPE 133,200 with M_w/M_n=6.6. There was no branch content information reported. They contended that blends of HDPE and LDPE consist

of three distinct phases, an amorphous phase and two crystalline phases (thus, two T_m or T_f). Based on this result, they concluded that HDPE and LDPE would be incompatible in their crystalline phases. On the other hand, they observed that blends of HDPE and LLDPE had only one T_m or T_f and reasoned that these blends had one amorphous phase and one crystalline phase, the latter therefore indicating miscibility of the components in the crystalline state. It was claimed that the DSC results were supported by their X-ray diffraction and mechanical measurements.

Kyu et al. [1987] and Ree et al. [1987] extensively studied crystallization kinetics for both HDPE/LLDPE and LDPE/LLDPE blends by wide angle x-ray diffraction (WAXD), small angle x-ray scattering (SAXS), Raman longitudinal-acoustic-mode spectroscopy (LAM), light scattering and DSC. The molecular information is as follows: LLDPE had M_w=114,000 with M_w/M_n=4.5, 18 short-chain branches per 1,000 carbon atoms; HDPE had M_w=126,000 with M_w/M_n=5.3, 1 short-chain branch per 1,000 carbon atoms, and LDPE had M_w=286,000 with M_w/M_n=16, 26 short-chain branches per 1,000 carbon atoms and 34 long-chain branches per weight-average molecule. Blend compositions were chosen with 20, 50 and 80% HDPE for HDPE/LLDPE while compositions were chosen with 25, 50 and 75% LDPE for LDPE/LLDPE. They observed a single melting peak in DSC measurements for all HDPE/LLDPE blend samples cooled from the melt both slowly and quenched, while two melting peaks were found for all LDPE/LLDPE blend samples in DSC measurements. Results from their different techniques were believed to be quite consistent; i.e., whenever a single endotherm was found in DSC (for HDPE/LLDPE blends), a single crystal population was observed in SAXS data, and when two

endotherms were found in DSC (for LDPE/LLDPE blends), two distinct crystal populations were observed in SAXS data. Therefore, they have concluded that co-crystallization (which implies that the components are miscible in crystalline phase) between HDPE and LLDPE components occurred, while separate crystals were found in the LDPE/LLDPE system. Further, based on polarized light microscopy (PLM) and light scattering experimental results, they proposed that "the LDPE/LLDPE solid blend system consists predominantly of volume-filling spherulites formed by primary crystallization of the LLDPE component and followed by a secondary crystallization process of the LDPE within the spherulites previously formed." Uniform-size, not mixed-size spherulites were found. Spherulites in the blend have a radius comparable to those in pure LLDPE. These arguments were based on the assumption that HDPE and LDPE or LDPE and LLDPE polyethylenes are miscible in the liquid state, which is still a controversial topic and the major focus of this thesis research work.

Tashiro et al. [1992; 1994] used DSC and Fourier transform infrared spectroscopy (FTIR) associated with a deuteration technique to investigate the cocrystallization and phase segregation behavior of polyethylene blends in the solid state. Because polyethylene molecules have very similar chemical structures with carbon and hydrogen atoms, it is often frustrating to investigate their phase behavior by using common spectroscopy or microscopy techniques. However, the infrared bands of CH_2 and CD_2 groups appear at different wave numbers so that it is possible to trace the change in the infrared bands of CH_2 and CD_2 species in order to investigate the phase behavior of H and D species and their corresponding components based on the deuteration technique. With this technique, Tashrio et al.

did some studies on the blends of deuterated HDPE (DHDPE) and LLDPE, and also they studied the effect of branch content of LLDPE on the phase behavior of the blends in terms of crystallization kinetics. The results were then compared with results of other researchers [Schelten et al., 1977; Cheam and Krimm, 1981] on the blends of DHDPE and HDPE, in which it was suggested that the DHDPE and HDPE showed co-crystallization behavior when samples were quenched rapidly, while phase segregation would occur when samples were slowly cooled from the melt. On the contrary, they showed that DHDPE and LLDPE (which was a 1-butene and ethylene copolymer) form co-crystals even if the melts of the blend were cooled slowly. In addition, they found that branching content played a role in the phase behavior of DHDPE and LLDPE blends in that DHDPE and LLDPE with lower branch content (17 ethyl groups/1,000 carbons) would form co-crystals for different blend composition from 0 to 100% even if the melts were cooled slowly while phase segregation was observed for the blends of DHDPE and LLDPE with higher branch content (41 ethyl groups/1,000 carbons).

Rego López and Gedde [1989], Iragorri et al. [1991] further studied the crystallization kinetics and melting behavior of polyethylene blends by DSC, polarized light microscopy (PLM), transmission electron microscopy (TEM) and small-angle light scattering (SALS) techniques. The HDPE had an M_w=2,500 with M_w/M_n=1.15 and the LLDPE an M_w=166,000 with M_w/M_n=6.1, about 7.5 ethyl branches per 1,000 backbone carbon atoms. They pointed out that the presence of a single melting peak would be a necessary but not sufficient condition for the existence of cocrystals. They have shown that a sample displaying unimodal melting

may have two separate crystallite populations of the same melting temperature. They concluded that the HDPE and LLDPE blend they studied showed the presence of two distinct crystalline types and the crystallization behavior (cocrystals or distinct crystallite populations) of polyethylene blends would be strongly influenced by crystallization temperature and blend composition. Therefore, care should be excised to analyze unimodal types of experimental results when cocrystallization issue is raised.

Zhao et al. [1997] studied crystallization behavior of blends of HDPE and a new type of LLDPE that was made by copolymerizing ethylene and 1-octene monomers with metallocene catalysts, called metallocene polyethylene (MCPE). Due to the new technology of metallocene catalysts, MCPE has both a narrow distribution of molecular weight and a narrow distribution of branches along the main chain. Besides, branches are usually distributed on the backbones' regularly. These characteristics make MCPE differ from conventional LLDPE made by Ziegler-Natta catalysts. In their study, they used MCPE with different branch contents and blended them with same HDPE at the compositions, 20, 50, 70 and 90% separately. The HDPE had an M_w=53,000 with M_w/M_n=3.3. Characteristics of three octene-based LLDPE samples were as follows: one with M_v=113,000, 3.6 branches per 1,000 backbone carbon atoms; the second one with M_v=68,000, 7.15 branches per 1,000 backbone carbon atoms and the third one with M_v=46,000, 24.1 branches per 1,000 backbone carbon atoms. The analytical techniques they used were DSC, small-ángle X-ray scattering (SAXS) and wide-angle X-ray diffraction (WAXD). By examining the melting peaks in DSC thermographs, Lorentz-corrected SAXS scattering pattern

and the changes of unit cell parameters obtained from WAXD measurements, they found that the crystallization behavior of blends of HDPE with MCPE differed significantly from that of blends of HDPE with conventional octene LLDPE by Ziegler-Natta catalyst. From the study of three pairs of blends of same HDPE and MCPE at different levels of octene branch content, they reported that when branch content of MCPE was low (3.6 branches/1,000 carbons, or 0.72% in mole percentage), the components mixed well and formed uniform cocrystals. However, when branch content was increased, separate crystallization occurred between the two components. There was a continuous transformation from cocrystallization to separate crystallization depending on the branch content. When branch content was above about 8 branches/1,000 carbons, separate crystallization began to take place. When branch content was above about 25 branches/1,000 carbons, they observed completely separate crystallization. In addition, they found also that the critical value of branch content for separate crystallization to occur in the blends of HDPE and MCPE was much lower than that in the blends of HDPE and conventional octene LLDPE reported in the literature (see the reference and therein) [Zhao et al., 1997]. And they suggested that the miscibility (in solid state) of the linear and branched polyethylenes would be affected by both the branch content and how the branches were distributed on the backbone.

Usually, three types of rheological behavior are observed for polymer blends in plots of a rheological quantity versus composition, i.e., 1. positive deviation from the linear rule of mixing; 2. negative deviation from the linear rule of mixing; 3. showing both of them in different composition ranges. However, all three types of

behavior have been observed in miscible and/or immiscible polymer blends [Utracki, 1989]. Therefore, deviation from linear rule of mixing itself cannot be viewed as an indication of immiscibility. In addition, in semicrystalline polymer blends, for most of the systems crystallization leads to phase separation of the constituents in the solid state which does not necessarily mean that the constituent polymers are immiscible in the melt. It is more difficult to judge the miscibility of non-polar polymer blends, eg., polyolefin blends, because of the similar thermodynamic interaction features from the hydrocarbon groups. Results from rheological study must be judged based on that of several physical properties to draw a conclusion on the miscibility or immiscibility of polymer blend systems. Utracki and Schlund [1987] indicated that presence of two indirect indications, i.e., deviation from linear rule of mixing of dynamic and steady state viscosities and a decrease of the maximum strain at break in uniaxial extensional flow could be used to imply immiscibility of components in the blend. However, they have also explained that the presence of the above two phenomena indicates immiscibility but the absence of them cannot be taken as the indication of the reverse. Based on aforementioned arguments and their experimental results, i.e., measurements of steady-state and dynamic viscosities and relaxation spectra, mostly from LLDPE and LDPE blends, they concluded that LLDPE/LDPE blends for 20, 50 and 80% LLDPE in weight that they studied showed two-phase mixture behavior with good interfacial interactions which they called emulsion-type blends and therefore LLDPE and LDPE are immiscible in the liquid state for the blends with those compositions. The molecular weights of the polyethylenes were about $M_w \sim 10^5$, and the LLDPE were ethylene and octene copolymers.

Müller et al. (1992; 1994) did a qualitative but extensive study on the miscibility of LDPE/LLDPE melt blends based on a DSC technique associated with controlling the cooling rate (quenching or slow cooling) to infer the melt miscibility of the blends. LLDPEs were ethylene and octene copolymers with $M_w \sim 1.3\times10^5$. LDPE had an M_w=110,000. Molecular weight distribution and branch content were not reported. They used two approaches to prepare the samples. One was melt blending and the other was physically assembling pieces of different polyethylene components together without any melt mixing. The samples prepared by the latter approach were called "unmixed". For DSC measurements, they found two melting peaks for melt blended samples. They suggested that the blends were immiscible in the molten state, existing in the form of a liquid-liquid phase segregation. However, the melting thermographs for melt blended and "unmixed" samples were not identical, which indicates that there is partial miscibility between the two components created by the melt-blending process. The term partial miscibility they used implies that the blend will show one or two phase regions in the melt depending on the exact shape of the phase diagram, i.e., depending on the melting temperature and composition of the blend. It is worth noting that, however, what the authors indicated in their papers: miscibility determination of semicrystalline polymer blends by DSC is not an easy task in that multi-melting transitions can happen even in pure LLDPE. Therefore, caution must be taken to draw a conclusion on the melt miscibility of polyethylene blends based on DSC experiments.

Martínez-Salazar et al. [1991] examined the branching effect of LDPE on the miscibility of HDPE/LDPE blends using melting point depression analysis and

discussed the issue in terms of Flory-Huggins theory for polymer-polymer mixtures. They derived the equilibrium melting temperature by observing the growing and disappearing of spherulites using an optical microscope equipped with a hot stage under polarized light. The HDPE had an M_w=100,000 and they used three LDPE samples with different molecular weights and branch levels. One had an M_w=120,000 with 7 branches per 1,000 carbon atoms; the second had an M_w=100,000 with 12 branches per 1,000 carbon atoms and the third had an M_w=51,000 with 18 branches per 1,000 carbon atoms. From the analysis of their data based on the Flory-Huggins lattice theory for polymer-polymer systems, they suggested that mixing of HDPE and LDPE molecules in the melt would take place whenever the branch content of LDPE was lower than 20 branches per 1,000 carbon atoms while phase separation might occur if the branch content was above 30 branches per 1,000 carbon atoms.

Plans et al. [1991] tried to develop a model based on their results to explain why the HDPE/LDPE system could undergo phase segregation. They modified the Flory-Huggins lattice by incorporating the holes caused by branching points to balance the free volume change during mixing and analyzed the entropy gain for mixing of the HDPE and LDPE molecules. They indicated that the entropy gain associated with the mixing of long chains was so low that one would expect that dispersive interaction between components would prevent miscibility, i.e., the enthalpy change would dominate in Flory-Huggins interaction parameter, χ. They concluded that their simple thermodynamic lattice model would satisfactorily explain the melting-point depression of HDPE containing some LDPE "solute" and support

the idea of phase segregation for a critical branch content of LDPE over 20 per 1,000 carbon atoms.

Nicholson et al. [1990] studied blends of HDPE and hydrogenated polybutadienes (HPB) having different levels of ethyl branching along the backbone, which are model polymers of butene-based LLDPE with very narrow molecular weight and branching distributions, using small angle neutron scattering (SANS) technique. To avoid more complicated questions of co-crystallization of dissimilar chains, they carried out all experiments in the melt state. Polybutadiene polymers were produced by anionic polymerization so as to give from 18 to 106 ethyl groups per 1,000 backbone carbon atoms. After being hydrogenated or deuterated over a palladium catalyst, these polymers would become models for butene-based LLDPE with different branch contents. The shape and magnitude of the scattering pattern for homogeneous and immiscible melt blends were much different and therefore the SANS technique is used as a powerful tool to determine the phase behavior for polyolefin blends. However, in SANS experiments, the contrast is due to the deuteration of one of the species, either HDPE or hydrogenated polybutadiene (HPB) in this case. Therefore, the isotope effect will become an issue when phase behavior is being discussed using SANS technique. This effect was analyzed and the χ value that the isotope effect contributes in SANS experiments was evaluated. They concluded this study with an expression for 50/50 HDPE/HPB blends at temperatures 150 ± 15 ^{0}C, as following:

$$\chi=0.4\times10^{-4} + 0.014\Delta X_{br}^2 \qquad (2\text{-}1)$$

where χ is the Flory-Huggins interaction parameter based on SANS; ΔX_{br} is the fraction of the repeat units with ethyl branches. The first term was attributed to the isotope effect and the second term to chemical composition differences between the components. They implied that the information drawn from this study of the model systems could be used to understand the phase behavior in complex copolymer systems such as those involving LLDPE.

Further, Rhee and Crist [1991] continued this work by examining the critical value of the branch content of HPB for the blends to phase-separate using SANS and morphological study with scanning electron microscopy (SEM) associated with etching and quenching techniques. They concluded with their study that a branch content over 60 per 1,000 backbone carbon atoms of the modeled branched polyethylene would be the critical value to phase segregate with HDPE in the blends with molecular weight M_w =118,000 at 150 ^{0}C. The domain sizes they observed ranged from 0.1 to 16 μm.

Hill and co-workers [1988-1998] did a series of studies on polyethylene blends by using DSC, TEM and some other techniques. Their main interest was focused on the liquid-liquid phase separation (LLPS) behavior in polyethylene blends. They have assumed that liquid state morphology existing at high temperatures ($T>T_m$) will be preserved if rapid quenching is applied to the melt. They have explained that because the rapid cooling impedes the movements of the molecules in the melt such that further segregation, which will need molecular diffusion, is not feasible [Kyu et al., 1987; Hill and Barham, 1992]. Therefore, the morphology

observed in the quenched samples should be closely related to the morphology in the liquid state.

By using TEM and DSC with quenching or isothermal crystallization, Barham et al. [1988] have shown that certain HDPE/LDPE blends (with HDPE content less than 40%) displayed two melting peaks in DSC endotherms after quenching treatment of the samples. They attributed the double-peak behavior to the liquid-liquid phase segregation within the melt not to the possible crystallization events during cooling process. They further showed TEM micrographs in support of this postulate. They argued that a homogeneous melt (above 50% HDPE blend) would result in a single featured micrograph after rapid quenching and its DSC endotherm would have only one peak. However, blends with HDPE content less than 40% would result in different features on their micrographs and two melting peaks in DSC endotherms after rapid quenching, which would be an indication of a two-phase melt.

In addition, Barham et al. [1988] have shown that if a homogeneous melt of HDPE/LDPE (with HDPE content about 50%) was held for a long time at a temperature between the melting temperatures of HDPE and LDPE, the resulting endotherm showed two peaks with melting points the same as that of their individual components. This phenomenon is an indication of liquid-solid transformation from an initially homogeneous melt. However, for a melt with HDPE content less than 40%, no matter how fast quenching was applied to the melt, the resulting endotherm of the quenched sample showed two peaks.

Hill et al. [1991] mapped out a melt phase diagram for HDPE/LDPE blend systems based on DSC, TEM, rheological measurement and hot stage electron

microscopy techniques. The phase diagram they mapped out is not an equilibrium one in that any mixing or demixing is time dependent and it can take a long time to reach equilibrium for polymer blend systems. Nonetheless, because it was difficult to get direct evidence of phase behavior for polyethylene blends in the molten state, they were investigating quenched samples to infer the liquid state miscibility as mentioned previously, which is still controversial in the literature. Based on their results, they constructed a closed-loop type of phase diagram (i.e. the system has both upper and lower critical solution temperatures within a certain composition range.), which gave the segregated region at low HDPE composition. They suggested that their results were not unique for the specific polyethylene pair they used and should be of common interest to all polyethylene blend researchers.

As indicated in their papers, polymer blend systems are very complicated in terms of blend composition. Neither of the homopolymers involved is a single component system. In HDPE/LDPE blend systems, HDPE has a broad distribution of molecular weights while LDPE has not only molecular weight distribution but branch content distribution as well. (In fact, there is also a distribution of branch length on the backbone carbons, which will be explored and discussed by using the MD simulation technique in this thesis work later.) Therefore, they further investigated [Hill et al., 1992; Hill, 1994] the effect of molecular weight and molecular weight distribution of HDPE on the melt phase behavior of HDPE/LDPE blends by DSC and TEM techniques, and examined the change of the shape and size of LLPS region in the phase diagram they proposed previously.

Hill and co-workers [1994; 1992] also investigated several blend systems of HDPE/LDPE with varying molecular weight of HDPE blended with the same LDPE. In general, they found that blend systems with lower molecular weights of HDPE showed greater miscibility. They analyzed their results with some conclusions as follows. When the molecular weight of HDPE is very low, the blend system does not show LLPS and the LLPS region on their phase diagram contracted to nothing. They suggested that a higher branch content of LDPE would give rise of greater phase separation. The phase separation is mainly due to the difference of the branch content between the two components but not due to the difference of the molecular weight of the components. In terms of their phase diagram, they suggested that the LLPS region would be larger if the molecular weight of HDPE is higher and the LLPS region would contract rapidly if the molecular weight of HDPE is below 20,000.

However, they reported [Hill and Barham, 1995] that no phase separation on a scale of micrometers was detected for blends of HDPE/HDPE with different molecular weight by the same techniques, i.e., DSC and TEM. In this study, they used four HDPE samples with M_w, 2.5K, 13K, 127K and one larger than 2 million. They blended two high molecular weight HDPE samples with two low molecular weight HDPE samples in turn for the whole composition range by melt blending between 140 to 160 °C and then quenched the samples for examining. From the results, they observed no phase separation for all HDPE fractions between 120 and 160 °C. However, some small-scale spatial separation was detected on isothermal crystallization for the blend of HDPE fractions with molecular weights between 127K and 2.5K. Thus, based on the above results, they claimed that the LLPS they found in

HDPE/LDPE and HDPE/LLDPE blends was a result of differences between the components with branch content or the combination of branch content and molecular weight difference but not a result of molecular weight difference alone.

By examining the TEM micrographs of the samples quenched from different temperatures outside and within the LLPS region, Hill and Barham [1992] intended to explain and expand the limit and use of their phase diagram for HDPE/LDPE blend systems. Their basic assumption is that the molecules at the surface of a quenched sample are unable to move quickly from their original positions in the melt. Therefore, by examining the surface morphology of a quenched sample, it is possible to infer the melt morphology and thus, find out the clear boundary of the phase diagram. They showed some specific TEM pictures of the micrographs of a sample of HDPE/LDPE blend with 20% HDPE, rapidly quenched from 230 °C (that was believed to be a homogeneous melt based on their phase diagram) and from 150 °C (that was believed to be a two-phase melt as identified on their phase diagram). The former picture showed uniform features but the latter dual features. Based on the above argument and analysis of their results from a close look at the temperature and composition boundary of their phase diagram, they claimed that their morphological studies confirmed their belief of its closed-loop shaped phase diagram and it should represent an equilibrium one.

In another paper [Barham et al., 1993], they intended to develop a model to explain the LLPS phenomenon as described by their closed-loop phase diagram qualitatively. They claimed that their reported phase behavior was based on their observations of over 20 different blends of HDPE/LDPE. And they reported that the

effect of molecular weight and molecular weight distribution was quite small. They showed that same type of phase diagrams were derived with HDPE varying molecular weight from 1,000 to 1,000,000 blended with the same LDPE. When the molecular weight of HDPE was increased, the LLPS region increased slightly. In addition, the phase diagrams for two different HDPEs (same average molecular weight but very different molecular weight distribution) with LDPE blends were essentially the same. Therefore, they concluded that molecular weight and its distribution would not affect the miscibility of polyethylene blends significantly except for some extreme cases.

Barham et al. [1993] also studied HDPE/LLDPE blend systems by the same techniques they usually used, i.e., TEM and DSC. They examined HDPE blends with octene-based LLDPE for different branch contents. They found that for lower branch contents (less than 8% in mole or 40 branches per 1,000 carbons) of the LLDPE the phase diagram of the HDPE/LLDPE system was similar to those they obtained previously from the studies of HDPE/LDPE blends. However, an unexpected behavior regarding the size of the LLPS region was observed: With the increase of the branch content of the octene-based LLDPE (beyond 8%), the size of the LLPS region (closed-loop) was decreased. Later, they investigated blends of HDPE and butene-based LLDPE with differing branch contents [Hill et al., 1993]. What they found was that the phase behavior of this blend system was basically the same as that containing octene-based LLDPE. In addition, they showed that the length of the LLDPE branches had to be of secondary importance in determining the phase behavior of polyethylene blends, as molecular weight of HDPE was. Based on the above studies and the investigation of the effect of molecular weights, they concluded

that branch content of polyethylenes would be the major factor that determines the phase behavior of their blends with HDPE.

Puig et al. [1994] compared the results from the studies of HDPE/LDPE blends using two different approaches of mixing the components. One approach to mix the components is by solution blending and the other by melt blending using a co-rotating twin screw extruder. DSC and TEM techniques associated with quenching technique were applied to infer the miscibility of the components in the liquid state. By comparing the phase diagrams derived by using two different sample preparation approaches, they concluded that the phase behavior of the melt-blended systems was similar to that of solution-blended systems. They suggested that melt mixing would be an efficient method to prepare uniformly blended samples for the purpose of studying the miscibility of the blend systems.

With regard to Alamo et al.'s [1994] SANS study on HDPE/LDPE blends with conclusion that this blend system is homogeneous in the melt for all compositions and temperatures, Schipp et al. [1996] accomplished a similar experimental study using SANS technique but contended that results from SANS could be ambiguous when data were interpreted to judge the phase behavior of the blends. As mentioned before, in SANS experiments, one of the species must be deuterated to enhance the contrast in order to detect the phase behavior of the mixture. In this study, linear polyethylene HDPE was deuterated, given the name DLPE. DLPE was blended with LDPE. Because of the deuteration, the isotope effect has to be taken into account when data are about to be interpreted to judge the miscibility of the blend system. Schipp et al. further argued that since the LLPS

region they found for polyethylene blends in general was typically of several micrometers in diameter, SANS technique is not sensitive to phase separation on such a large domain size. Therefore, the data from the SANS experiments for the blends of DLPE/LDPE can be interpreted as being either due to a homogeneous melt (as concluded by Alamo et al.) or just simply due to a biphasic melt with a large phase domain size (which would contradict Alamo et al.).

In polymer research, TEM is a useful tool for morphological studies. However, the samples for TEM examinations must be very thin, usually less than about 100 nm in thickness to let the electrons go through the samples. Therefore, specimen preparation techniques should be taken into account when TEM data are interpreted. In general, there are two major techniques used in TEM specimen preparation in polyethylene studies. One is the fixation with chlorosulfonic acid followed by sectioning developed by Kanig [1973; 1975]. The other is the permanganic etching followed by replication developed by Olley et al. [Olley et al., 1979; Bassett and Hodge, 1978]. Both methods have been widely used in the polymer TEM field. Patrick et al. [1996] did a study to compare the two methods for bulk polyethylene associated with the application of SAXS technique to examine the lamellar thickness of the samples prepared by these two methods. They suggested that the permanganic etching and replication method was preferred for the morphological studies in that this method would give a clearer view of morphological structures. However, in terms of lamellar spacing characterization, this method might give a value that would be a little higher than that from the SAXS examination, while the chlorosulfonation and sectioning method would give a value a little lower than that

from the SAXS determination. In their view, it would be better for lamellar spacing study using the chlorosulfonation and sectioning method but it would be preferable for morphological structure appreciation to use the permanganic etching and replication technique that is their commonly used method for miscibility study of polyethylene blends.

Hill and Puig [199?] further studied the melt miscibility of blends of octene-based LLDPE and LDPE using the same techniques, TEM and DSC, associated with application of rapid quenching. Their purpose of doing this research was to see if their previous studies on HDPE/LDPE and HDPE/LLDPE blends could be applied to understand the phase behavior of this more complex LDPE/LLDPE blend system. In fact, many researchers suggested that LLDPE was not a single component system itself [Wardhaugh and Williams, 1995; Mirabella et al, 1988; Channell et al., 1994]. If it is true that LLDPE itself can be phase-separated, then it is not surprising that blends containing LLDPE components can have multiphase behavior. Based on their experiments, Hill and Puig deduced that their previous work could be applied to explain the phase behavior of LDPE/LLDPE system with similar conclusions: there was a closed-loop phase diagram at low LLDPE composition and the phase domain size was around some microns in diameter. Two different types of LLDPE were used in their study; one was an ethylene-octene copolymer and the other had more than one branch type. However, different blends of LDPE with either one of the above LLDPE showed similar phase behavior, i.e., similar LLPS region and domain size. Accordingly, they further contended that it would be the number of branches that was of primary importance and that branch type was not of importance in determining the

extent of phase separation. They also suggested that the phase separation in melts would very likely affect the rheological properties of these blends.

Alamo et al. [1994-1999] studied the phase behavior of HDPE/LDPE blends by SANS and DSC. They claimed that their results were in conflict with those from Hill's studies. The LDPE used in their study had following branching characteristics: branch content from 2 to 3 long branches and from 12 to 16 short branches per 1,000 backbone carbon atoms. Thus, the total branch contents of the LDPE were from 14 to 19 branches per 1,000 backbone carbon atoms (Note: the branch content of LDPE used in Hill et al's studies was about 10 long branches and 16 short branches, thus 26 in total, per 1,000 carbon atoms [Hill et al, 1991]). By analyzing and accounting for the isotope effect of SANS data and combined with DSC analysis, Alamo *et al.* [1994] concluded that unlabeled HDPE/LDPE blends with $M_w \sim (1\text{-}2)\times 10^5$ would be homogeneous in the melt over the complete composition range. They believed that the segregated crystalline state detected by DSC and SANS was due to the crystallization process from homogeneous melt. They further suggested that the conflict between their results and Hill's reports was because the latter work was focused on the crystalline state. In regard to the argument that the SANS data for this study can be interpreted either as from a homogeneous melt or from a heterogeneous melt with a large domain size, around 3 μm, Londono et al. [1995] investigated the cooling rate effect on the phase separation during crystallization by SANS, SAXS and DSC. Once again, they indicated that HDPE/LDPE blends in the melt were homogeneous throughout all compositions, and the possibility of forming larger domains ~ 10^3 Å was ruled out. Furthermore, the various solid state morphologies

were not the function of the state-of-mixing in the melt but a function of composition and cooling rate from the melt instead.

As mentioned before, Schipp et al. argued that SANS technique might not be sensitive to phase separation on large domains, such as micron size. In this regard, Alamo et al. [1997] addressed their hypothesis that HDPE/LDPE blends would be homogeneous in the melt for all compositions by further studies of the blends of linear and branched polyethylene and focused on the branching effect on the miscibility of the components in the blends. In addition to two LDPE polymers as they used before, they used hydrogenated HPB as model polyethylene with different levels of branching that are essentially monodisperse model LLDPEs. They concluded based on their results that mixtures of linear and branched polyethylene would be homogeneous for all compositions when the branch content of the branched polyethylene was low, typically less than 40 branches/1,000 backbone carbon atoms when $M_w \sim 10^5$. However, linear and branched polyethylene molecules would phase separate if the branch content of the branched polyethylene was higher, typically larger than 80 branches/1,000 backbone carbon atoms. Moreover, phase segregation could be driven by isotope effects if the molecular weight of deuterated polyethylene was sufficiently high so that the product of degree of polymerization and χ between deuterated and hydrogenated species exceeds 2. The isotope effect driven phase separation could also be observed in the isotopic mixtures of the same species, say a deuterated and hydrogenated HDPE blend. They further indicated that for a LLDPE system itself with a wider range distribution of branch contents, a fraction of the highly branched molecules could phase separate from the lightly branched majority,

even when the average branch content was low, say, 10-20 branches/1,000 backbone carbon atoms. It was commented that the key would be the level of branch content that would determine the miscibility of the components in the blend systems. It is worth pointing out that the effects of long chain branching and branch content in their studies were not investigated extensively for HDPE/LDPE systems.

In order to clarify their SANS results, Agamalian et al. [1999] studied the linear and branched polyethylene blends using an ultra-small-angle neutron scattering (USANS) technique that can resolve particle dimensions up to ~30 microns as they indicated. They argued that USANS could show phase separation on micron level domains when it existed in blends of HDPE/HPB with high branch contents of HPB. However, no such evidence had been detected from HDPE/LDPE blends. Therefore, they further contended that their previous SANS results and interpretations of them would be valid; i.e., HDPE/LDPE blends were homogeneous in the melt throughout all compositions at the experimental temperature, 160 ^{0}C. Once again, it is worth noting that the LDPE samples they used had lower branch content than the ones used in Hill's work.

Crist and Hill [1997] provided an extensive review on the miscibility studies of polyolefin melt blends, especially for polyethylene blends. They indicated that more complicated systems such as blends of commercial polyethylenes could be understood by studying blends with model polymers that have uniform chemical structures and narrow molecular weight and branch content distributions. HPB model polymers are good examples. Most of the studies regarding the miscibility issue for polyolefin blends are based on the Flory-Huggins interaction parameter theory. This

approach shows its simplicity and power for expressing thermodynamic interactions in terms of a single parameter, χ. It has been pointed out that morphological investigations on this issue must be taken very carefully in order to draw a conclusion on the melt miscibility between the components in the blends based on the morphologies observed in the solid state. As mentioned before, Hill et al. developed an indirect method by using TEM and DSC to characterize the polyethylene melt morphology based on observations of quenched samples. Hill emphasized that the Ostwald ripening behavior was exhibited in her and her co-workers' previous work regarding the LLPS of polyethylene blends, thus assuring that their conclusions based on the solid state morphological studies were applicable to the liquid state.

As for SANS technique, it is very powerful in determining the melt miscibility through evaluating the thermodynamic interaction (χ) between chemically different polyolefins but this technique requires one of the components be deuterated, which may cause additional ambiguity. Therefore, isotope effect must be taken into account. In general, measurements of interaction parameter, χ, should be done twice for each set of components, once with one of the two components deuterated and once with the other component deuterated. The geometric mean of the value of χ should be taken as the reliable value without isotope effect [Mark, 1996].

In summary, extensive studies on the miscibility of polyethylene blends have been done and very useful information has been drawn from these studies as aforementioned. However, huge amount of work on the subtle structural differences and interactions which would contribute to the control of phase behavior for

polyethylene blends is still left for further studies on these complex systems. For example, it is still controversial on the topic of melt miscibility of HDPE/LDPE blends and of the critical branch content value of LLDPE for HDPE/LLDPE to phase segregate or on the miscibility of the more complex system of LLDPE/LDPE. Therefore, there is still need to construct more suitable model polymers, such as more proper model polymers for LDPE, and to develop new experimental techniques or other miscibility characterization techniques. Also, a more reasonably quantitative theory for describing the phase behavior of polyethylene blends is yet to be developed.

As mentioned in Chapter one, the molecular dynamic (MD) simulation technique has been explored and successfully applied to compute the solubility parameters of HDPE and LLDPE molecules, with which Flory-Huggins interaction parameters have been calculated to determine the miscibility between the components of blends of HDPE and LLDPE [Choi, 2000]. One of the major objectives of this thesis work is to continue utilizing, justifying and developing the MD simulation technique to predict and determine the phase behavior of various kinds of polyethylene melt blends. Other techniques, such as SEM and PLM, were also explored to characterize the phase behavior of polyethylene blends in this thesis work in addition to MD studies. Introductions to the related techniques will be given in the following appropriate chapters separately.

Chapter 3

Polymer Mixtures

3.1 Thermodynamics of Mixtures

Polymer mixtures including polymer-solvent systems and polymer-polymer systems are widely used in industry. Nowadays, over a few hundred polymer mixtures have been used to meet various kinds of requirements of processing and final product properties. It is easier and cheaper to make polymer products by blending existing polymers (or dissolving polymers in certain kind of solvents) than to produce new polymers. It is known that miscibility between components of a mixture will affect mixture melt rheology and solid state properties. In general, miscible components produce useful mixtures that are thermodynamically stable. However, thermodynamically immiscible polymer systems that are practically compatible are often utilized in many applications [Utracki, 1989]. The key is to make immiscible components compatible, which requires knowledge about the thermodynamics of mixtures.

In general, the concept of miscibility for polymer mixtures means that components of the mixtures mingle well at the segmental level. In practice, the appearance of a single T_g for the blend, intermediate between the T_gs of the pure components, is considered as a well-accepted criterion for miscibility of two

amorphous polymers. Problems arise when such a criterion is applied to semi-crystalline polymer mixtures. Even pure semi-crystalline polymers have more than one phase in the solid state, crystalline and amorphous phases. Therefore, a single T_g cannot be considered as an indication of overall homogeneity for semi-crystalline polymer blends. Nonetheless, "compatibility" is often used in industry to imply useful mixtures, which usually show synergism even if separated domains are observed. Another difficulty is regarding the domain size for the definition of miscibility. Actually, 50-100 Å inhomogeneities in polymer-polymer solutions are not uncommon and the existence of inhomogeneities at this order is not an indication of two phases. Heterogeneities at this order have been observed in amorphous single-component polymer systems, too [Geil, 1975]. In fact, as long as the mixtures do not deteriorate over long enough period of time during their application, compatibility is assumed regardless of the thermodynamic miscibility issue for practical purpose.

However, the thermodynamic conditions for miscibility applies to any mixture systems. Thermodynamic theories assume that a polymer molecule dissolves in a solvent at a certain temperature and pressure if the total Gibbs free energy change on mixing (ΔG_{mix}) is negative, i.e., the following relations must be satisfied:

$$\Delta G_{mix} = \Delta H_{mix} - T\Delta S_{mix} < 0 \qquad (3\text{-}1A)$$

$$\partial^2 \Delta G_{mix} / \partial \phi^2 > 0 \qquad (3\text{-}1B)$$

where ΔH_{mix} is the enthalpy change of the mixing process and ΔS_{mix} is the entropy change of mixing; ϕ is the volume fraction and T is the thermodynamic temperature.

3.2 Theories of Characterizing Phase Behavior of Mixtures

3.2.1 Ideal Solution

As explained before, equations (3-1A) and (3-1B) are the thermodynamic criteria for mixing. Therefore, various kinds of theories were developed to calculate the Gibbs free energy change of mixing, ΔG_{mix}, i.e., ΔH_{mix} and ΔS_{mix}. The simplest one is the ideal solution theory that assumes zero enthalpy and ideal entropy changes of mixing. Thus, in this theory, the calculation of Gibbs free energy change reduces to the calculation of the ideal entropy change of mixing based on the Boltzmann principle. For small molecules, the requirements are that all molecules have the same size or equal volume and no volume change on mixing. The entropy change for ideal solution is computed as following:

$$\Delta S_{mix} = -k_B(N_1 \ln x_1 + N_2 \ln x_2) \qquad (3\text{-}2)$$

where N_1 and N_2 are the numbers of molecules of components one and two respectively; k_B is the Boltzmann constant. x_1 and x_2 are mole fractions of components one and two, respectively.

3.2.2 Regular Solution

Although there exits solutions exhibiting ideal solution behavior, e.g. CCl_4 and cyclohexane system [Geil, 1975], most solutions' behavior deviates from the ideal solution model significantly. Therefore, more appropriate theories were required to be developed in order to characterize typical solution properties. The concept of the regular solution was first introduced by Hildebrand [Hildebrand et al., 1964] for small-molecule mixtures. One of the main assumptions of the regular solution theory

is that the ideal entropy still holds but a non-zero enthalpy part was introduced and the presence of the non-zero enthalpy was assumed not to affect the ideal entropy part. The enthalpy part was computed as the sum of total interaction energies, e,:

$$e = e_{11}/2 + e_{22}/2 - e_{12} \qquad (3\text{-}3)$$

where e_{ij} is the interaction energy between molecules i and j. Thus, e_{11} represents total interaction energy between two molecules of component 1 and e_{22} represents the total interaction energy between two molecules of component 2 while e_{12} indicates the total interaction energy between molecules 1 and 2. Providing that each site of the lattice has z neighboring sites, i.e., the coordination number, the enthalpy change of mixing can be approximated as:

$$\Delta H_{mix} = (N_1 + N_2) z e x_1 x_2 \qquad (3\text{-}4)$$

By combining equation (3-4) with equation (3-2), ΔG_{mix} can be obtained as in equation 3-1A.

3.2.3 Polymer Systems

For polymer-solvent systems, in a modified model, it is assumed that the volume of a polymer segment is the same as that of a solvent molecule. For polymer-polymer systems, a reference segment volume, which is usually the smallest one among the component polymers, is assumed. Therefore, the equations for entropy developed from small molecules may work well for polymer systems with some modifications. However, it is worth noting that the entropy change for polymer systems is much smaller than that for small molecule systems in that the possible

numbers of arrangements of polymer segments during mixing are greatly reduced because of connectivity of the segments of polymers.

Based upon an incompressible lattice model, Flory [1941; 1942] and Huggins [1941; 1942] independently obtained the expression for entropy change shown as equation (3-5).

$$\Delta S_{mix} = -k_B(N_1 \ln\phi_1 + N_2 \ln\phi_2) \qquad (3\text{-}5)$$

where ϕ_1, ϕ_2 are volume fractions of components one and two, respectively. Note that equation (3-5) is quite similar to equation (3-2) but volume fractions have replaced the mole fractions. It is worth noting that volume fraction must be used in the polymer field because the ratio of segments occupying adjacent lattice sites, not the ratios of whole molecules, determines interaction energies. It should be pointed out that, in equation (3-5), N_1 represents the number of molecules of solvent for polymer-solvent systems but it represents the number of the segments of polymer one for polymer-polymer systems. In either polymer-solvent or polymer-polymer systems, N_2 represents the total number of segments of polymer two, not the number of polymer molecules. And equation (3-5) can be used for the expression of entropy change for polymer-solvent or polymer-polymer systems with the changes of the meanings of N_1 and N_2 aforementioned.

3.3.1 The Solubility Parameter Approach

The ideal solution theory produces a very simple model while the regular solution theory provides a basic tool to characterize the phase behavior of lots of existing-mixtures. However, for practical applications in industry, more convenient

and applicable approaches are required to be developed. Among those, Hildebrand solubility parameter approach is the most popular and widely used. In this thesis, only solubility parameter is discussed. Because the Hildebrand solubility parameter approach is combined with Flory-Huggins interaction parameter approach to determine the miscibility of the blends in my MD simulation studies, the Flory-Huggins parameter theory is also introduced.

Solubility parameter approach was first introduced by Hildebrand [Hildebrand and Scott, 1964] for small molecules and extended to polymer-polymer systems by Bohn [Bohn , 1968]. The symbol δ is designated for solubility parameter and defined as the square root of cohesive energy density (CED) that is the internal energy change upon vaporization per unit volume of material [Hildebrand and Scott, 1964].

$$\delta = (CED)^{1/2} = (\Delta E_v/V)^{1/2} \qquad (3\text{-}6)$$

where ΔE_v is the vaporization energy of a material and V the molar volume of the material. The rationale for using δ to characterize miscibility of components of mixtures is that molecules with close solubility parameters (i.e., close cohesive energy densities) dissolve into each other easily. There are some exceptions, however. For example, this simple solubility parameter approach is not reliable with materials exhibiting specific interactions such as hydrogen bonding and significant volume change on mixing. A modified solubility parameter approach works better in dealing with those cases, in which a three-dimensional solubility parameter concept was introduced [Hansen, 1967].

The solubility parameter approach is appealing in that no information about a mixture is needed in order to characterize the phase behavior of the mixture. Only solubility parameters of pure components of the mixture are required for judging the miscibility between the components of the mixture.

By taking the Scatchard geometric mean assumption on the cross interaction energy term of e_{12} in the enthalpy expression of equation (3-3) and replacing molar fractions with volume fractions and using the solubility parameter concept, Hildebrand and Scott [1964] derived the following expression for ΔH_{mix}:

$$\Delta H_{mix}/V = [\delta_1-\delta_2]^2\phi_1\phi_2 \qquad (3\text{-}7)$$

It has been observed that the geometric mean assumption is reasonable for systems of small non-polar or slightly polar molecules [Olabisi et al., 1979; Kern, 1956].

3.3.2 Determination of Hildebrand Solubility Parameters

Determination of solubility parameters for small molecules is straight-forward as its definition says. Once the internal energy change of vaporization of a material is measured, its solubility parameter can be calculated according to equation (3-6). Direct determination of δ for polymers is impossible because polymers cannot be vaporized. As a result, indirect methods have been developed. One of the simplest ways is the swelling method. A polymer material for which its solubility parameter is going to be determined is lightly cross-linked and allowed to swell in various kinds of solvents having a range of solubility parameters (δ_1). The solubility parameter of the polymer (δ_2) is assigned to be the same as the solubility parameter of the solvent in which the polymer swells the most. The rationale is that when the ($\delta_1=\delta_2$) then ΔH_{mix}

is zero or minimum and $\Delta G_{mix}=-T\Delta S_{mix}<0$ so tendencies to dissolve are maximized (prevented only by the crosslinks) and, the solvent will swell the polymer to the maximum. This approach of determining δ values of polymers holds well for non-polar systems but may be not good for polar systems [Olabisi et al., 1979]. This method has been widely used in the polymer field and gives a good estimation of polymer solubility parameters. Once the data are recorded for most common polymers, one can choose certain components to make a mixture that shows desired-properties based on δ values of components.

Olabisi and Simha [1977] first developed a method for the estimation of solubility parameters for polymers based on fundamental thermodynamic consideration, i.e., the internal pressure approach. They suggested that:

$$\delta^2 = \Pi \equiv (\partial U/\partial V)_T \equiv T\alpha/\beta \qquad (3\text{-}8)$$

where Π is the internal pressure; α is the thermal expansion coefficient and β the compressibility. By measuring α and β, one can estimate solubility parameters through equation (3-8). This method can then estimate temperature dependence of solubility parameters [Olabisi et al., 1979]. Recently, It has been reported that Π was computed by using molecular dynamics simulations [Janna et al., 1998 and Londono et al., 1998]. However, a proper equation of state must be known in order to evaluate the temperature and pressure dependence of δ.

The MD simulation is another approach to compute δ that is a theoretical method based on statistical thermodynamics and computer simulations. It has been successfully applied to compute δ of polyethylene molecules [Choi, 1995]. Although the internal energy change of vaporization cannot be measured for polymers, which

makes direct measurement of solubility parameters for polymers impossible, it could be computed by computer simulations. Molecular dynamics and computer simulations will be discussed in detail in Chapter 4. Here, only the idea of how to calculate the internal energy change of vaporization is introduced. By modeling the molecular motion due to inter- and intra-molecular forces, the total energy of a molecular system can be calculated at a certain temperature and pressure when the system is in equilibrium. Therefore, by simulating a molecular system both in random condensed state (liquid state) and in vacuum (equivalent to in the gas state, i.e. there are no intermolecular interactions between molecules), the internal energy change of vaporization can be estimated as the difference of the total energies of the system in vacuum and in condensed state. However, only very simple molecular systems can be simulated due to the limited computation resources. Therefore, effects such as molecular weight, molecular weight distribution and branch distribution, etc. are still not practical to study by this approach.

3.3.3 The Flory-Huggins Interaction Parameter

As mentioned previously, Flory and Huggins independently modified the entropy part for polymer systems using a lattice model and pure statistical calculation on the entropy of chain molecules. Therefore, it is called Flory-Huggins approach or Lattice Model approach. A few assumptions were made. It was assumed that there is no volume change on mixing and no vacant site in the lattice is allowed, i.e., all sites are taken by either a solvent molecule or a polymer segment. In addition, a spatially uniform polymer concentration in solutions was assumed. Based on the lattice model

and above assumptions, they derived the expression for ΔG_{mix}. For the treatment of the enthalpy part, they suggested a new dimensionless parameter, χ_{12}, called Flory-Huggins interaction parameter, to characterize the enthalpy part in the Gibbs free energy change expression. χ_{12} is defined as:

$$\chi_{12} = ze/kT \qquad (3\text{-}9)$$

where z is the coordination number as before and e is the total interaction energy change of mixing given by equation (3-3). The subscripts in χ_{12} indicate components one and two in a binary mixture. It can be seen that χ_{12} is a dimensionless quantity from its definition.

Therefore, the Gibbs free energy change of mixing can be written in terms of R (=k_BA) as follows:

$$\Delta G_{mix} = kT[N_1 \ln\phi_1 + N_2 \ln\phi_2 + \chi_{12}(N_1 + N_2)\,\phi_1\phi_2] \qquad (3\text{-}10)$$

If using number of moles (n_i) instead of number of molecules (N_i) in the above equations ($n_i = N_i/A$, A is the Avogadro's constant), the above equations can be rewritten as follows:

$$\Delta H_{mix} = RT\chi_{12}(n_1 + n_2)\,\phi_1\phi_2 \qquad (3\text{-}11)$$

$$\Delta S_{mix} = -R[n_1 \ln\phi_1 + n_2 \ln\phi_2] \qquad (3\text{-}12)$$

Note that, in equation (3-10), the first two terms (the entropy contribution to mixing) in the bracket are always negative because volume fractions are less than unity and the sign of the third term (enthalpy contribution to mixing) depends on the sign of the Flory-Huggins interaction parameter. χ_{12} can be positive or negative in nature depending on the characteristics of the interactions between solvents and segments of

polymers or between polymer-polymer segments. In favor of miscibility, the value of χ_{12} must be negative or, if positive, small enough in order to have a negative ΔG_{mix}.

Equation (3-9) predicts that χ_{12} decreases with increasing temperature. Based on equation (3-10), increasing molecular weight of polymer components of a mixture at fixed ϕ_2 will decrease the total number of polymer molecules, N_2, while keeping other variables constant. Therefore, it will reduce the negative entropic term and result in a less negative Gibbs free energy change, indicating that higher-molecular-weight polymers are more difficult to dissolve in solvents or other polymers than are lower-molecular-weight polymers. However, the behavior of non-1/T dependence of χ has been observed for many polymer mixtures and it is believed that χ should include enthalpy and entropy contributions [Olabisi et al., 1979]. Therefore, many theories were developed to account for the entropy contribution. Lattice cluster theory (LCT) has been developed and applied to polyolefin blend miscibility study quite recently to describe the monomer structures, nonrandom mixing and blend compressibility, explicitly to overcome the drawbacks imbedded in the Flory-Huggins lattice model [Freed and Dudowicz, 1998; Foreman and Freed, 1997 (1), (2); Dudowicz and Freed, 1996]. Inevitably, the expression for ΔG_{mix} in (LCT) becomes much more complex to get these significant advances.

When combining equation (3-11) with equation (3-7), one can obtain the following useful expression:

$$\chi_{12} = V_s [\delta_1 - \delta_2]^2 / RT \qquad (3\text{-}13)$$

where $V_s = V/(n_1 + n_2)$ is the molar volume of the solvent for polymer-solvent mixtures or the molar volume of the smallest polymer segment for polymer-polymer mixtures. In this expression for V_s, n_1 is the number of moles of the solvent while n_2 is the number of moles of polymer segments for polymer-solvent systems, not the number of moles of the polymer molecules and usually not the number of moles of the polymer repeat unit. For polymer-polymer systems, n_1 and n_2 represent the number of moles of the segments of polymer one and polymer two, respectively. By using this simple expression, χ_{12} can be calculated from individual solubility parameters of the pure components without appealing to the simulations of the blends, which saves much computation work. In addition, this approach can have the non-1/T temperature dependence of χ_{12} because in this approach, χ_{12} is calculated through δ that has non-1/T temperature dependence. In fact, polyethylene blends did show complicated temperature dependence of χ_{12} that is calculated from solubility parameters computed from my MD simulation work. It has been validated both experimentally and theoretically for non-polar systems [Olabisi, 1979; Schweizer, 1997]. Equation (3-13) has been utilized through all my MD simulation studies on various kinds of polyethylene blends discussed later in this thesis.

Because χ_{12} is always positive in this approach as described in Equation (3-13), the smaller χ_{12}, the more miscible or compatible the components. For polymer blends, the critical value of $\chi_{12,\,critical}$ for the components to phase-separate is rather small and close to zero in many cases. In polyethylene blends, the χ_{12} values of linear and branched polyethylene blends are usually larger when the branch content of branched polyethylene is larger, which will be discussed in Chapter 5.

Chapter 4

Molecular Dynamics Simulation

4.1 Introduction to Statistical Mechanics and Molecular Simulation

With the advent of modern experimental techniques, researchers have been able to draw more and more information of systems at the molecular level. The most important information of a molecular system in statistical mechanics is its energy levels. Once energy levels and distributions are known, the total energy of the system can be calculated using statistical mechanical theories. This, in turn, can be used to derive many thermodynamic properties. The total energy of a molecular system (including kinetic and potential energies of the motions and interactions of the molecules) is referred to as the internal energy of the system. The kinetic energy is determined by individual molecular velocities. Contrary to the kinetic energy, potential energy is not a property of a single molecule; rather, it is a property of the collection of molecules representing the whole system. Molecules interact with each other and the molecular interaction gives rise to most of the important macroscopic behavior, like phase equilibrium. The knowledge of molecular interactions is the key to understanding of the quantitative thermodynamic behavior of a real system.

Usually, the possible energy states of a molecular system can be calculated from the solution of the Schrödinger equation, i.e., so-called "ab initio" calculation in quantum mechanics:

$$H\psi = E\psi \qquad (4\text{-}1)$$

where H is the Hamiltonian operator and the wave function ψ is the eigenfunction of H corresponding to the eigenvalue E that is the total energy of the system, representing the different energy levels of the microstates of the system. Eigenvalues of energy play an important role in statistical ensemble theory.

However, these kinds of solutions are rarely available or practical for a real system. Thus, in order to get molecular information (microstate energies) of a system, one needs a molecular model or molecular theory. The molecular model provides us the necessary equivalent information representing the real system. Once the model is set up, one can use statistical thermodynamics to relate the thermodynamic properties with microstate information through statistical mechanics ensemble theory. The molecular information about the system is contained in the so-called partition function that gives us the energy distribution of a system and will be discussed later. However, the microstate energy levels are usually not available for most systems except for very simple cases due to our inability to solve the Schrödinger equation. Most of the time, the energy levels are evaluated numerically through applied statistical thermodynamics. The calculation of thermodynamic properties within technical accuracy by molecular simulation becomes possible nowadays because of the availability of high-speed computers.

A microstate can be defined in terms of fixed values of the position and momentum coordinates of all atoms in the whole system. However, due to Brownian motions, the system can be in many different microstates when macroscopic

properties are fixed. Therefore, any macroscopic thermodynamic properties are the result of averaging vast numbers of microstates over the period of observation.

Unfortunately, there is no well-accepted theory that allows accurate evaluation of expressions for the thermodynamic properties in terms of an intermolecular force model for condensed state. The only available method for essentially accurate evaluation for that is provided by molecular simulations based on a specific molecular model, i.e. force-field-based computer simulation.

In general, macroscopic thermodynamic properties can be defined as the time average for the system in each microstate over a long enough period of time. Therefore, any thermodynamic property, Z, can be estimated as the average value of observed values over the period of time, t. Thus, the following expression holds:

$$Z = \langle Z \rangle_t = \lim 1/t \sum_i Z(t_i) \quad t \to \infty \tag{4-2}$$

If the time interval for observation is very small and the number of the time intervals is huge (in another word, the total time of observation, T, approaches infinity), the sum can be replaced by an integral, that is:

$$Z = \langle Z \rangle = \lim_{T \to \infty} 1 / T \int_0^T Z(t)\, dt \tag{4-3}$$

In statistical thermodynamics, the ensemble average, not the time average of a property, is taken as the macroscopic thermodynamic property. However, the time average is assumed to be equal to ensemble average in statistical mechanics.

Statistical thermodynamics takes ensembles of molecular systems containing enormous amount of molecules, typically on the order of 10^{23}. Therefore, it is not

feasible to simulate such systems by a computer so far due to the limited computing resources. However, if a sampling system containing a few hundred or thousand molecules (or atoms) is properly chosen, suitable molecular simulation can be done on such a small sampling system over a reasonable time period within technical accuracy. Essentially, there are two molecular simulation approaches. One method is referred to as molecular dynamics simulation while the other is referred to as Monte Carlo (MC) simulation.

In MC simulation, a molecule is chosen at random from the total of N molecules in the system. Then by defining a displacement length based on molecular information, another molecule is found adjacent to the first one and so on until all molecules are arranged. Thus, this is one of the possible microstates (configurations) for such a system at specified temperature and volume (NVT ensemble). Then another state is created at random according to the same rule and another and so on. By collecting all the configurations created, one can choose a suitable integral method and do an ensemble average to get the macroscopic thermodynamic property. The starting configuration usually is not consistent with the specified constraints, such as temperature and density. Thus, initial MC simulation run is required until equilibrium of the system is reached. This is called the equilibration process. The equilibration ends when energy and pressure start to fluctuate around steady mean values. In order to get the consistent ensemble averages, about 10^6 configurations should be created for a complete MC simulation.

In MD simulation, microscopic evolution of the molecular system with time is traced and recorded. By creating an initial structure of the system (configuration), i.e.,

specifying the momenta and positions of all atoms in the system, then find the next structure (configuration) by solving Newton's equation of motion to obtain changes occurring during the next time step and so on. The MD simulation will run until the equilibrium is reached, i.e. all thermodynamic properties start to fluctuate randomly around certain steady mean values as in MC simulations.

As defined previously, an ensemble is a collection of a large number of systems (microstates) having the same observed macrostate. If the system is defined macroscopically in terms of N, V, T, the ensemble is called the canonical ensemble, corresponding to a closed system. If the system is defined in terms of N, V, E (E is the total energy of the system), it is called the microcanonical ensemble, indicating an isolated system. If the system has fixed values of V, T, and chemical potential, denoted as μ, it is called grand canonical ensemble, representing an open system.

In practice, averages over a series of microstates as the result of the evolution of the system with time are often used instead of ensemble averages as is MD. Therefore, ergodicity must be assumed. In statistical thermodynamics, we always study systems in equilibrium. Therefore, an ensemble being studied is usually a stationary one. Thus, the ensemble average of any thermodynamic property should be independent of time. Accordingly, the ensemble average must be the same as the time average. This is the so-called ergodicity hypothesis [Lucas, 1991] in statistical mechanics.

The microstate of a given system can be described by specifying the positions and momenta of all the particles (atoms for example) in the system at time t. Each particle requires 3 position coordinates and 3 momentum coordinates to be specified.

If the system contains N particles, then we need 6N coordinates to describe completely the system at time t. Therefore, the system constitutes a 6N dimensional space and it is referred to as a phase space. Each of the particles with given position coordinates and momentum coordinates constitutes a point in the space, called a phase point. It is clear that the coordinates will change with time. Therefore, the next positions and momenta of the particles of the system can be found by solving the equations of motion, usually in the form of the Hamiltonian. In statistical mechanics, it is not convenient to use Newton's equation of motion in terms of force:

$$\mathbf{F} = d\mathbf{p}/dt \qquad (4\text{-}4)$$

where $\mathbf{p}$ is the momentum in the form of a vector. Instead, it is more convenient to use the canonical type of equation of motion in terms of the Hamiltonian that is the total energy of the system:

$$\mathbf{q} = \partial H(\mathbf{q}, \mathbf{p}) / \partial \mathbf{p} \qquad (4\text{-}5a)$$

$$\mathbf{p} = -\partial H(\mathbf{q}, \mathbf{p}) / \partial \mathbf{q} \qquad (4\text{-}5b)$$

where $\mathbf{q}$ is the position coordinate in the form of a vector. It is understood that $\mathbf{q}$ contains 3N position coordinates and $\mathbf{p}$ contains 3N momentum coordinates in a phase space containing N particles.

Strictly speaking, it is not proper to define a given macro system in terms of microstates specified by the position and momentum coordinates of all particles in the system simultaneously according to Heisenberg's uncertainty principle. Quantum effects have to be taken into account in describing the molecular world. However, in classical statistical mechanics, quantum effects are not considered explicitly. Firstly, because statistical mechanics calculations are force-field based and require a

molecular model that collects all the necessary information about the molecular system and lumps it together and simplifies the actual problems. A force field is the collection of expressions and parameters that are used to describe molecular systems. Therefore, quantum effects have been taken into account when the expressions of the force field are set up or the parameters are experimentally determined. Secondly, if the systems dealt with are at high temperatures, far above zero K, the quantum effect is usually negligible. Thus, the system can be treated as a continuous phase space at high temperatures.

4.2 Force-Field

As mentioned before, molecular dynamics is the force-field based computational method. In order to carry out the molecular dynamics computations, a proper force-field is firstly required to be chosen. The core of a force-field-based computational simulation is the calculation of the potential energy of the system for a specified configuration of atoms. A force-field is the collection of expressions of the potential energy and the parameters required in the expressions. The potential energy is characterized by intra- and inter-molecular interactions that have additive contributions from bonded (E_b) and non-bonded (E_{nb}) interactions:

$$E = E_b + E_{nb} \qquad (4\text{-}6)$$

Usually, the expressions are partly derived based on ab initio calculations that have quantum mechanics basis. The parameters in the expressions are both experimentally determined and through ab initio calculations and therefore, the quantum effect has been incorporated in these expressions as mentioned in previous

section. Basically, there are three categories of force-fields. First category of force-fields was developed on the purpose of being very generic so that these force-fields can cover as many as possible atom types and combinations of them. UFF (universal force-field) [Rappé et al., 1992] and DREIDING [Mayo et al., 1990] are only two examples of them. This category of force-fields is usually expected to produce only approximately correct predictions of molecular structures due to the generic parameterization. The second category of force-fields was developed on the purpose of improving the quality of the prediction in a relatively focused area of applications, especially in biochemistry field. Examples of these force-fields are new versions of CHARM [Mackerell et al., 1995], AMBER [Cornell et al. (1), 1995; Cornell et al. (2), 1996] and OPLS/AMBER [Jorgensen et al., 1996]. Similar to first category, these force-fields still use simple functions in potential energy expressions but parameterization is more precise. Another category belongs to high-precision prediction of various molecular properties with relatively large coverage of atom types. Unlike the above two categories, complicated potential expressions and high-order force constants are utilized in these force-fields in order to achieve the high accuracy of prediction of molecular properties. As a result, more powerful computation resources are required for this type of force-field-based simulations. Examples are CFF93 [Hwang et al., 1994; Maple et al, 1994; Peng et al., 1997], MMFF [Halgren (1), 1996; Halgren (2), 1996; Halgren and Nachbar, 1996] and COMPASS [Sun and Rigby, 1997; Rigby et al., 1997; Sun, 1998]. The parameterization of these force-fields is based on high quality experimental data and/or quantum mechanics ab initio calculations.

In MD simulations, one must carefully choose appropriate force-fields based on one's interests in the specific molecular systems and properties to be studied. Meanwhile, considerations of available computation resources have to be taken and sometimes, accuracy and computation time have to be compromised. Since I am mainly concerned about the non-bonded interactions between different polyethylene molecules and segments that only contain carbon and hydrogen atoms, it is natural that a simple force-field is preferred. In addition, the major task in my simulations is the calculation of the difference of solubility parameters. Thus, seeking the accuracy of the absolute values of individual solubility parameters is not my target in this thesis work. Therefore, for the energy minimization and MD simulations in this work, a generic force field, DREIDING 2.21, developed by Mayo et al. [1990], was adopted because of its simplicity and the availability of united-atom model parameters. This can meet my needs for computing hundreds of solubility parameters for different polyethylene molecules at different temperatures within reasonable computational time.

In the DREIDING force-field, the total potential energy of a system is expressed straightforwardly in equation (4-6). Bonded interactions include bond stretching (E_S), bond angle bending (E_A), torsion angle rotations (E_T) and four-body central inversion (E_{INV}). Non-bonded interactions include dispersion (van der Waals, E_{vdw}), electrostatic interaction (E_{elec}) and hydrogen bond (E_{hb}). Therefore, the total potential energy can be described as:

$$E = E_S + E_A + E_T + E_{INV} + E_{vdw} + E_{elec} + E_{hb} \qquad (4\text{-}7)$$

There are many different forms and parameters to express individual interactions in various force-fields. In the DREIDING force-field, the bond stretching energy is described as a simple harmonic oscillator:

$$E_S = 1/2K_S(R-R_o)^2 \qquad (4\text{-}8)$$

where R is the stretched bond length and R_o is the equilibrium bond length while K_S is a force constant. Bond angle bending interaction is described by a harmonic cosine form:

$$E_A = (1/2)K_A(\cos\theta - \cos\theta_o)^2 \qquad (4\text{-}9)$$

where θ and θ_o are instantaneous bond angle and equilibrium bond angle respectively, and K_A is a constant. Torsional angle rotation is a type of motion wherein two bonds rotate around a common bond. It takes the form:

$$E_T = (1/2)K_T\{1-\cos[n(\phi-\phi_o)]\} \qquad (4\text{-}10)$$

where ϕ and ϕ_o are dihedral (torsion) angle and equilibrium torsional angle respectively; n is the periodicity (an integer) while K_T is a constant related to rotation energy barrier. Inversion describes a four-body tetrahedral central interaction (out-of-plane) potential and takes the spectroscopic form:

$$E_{INV} = 1/K_{INV}(\Psi-\Psi_o)^2 \qquad (4\text{-}11)$$

where Ψ is the plane angle and Ψ_o is defined as zero for a planar molecule while K_{INV} is a constant.

van der Waals interactions are described by a Lennard-Jones 12-6 potential:

$$E_{vdw} = D_o[(R_o/R)^{12} - 2(R_o/R)^6] \qquad (4\text{-}12)$$

where R is the van der Waals interaction distance and R_o is the van der Waals bond length or equilibrium intermolecular distance. D_o is the van der Waals energy well depth. Electrostatic interactions are described by using the Coulombic form:

$$E_{elec} = 332.0637 Q_i Q_j / \varepsilon R_{ij} \qquad (4\text{-}13)$$

where Q_i and Q_j are atomic charges; R_{ij} is the distance between the two charges and ε is the dielectric constant. The hydrogen bond is described by a special form of Lennard-Jones 12-10 potential:

$$E_{hb} = D_{hb}[5(R_{hb}/R_{DA})^{12} - 6(R_{hb}/R_{DA})^{10}]\cos^4(\theta_{DHA}) \qquad (4\text{-}14)$$

where R_{DA} is the distance between atoms of hydrogen bonding donor and acceptor while θ_{DHA} is the bond angle between atoms of hydrogen bonding donor, hydrogen atom and the hydrogen bonding acceptor. D_{hb} is the hydrogen bond length.

The corresponding Lennard-Jones parameters for van der Waals potential, estimated from lattice spacing and heat of sublimation measurements for low molecular weight hydrocarbons, are shown in Table 4-1. Equilibrium bond length (R_o) and energy well depth (D_o) used were 1.53 Å and 2,930 kJ/mole, respectively, for all carbon-carbon bonds. Detailed descriptions of DREIDING force field are given in the reference [Mayo et al., 1990].

Table 4-1 Lennard-Jones Parameters for van der Waals Potential

United Atom Group	R_o, nm	D_o, kJ/mol
CH	0.3983	0.615
CH_2	0.4068	0.829
CH_3	0.4152	1.047

Here, non-bonded interactions computed in the simulations include inter- and intra-molecular interactions. The original parameterization of the DREIDING force-field in the Cerius2 MD simulation engine has been utilized throughout the MD simulation works in this thesis. (Regarding the details of the DREIDING force-field, see [Mayo et al., 1990]. DREIDING 2.21 is the most updated DREIDING force-field [MSI, 1997].)

I am aware that more accurate force-fields have been developed [Laso et al., 1992; de Pablo et al., 1992], one of which is called NERD force-field and has been successfully applied to olefins to study the phase equilibria quite recently [Nath et al., 2001].

4.3 Nosé Formalism for NVT Canonical Ensemble Dynamics

As mentioned before, molecular dynamics studies the evolution of a molecular system with time. In order to achieve this, a trajectory file needs to be created when an MD run is completed. A trajectory is a set of records of position and velocity coordinates of a molecular system for a whole MD simulation run. In MD simulations, trajectory files are obtained by solving Newton's equation of motion step by step. At the beginning of an MD simulation, the initial position coordinates are determined by a Monte Carlo method subjected to density and conformational constraints. An energy minimization step is preformed and the initial velocity coordinates are assigned based on the Boltzmann principle at the simulation temperature before an MD run. Thus, MD simulations cannot be repeated exactly because of the random selection of the initial position coordinates and velocity

coordinates. However, MD run results should not depend on the initial condition although no identical trajectories can be generated. This is assured by appropriate selection of the initial configurations of the molecules (or atoms) and their momenta. This includes proper construction of molecular models and suitable energy minimization. If this is done correctly, the energy (energies) of the modeled system at equilibrium for each MD run should keep at the same level regardless of the difference of trajectories.

Once the initial condition is selected, the position and velocity coordinates of the next time step can be calculated using a numerical method (called an integrator in MD simulation engines) according to the present position and velocity coordinates. In the Cerius2 MD simulation engine, the Verlet leapfrog integrator is used [Verlet, 1967]. This method requires only one energy evaluation at each step and requires only modest memory and also permits large timestep applications. However, if the timestep is too large, instability and inaccuracy will occur in the integration process. In my simulation work, a small timestep of 1 femtosecond (fs) is used to assure the smoothness of MD trajectories.

There are many statistical ensembles that can be used in MD simulations [MSI, 1997; Lucas, 1991; Pathria, 1972; McQuarrie, 1976]. In particular, the constant-number of particles, constant-temperature and constant-volume (NVT) ensemble (also called canonical ensemble) is used in my MD simulations. By using the NVT ensemble, the densities (N/V) of the simulated systems can be easily controlled at the experimental values. It was reported that an NPT ensemble approach would be slightly worse than an NVT approach in predicting solubility

parameter [Sun and Rigby, 1997]. More accurately speaking, the term of constant-temperature is misleading and should be replaced by controlled-temperature. Because direct temperature scaling suppresses the natural fluctuations of a modeled system, it cannot generate realistic thermodynamic ensembles. In order to produce real canonical ensembles, Nosé developed a controlled-temperature dynamics method [Nosé, 1984]. The central theme of Nosé formalism is that an additional term is put into the original equation of motion to balance the heat bath with the system. In Nosé dynamics, the smaller the timestep, the closer it reaches the controlled temperature.

4.4 MD Simulations for Condensed State

As discussed before, limited by today's computation resources, only very small molecular systems compared with a real molecular system (a typical molecular system contains a number of molecules at the order of 10^{23}) can be studied by MD simulations. In general, a system containing hundreds to thousands of atoms is typical in molecular simulations. Such a small system imposes a problem of surface effects when bulk materials properties at condensed state are of interest. In such a small system, a large part of molecules would undergo interactions with the boundaries of the system and thus, the simulation could not represent a small volume element in the bulk of a liquid. To remove this surface effect, the condensed state of molecular systems is modeled with the use of a cubic unit cell subject to periodic boundary conditions [Allen and Tildesley, 1987; Colbourn, 1994]. Figure 4-1 shows the idea of periodic boundary condition. The central unit cell (called the primary cell) is surrounded by its replicas (called image cells). The position and velocity coordinates

of molecules in the image cells are identical to the ones in the primary cell. When simulation proceeds, the molecules leaving the primary cell will be replaced by its images. No boundary exists between each pair of cells. This method of eliminating the surface effect is called the periodic boundary condition.

Figure 4-1 Primary Cell and Image Cells Under Periodic Boundary Conditions

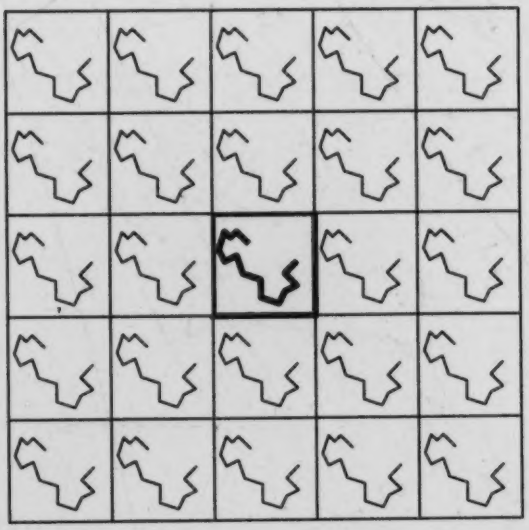

4.5 Model Construction

In the MD simulations, I first constructed a desired model for polyethylene molecules according to research interest. Extreme care has to be taken in order to build up an appropriate model. Factors such as bond length, bond angle, and proper connections of the atoms, etc, should be carefully examined. Then, an amorphous state (initial structure) of the molecule under periodic boundary condition was generated based on interdependent rotational isomeric states (RIS) method [Flory, 1988] at a given temperature and density with a Monte Carlo method built into the Cerius2 simulation engine. Torsion is a bonded interaction of substituted groups rotating around a central bond of the backbones. There are three most important features (minima) in the rotational potential curve for n-butane, the simplest molecule for the explanation of rotational isomeric state conformations. One is the trans (at 180^{o} or 0^{o}) and the other two gauche (at about $\pm 120^{o}$ or $\pm 60^{o}$) conformations. In RIS theory, each molecule, or bond is assumed to occur in one of these three discrete rotational isometric states associated with rotational potential minima, and dynamic possibilities about the minima are ignored [Flory, 1969].

For polymers, because of the long chain and branches (the substituted groups), the trans and gauche conformations will be perturbed relative to butane case. Rotational isomeric state can also be affected by temperature and microstructure difference in terms of branch content of branched polyethylenes.

In these simulations, each cubic unit cell (the periodic boundary box in Figure 4-2) contained a single molecule and the cell was constructed in a way that its density would match with the experimental value (see Table 5-2 for experimental density

values of polyethylenes at different temperatures). Figure 4-2 depicts the initial structures created in this way for the MD simulations. The density values at the chosen simulation temperatures would be determined based upon an empirical correlation [Rudin et al., 1970]. Usually, the initial structures generated in this way are at high-energy level. Therefore, all initial structures created in my MD simulations were energy-minimized using the conjugate gradient method built into the Cerius2 simulation engine before the MD simulations were begun.

In the MD simulations for the studies of miscibility of polyethylene blends, I constructed polyethylene molecules by polymerizing 500 ethylene monomers to give 1,000 carbon atoms on the main chain for each of all HDPE and LLDPE models. For LDPE, I used a main chain (strictly speaking, there is no main chain in LDPE molecules) with 500 carbon atoms, and two long branches with 200 and 300 carbon atoms respectively. Therefore, the total number of carbons on the long chains in each LDPE model is 1,000, which makes the molecular weight of LDPE models equivalent to corresponding HDPE and LLDPE models. The short-branches on branched polyethylenes were assigned and attached randomly to the long chain atoms according to the branch content of interest. Every effort has been made to construct the models to be realistic representatives of their corresponding commercial products.

Figure 4-2 An amorphous HDPE molecular model in condensed state, generated as an initial structure in the MD simulations

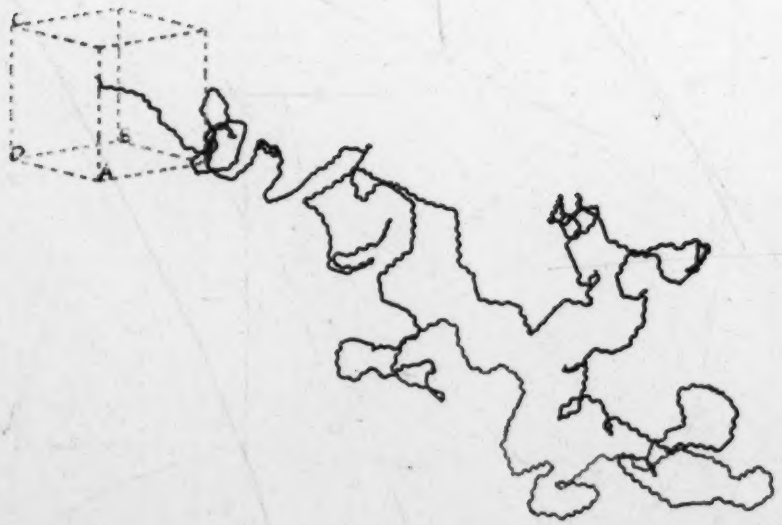

Simulation time was 1,000 pico-seconds (1ps=10^{-12} s) with a time step of 1 fs (10^{-15} s). During the MD simulation progress, data such as energy, pressure, etc., for every 1,000 fs were collected and recorded in the trajectories. Energy and pressure of the NVT ensemble for each MD job were monitored frequently. All simulations have shown that the total energy was leveling off within the last few hundred pico-seconds in the MD annealing, signifying that the systems have reached thermodynamic equilibrium. In theory, 1,000 pico-seconds should not be long enough to get these large molecules fully relaxed. In this regard, I have repeated some of the calculations with different initial structures for the same molecular models and found that they all reached approximately the same energy level. In addition, I have checked and energy-minimized all the initial structures very carefully. Therefore, it is believed that the system should be close to equilibrium. Figure 4-3 describes a total energy MD simulation profile for a hexene-based LLDPE model (HLLDPE) simulated at 475 K and Figure 4-4 shows the profile for a LDPE model at 475 K.

Here, the vaporized state of polyethylene molecules was simulated by putting the amorphous state molecules in the vacuum without periodic boundary conditions and density constraint at chosen temperatures. It is worth noting that the vaporized state of polyethylene molecules is completely imaginary because polymer molecules cannot be vaporized in practice. This is the power of computer simulations, which can provide information that cannot be normally obtained experimentally. This advantage of computer simulation balances its drawbacks of being criticized for being unreal compared with experimental methods.

Figure 4-3 A total energy MD simulation profile for an HLLDPE model

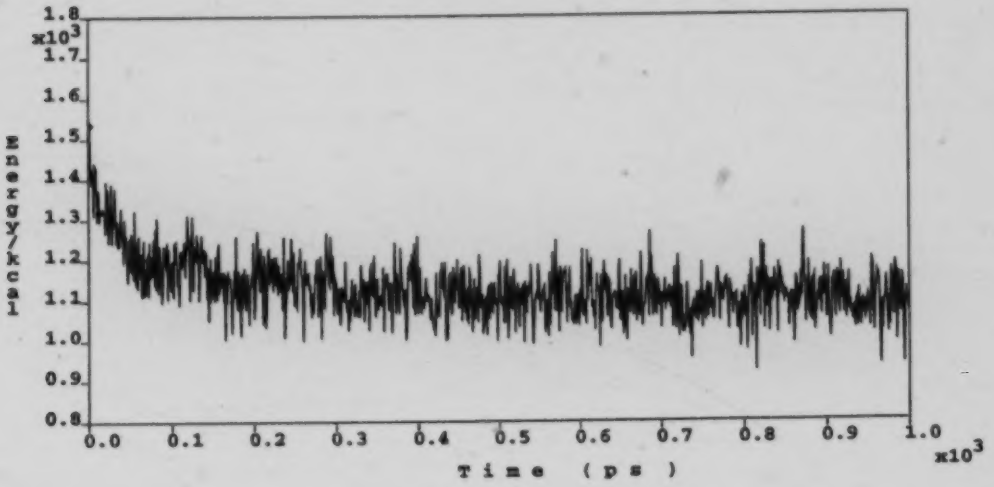

Figure 4-4 A total energy MD simulation profile for a LDPE model

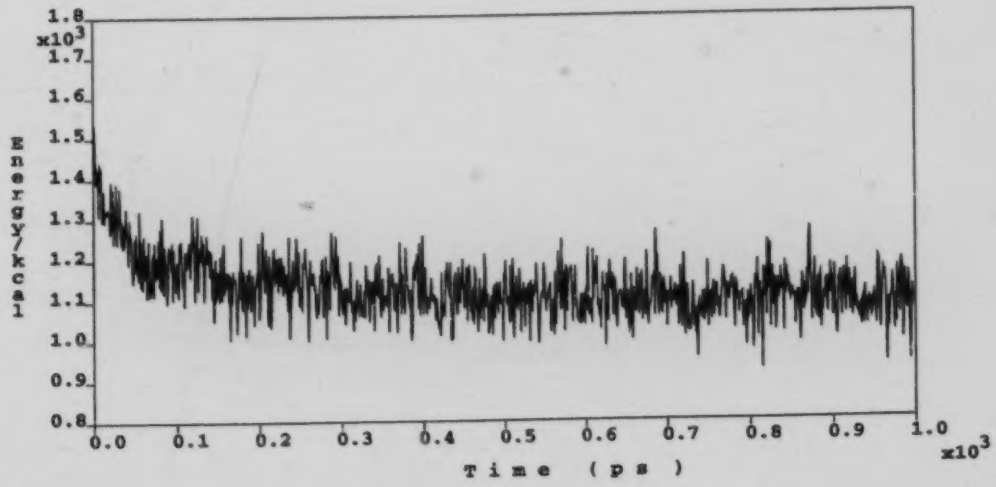

Once the MD trajectories were successfully generated, the total energy values of the molecules in vacuum states and condensed states, for every 10 pico-seconds in the last 100 pico-seconds of the MD annealing, were taken and averaged to get the E_{vac} and E_{cond}, separately. Here, E_{vac} and E_{cond} are the total energy of the molecular system of interest in vacuum and condensed state (i.e., melt state), respectively. The maximum standard deviation of the E_{vac} and E_{cond} values was less than 5% of the average values. In turn, E_{vac} and E_{cond} were used to calculate the solubility parameter of the molecular system.

Molecular dynamics simulations were run by using a commercial software package, Cerius2, version 3.5 and 4.0, developed by Molecular Simulations Incorporated (MSI) of San Diego, CA. All the computer simulations were carried out on a Silicon Graphics Octane workstation with two processors, produced by Silicon Graphics Incorporated (SGI) of Mountain View, CA.

4.6 Comparison of DREIDING and COMPASS Force-fields

As mentioned before, the DREIDING force-field is a generic force-field. In order to justify the use of this simple force-field, I carried out a few MD simulations only for the sake of comparison with the DREIDING force-field by using a more accurate force-field, COMPASS (condensed-phase optimized molecular potentials for atomistic simulation studies), developed quite recently, and built-in Cerius2 MD simulation engine. COMPASS force-field is designed for organic molecules and polymers in the condensed state [Sun, 1998; Sun and Rigby, 1997; Rigby et al., 1997; Sun et al., 1998]. It is believed that the COMPASS force-field is the most accurate

one to reproduce P-V-T behavior for polymer melts so far. Because COMPASS force-field requires explicit hydrogen atoms, the number of atoms in these molecular models had to be reduced. I ran MD simulations for HDPE and butene-based as well as hexene-based LLDPE using both COMPASS and the DREIDING 2.21 force-fields. In COMPASS-based simulations, I built up LLDPE models by using 100 backbone carbon atoms and attached 5 branches randomly on the backbone carbon atoms. The number of carbons in all branches is 2 for butene-based linear low-density polyethylene (BLLDPE) and 4 for hexene-based linear low-density polyethylene (HLLDPE), respectively. These models are equivalent to those having 1,000 backbone carbon atoms with 50 branches that were used in the DREIDING2.21-based simulations. (All the hydrogen atoms in these models were explicitly incorporated in COMPASS-based simulations. However, considering the large size of the modeling systems, it is not practical to mimic the systems with explicit hydrogen atoms in DREIDING-based computations. As a result, a united-atom model that incorporates implicitly all hydrogen atoms into their corresponding carbon atoms was employed to reduce computation efforts in all DREIDING-based simulations throughout the thesis work. The validity of the united-atom model in predicting the phase behavior of polyolefin blends has been confirmed although different approaches were adopted in characterizing the phase behavior of polyolefin blends [Dudowicz and Freed; 1996, Foreman and Freed, 1997; Luettmer-Strathmamm and Lipson, 1999].

The MD simulations for this particular interest were carried out at two temperatures, 425 and 525 K separately. As mentioned in the last chapter, I am targeting the difference of solubility parameters of different polyethylenes, $(\delta_1 - \delta_2)$,

as expressed in equation (3-13) instead of the absolute values of individual solubility parameters. Thus, I will compare the results of computed $(\delta_1-\delta_2)$ when using the two different force-fields. Please refer to the following related sections and chapters for details of running MD simulations and computing $(\delta_1-\delta_2)$. Here, results are presented in Table 4-2. Attention should be paid not only to the absolute value of the computed individual solubility parameters but also to the difference of the computed solubility parameters by these two different types of force-fields.

From Table 4-2, it can be seen that the values of solubility parameters computed by using these two force-fields vary significantly. Note that there is no experimental method to measure the absolute values of solubility parameters for polymers exactly so far, as discussed in chapters 2 and 3. Recently, solubility parameters of various polyethylenes in the melt state have been measured by Pressure-Volume-Temperature (P-V-T) experiments [Han et al., 1999] and data from their work is listed in Table 5-8A. The computed differences of solubility parameters of different polyethylenes $(\delta_1-\delta_2)$ also vary significantly by using these two force-fields in my simulation results. However, it seems that the differences of δ using COMPASS simulations are bigger than those using DREIDING systematically. Remember that I am trying to capture the trend of the dependence of Flory-Huggins interaction parameters, χ, i.e. $(\delta_1-\delta_2)$, on branch content and temperature. Therefore, I positively think that this systematic shift of $(\delta_1-\delta_2)$ would not affect the results of the studies of interests. Furthermore, considering the computation time, it is not feasible to use COMPASS for my purpose. It takes about 9 days (24 hour/day) to run one MD simulation for only one solubility parameter calculation using COMPASS compared

with about 30 hours for each solubility parameter computation using DREIDING. These results justify using DREIDING2.21 force-field with technical accuracy throughout the MD simulations. In fact, it can be seen that the computed δ values using DREIDING force-field provide a good match with those from the P-V-T experimental measurement (see Table 5-8A).

Table 4-2 Computed Hildebrand Solubility Parameters, $(MPa)^{1/2}$,
Using COMPASS and DREIDING Force-Fields
for Model Blends of HDPE and LLDPE

T=425 K	COMPASS	DREIDING
δ_{HDPE}	15.7 ± 0.2	18.5 ± 0.1
δ_{BLLDPE}	14.0 ± 0.2	17.4 ± 0.1
δ_{HLLDPE}	14.2 ± 0.2	17.8 ± 0.1
$(\delta_{HDPE} - \delta_{BLLDPE})$	1.7 ± 0.2	1.1 ± 0.1
$(\delta_{HDPE} - \delta_{HLLDPE})$	1.5 ± 0.2	0.7 ± 0.1
T=525 K		
δ_{HDPE}	14.2 ± 0.3	17.9 ± 0.1
δ_{BLLDPE}	11.1 ± 0.3	15.3 ± 0.2
δ_{HLLDPE}	11.7 ± 0.3	16.2 ± 0.1
$(\delta_{HDPE} - \delta_{BLLDPE})$	3.1 ± 0.3	2.6 ± 0.2
$(\delta_{HDPE} - \delta_{HLLDPE})$	2.5 ± 0.3	1.7 ± 0.1

Note: the branch content of both BLLDPE and HLLDPE was the same in this computation, 50 branches per 1,000 backbone carbons.

4.7 Molecular Weight Effect

In order to ensure that the molecular models constructed in my MD simulations are large enough to be representatives of the real ones, I carried out a study of the molecular weight effect on the solubility parameter values of polyethylene molecules computed in my MD simulations.

In particular, I constructed 7 HDPE models with 100, 200, 300, 400, 500, 600 and 1,000 carbon atoms on backbones. MD simulations were carried out at 450 K. The procedure of running molecular dynamics is the same as I used in the miscibility studies of polyethylene blends. Table 4-3 and Figure 4-5 show the simulation results.

Table 4-3 Effect of Molecular Weight on the Computed Hildebrand Solubility Parameters of HDPE

Number of carbons	Solubility Parameter	Standard Deviation
n	$(MPa)^{1/2}$	$(MPa)^{1/2}$
100	18.8	0.3
200	18.6	0.2
300	18.8	0.2
400	18.9	0.2
500	18.4	0.2
600	18.2	0.2
1000	18.3	0.1

Figure 4-5 Effect of Molecular Weight on the Computed Hildebrand Solubility Parameters of HDPE

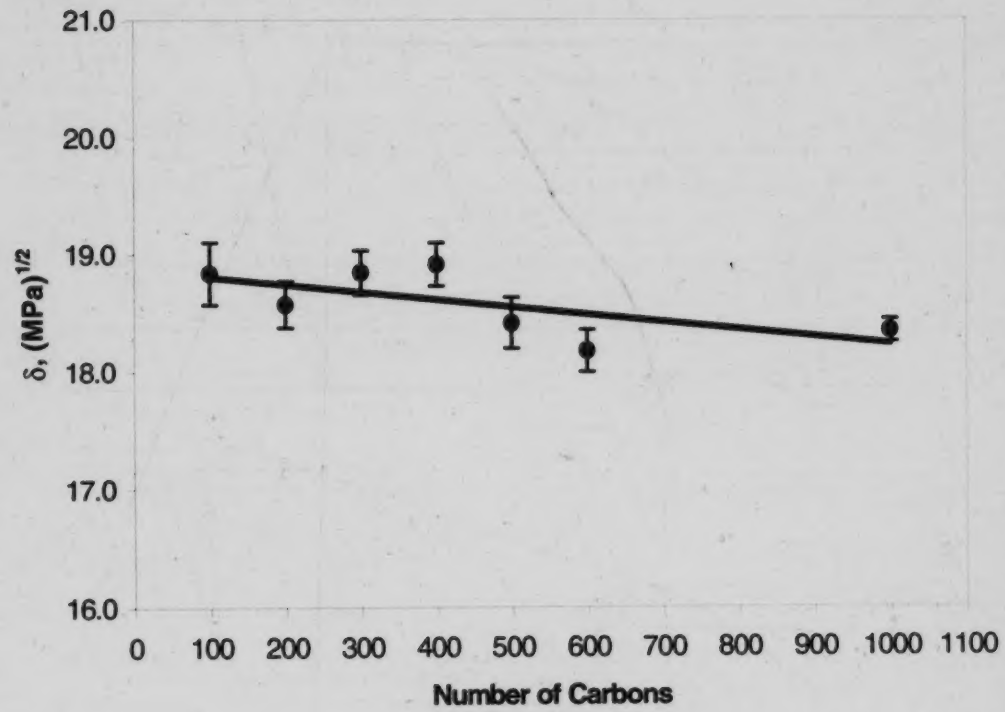

From the results, it can be seen that the values of solubility parameters of HDPE decrease with increasing chain length from 100 to 1,000 backbone carbon atoms slightly. However, because I am targeting the difference of individual solubility parameters (δ_1-δ_2), it is believed that the slight effect of molecular weight

on the calculation of the individual solubility parameters will not cause serious problems on the results of my research. In fact, simulations on short chains have been demonstrated to be sufficient to capture the behavior of their long chain polymer representatives in practice [Londono et al, 1998]. This ensures the appropriate use of 1,000 backbone carbon atoms in my models. The very reason that I choose 1,000 carbon atoms in the long chains (relatively large molecules) is that I am going to investigate the branching effect of branched polyethylenes (including LLDPE and LDPE) on their miscibility with linear polyethylene (HDPE). Therefore, the randomness of the branch-distribution on the main chains has to be considered. If the molecules were too short, it would be difficult to incorporate the random branch-distribution effect in the main chains of molecules. This further explains why the generic force-field, DREIDING2.21 was chosen: the models are quite large and require much computation effort even with the simplest force-field.

It should be pointed out that the conclusion about the molecular weight effect we presented here is only valid for the solubility parameter calculations using MD simulations. It is well known that polymer miscibility is a function of molecular weight as indicated in Flory-Huggins theory, shown in equation (3-10). It is also observed experimentally that solubility of polymers in solvents or other polymers decreases with increasing molecular weight of polymers [Hill, 1994; Crist and Hill, 1997]. It is also found in our DSC study that miscibility of polyethylene blends decreases with increasing molecular weight [Fan et al., 1997]. However, in my MD simulation approach, limited by computation resources, it is not feasible to mimic molecules as large as actual ones. Neither is it our interest to study the molecular

weight effect on the miscibility of polyethylene blends by MD simulation approach. As shown in the above results, computed solubility parameters change insignificantly with molecular weight by this approach, indicating that this approach is not eligible to be used for the purpose of studying molecular weight effect on the miscibility of polyethylene blends (and most likely other polymer blends either).

4.8 Pressures in MD Simulations

Pressure is another important thermodynamic property that can be used to define the state of a system. It bears its usual thermodynamic meaning (i.e. the force per unit area) in MD simulations. A positive pressure indicates a compressive force pushing the system inward in molecular simulations. The unit of pressure often seen in the literature of molecular simulations is expressed in terms of bars. 1 bar = 10^5 Nm^{-2} (Pa). GPa is used in Cerius2 simulation engine as default. 1 GPa = 10^4 bar. Pressure is only defined when fluid is confined in a definite volume. In a computer simulation of condensed systems, the periodic boundary box (unit cell) is recognized as a container with definite volume. In NPT ensemble simulations, the pressure control is done by coupling the system with a pressure "bath", i.e., changing the size of the unit cell under periodic boundary conditions [Berendsen et al., 1984]. In an NVT ensemble simulation, the volume or dimension of the unit cell under periodic boundary condition is determined by the experimental density value (N/V) at the controlled temperature. The pressure fluctuation has been observed to be large in both NVT and NPT ensemble simulation studies, typically thousands of bars off (either positive or negative) of one atmosphere imposed by experimental densities in MD

simulations [Brown and Clark 1984; Sun and Rigby, 1998; Sun, 1998; MSI, Forcefield-Based Simulations Manual, 1997]. By using high-quality force-fields in MD simulations, a pressure deviation of hundreds of bars off is normal and this corresponds to a density deviation about 2-3 percent in condensed-state simulations [Sun and Rigby, 1998; Sun, 1998], which is quite satisfactory.

The major reason that deviations of pressure-volume-temperature (P-V-T) are found in force-field-based MD simulations at condensed state, especially for pressure, is becoming clear now. The potential expressions and parameters were quantum-mechanically derived from the calculations of two, isolated small molecules, and thus, many-body effects are ignored. In addition, the experimental data are measured at finite temperature, while the parameters in potential expressions are derived based on static simulations (energy minimization) corresponding to a classical state at 0 K. Thus, the parameters developed in such an approach encounter quantum effects at finite temperature (which is not correct), indicating an inconsistency with the use of potential expressions and parameters in MD simulations at given conditions [Sun and Rigby, 1997; Sun, 1998]. In addition, using cut-offs to the inter-molecular interactions in MD simulations also gives rise to an error in the computed energy and pressure [Verlet, 1967]

In order to meet the needs for high-quality prediction of P-V-T behavior in some MD simulation studies, Sun et al. developed and tested a high-precision force-field [Sun et al., 1997; Sun, 1998] and observed good agreement between simulated and experimental cohesive energy densities, indicating ~2% deviation in solubility parameters. The pressure values obtained by using the optimized parameters in the

potential expressions were reported to be around 200-300 bars off from the experimental values. It is worth pointing out that large deviation in pressures causes only very small deviation in densities because the compressibilities for polymer melts are quite small, typically on the order of 10^{-4} bar^{-1}.

Once again, I address that the focus of my MD simulation studies is the calculation of the difference of solubility parameters, not the absolute value of solubility parameters. As shown before, by using a COMPASS force-field, the absolute values of solubility parameters vary significantly compared with those using DREIDING. However, the difference of solubility parameters of interest shows a systematic shift with different force-fields, which is believed not to affect the trend of the dependence of χ (i.e., δ_1-δ_2) on temperature and branch content. The pressure values obtained in my simulations using such a simple force-field and united atom model are typically less than 1,700 bars off from one atmosphere imposed by the experimental densities, within the normal range reported in the literature. Moreover, the pressure values in my MD simulations using COMPASS for the purpose of comparison were indeed improved to a certain extent but were essentially in the same range as those computed by using DREIDING2.21 (see next chapter for reference), indicating that the potential form and parameters used throughout my MD simulations are consistent and satisfactory. Therefore, it is believed that the error in simulated values of the differences of solubility parameters are not influenced by error in pressure in the results of these research interests.

Chapter 5

MD Simulation Results on Polyethylene Blends

5.1 Introduction

In previous chapters, the objectives and methods of my MD simulation studies on the miscibility of different polyethylene blends have been addressed. The work presented in this chapter includes the effect of the branching characteristics of branched polyethylenes on their miscibility with HDPE and with different types of branched polyethylenes. The temperature dependence of χ of polyethylene blends is also given. Moreover, the effect of microstructure difference of polyethylene molecules, quantified by the trans/gauche ratios of the molecules in the melt state, is explored as well. In this chapter, I am going to present MD simulation results for δ of various kinds of polyethylene molecules, followed by discussion on the miscibility of various kinds of polyethylene blends in terms of microstructure difference, including HDPE/LLDPE, HDPE/LDPE and LDPE/LLDPE blends. The effects of branch content of the branched polyethylene and temperature on the miscibility of various polyethylene blends are major concerns in this study. The effect of the length of short branches on the miscibility of polyethylene blends was also studied and discussed. Consistency of the results with experimental findings of other researchers will be discussed.

5.2 HDPE/LLDPE Blend Systems

In the literature, based on different experimental approaches, researchers proposed some critical values of branch content in terms of numbers of branches per 1,000 backbone carbon atoms for LLDPE above which LLDPE/HDPE blends would phase-separate as reviewed in chapter 2. Critical values of 40, 60 and 80 branches per 1,000 carbon atoms have been proposed in the literature (see chapter 2 and therein for references). Therefore, the MD simulation work in this thesis was initiated with HDPE/butene-based-LLDPE system to study the effect of branch content on the miscibility of the blends. I also wanted to know how consistent my MD simulation approach is with others' experimental methods to determine whether the novel MD simulation approach is valid for the miscibility study of polyethylene blends. Once the approach was verified [Choi, 2000], I started a systematic study on the miscibility of HDPE/LLDPE with changing the branch length by simulating hexene-based and octene-based LLDPE molecules. My MD simulation results are compared with other researchers' experimental results reported in the literature. Good agreement has been found between these results.

Note that my work differs from that of Choi in one way: The LLDPE molecular structures were assembled by Choi by allowing the computer to co-polymerize randomly certain monomers defined by himself to form BLLDPE molecules with certain number of short branches, whereas I began with polymerizing 500 ethylene monomers to form a linear chain and then attached short branches at randomly spaced positions. Both methods of constructing LLDPE molecules gave

similar δ, but Choi's method gave an incorrect dihedral distribution. My method, however, gave a correct dihedral distribution.

5.2.1 HDPE and Butene-Based LLDPE Systems

5.2.1.1 Molecular Models

Six molecular models were created and studied by MD simulations in this particular work. The characteristics of the models are shown in Table 5-1. In the table, model 0 is an HDPE molecule without any branches; models 1 to 5 are butene-based LLDPE with different branch contents with random distribution (thus representing Ziegler-Natta types of LLDPE). The HDPE molecule was modeled as a linear chain with 1,000 carbon atoms by polymerizing 500 ethylene monomers using polymer builder in Cerius2. Each LLDPE molecule was modeled with a linear main chain with 1,000 carbons (built by using the same procedure as building an HDPE molecule of 500 monomers) and a specific number of short branches depending on the particular interest of research. Short branches, containing two carbons, were arbitrarily assigned to the linear main chain one by one manually. Here, the branch contents for butene-based LLDPE models were chosen with 10, 20, 40, 50 and 80 branches per 1,000 linear chain carbon atoms. Therefore, in Table 5-1, model 0 had no branches representing HDPE and model 1 had 10 branches with 2 carbons randomly attached on its linear main chain. Model 2 had 20 branches with 2 carbons on the main chain and so on.

Table 5-1 Characteristics of the Models Used in the Simulations

Model	Molar mass, g/mol	Branch content, number of branches per 1000 main chain carbons
0 (HDPE)	14029	none
BLLDPE		
1	14310	10
2	14590	20
3	15151	40
4	15432	50
5	16274	80

5.2.1.2 Results and Discussion

The Hildebrand solubility parameters were calculated using Equation 3-6 which can be rewritten as:

$$\delta=[(E_{vac}-E_{cond})\rho/M]^{1/2} \qquad (5\text{-}1)$$

The quantity, $(E_{vac}-E_{cond})\rho/M$, is the cohesive energy density of the melted material, while ρ is the density and M the molar mass. Simulation temperature was chosen at 425, 450, 475, 500 and 525 K separately, within the normal temperature range at which polyethylenes are melt blended in industry [Mark et al., 1985]. The polyethylene density values specified in the MD simulations at these temperatures are shown in Table 5-2. The density values of polyethylene melts were determined using the following correlation:

$$1/\rho=1.282+9.0\times10^{-4}(t-150) \qquad (5\text{-}1A)$$

where ρ is the density in g/cm^3 and t is the temperature in ^{o}C. Note that the density values of linear and branched polyethylene in the melts are equivalent. The

correlation was compared with three other published density-temperature relations and good agreement was observed (see the reference and therein [Rudin et al., 1970]).

Table 5-2 Experimental Densities of all Polyethylenes at Different Temperatures

Temperature, K	425	450	475	500	525
Temperature, °C*	152	177	202	227	252
Density, g/cm^3	0.779	0.766	0.753	0.740	0.728

*Please see page 3 for melting temperatures of different polyethylenes

Once the MD trajectories were generated, the total energy values of the molecules in vacuum states and condensed states, for every 10 pico-seconds in the last 100 pico-seconds of the MD annealing, were taken and averaged to get the E_{vac} and E_{cond}, separately. The standard deviation of the E_{vac} and E_{cond} values is less than 5% of the average values. The Flory-Huggins interaction parameter was obtained by using Equation 3-13.

The computed Hildebrand solubility parameters of the polyethylene models are summarized in Table 5-3 and visually presented in Figure 5-1. In Table 5-3, the model number (code) bears the same meanings as in Table 5-1. As shown, the computed δ values decrease with increasing temperature as well as with branch content generally. This is reasonably understandable because due to Brownian motion, increasing either temperature or the number of branches enlarges the average separation of molecules and chain segments so that it lowers the cohesive energy densities of the molecules. In fact, these trends of temperature and branch content

dependence of δ for polyethylene melts are in agreement with P-V-T measurement of δ [Han et al., 1999].

When the δ values were used to calculate χ, while the resulting χ is plotted against temperature, a non-inverse pattern of temperature dependence, as shown in Figure 5-2, is obtained. This is somewhat expected because χ does not follow the expected inverse temperature dependence predicted by Flory-Huggins theory [Flory, 1953]. Since the χ values in my approach were calculated from the computed δ values of pure component using Equation (3-13), it is understandable that a non-1/T temperature dependence of χ was observed in my MD simulations. In fact, such non-inverse temperature dependence of χ was also observed experimentally [Zhao and Choi, 2000].

Table 5-3 Computed Hildebrand Solubility Parameters, δ, of the Models, $(MPa)^{1/2}$

Model Code	Simulation Temperature, °C				
	152	177	202	227	252
0	18.4±0.1	18.3±0.1	18.1±0.1	18.0±0.1	17.9±0.1
BLLDPE					
1	18.3±0.1	18.1±0.1	17.5±0.1	17.2±0.1	16.7±0.1
2	18.2±0.1	18.0±0.1	17.3±0.1	17.2±0.1	16.7±0.2
3	18.0±0.1	17.6±0.1	17.2±0.1	16.9±0.1	16.7±0.1
4	17.4±0.1	17.1±0.1	16.8±0.2	15.9±0.2	15.3±0.2
5	17.4±0.1	17.2±0.1	16.8±0.1	15.6±0.2	15.4±0.2

Figure 5-1 Computed δ of HDPE and Butene-based LLDPE vs. Temperature

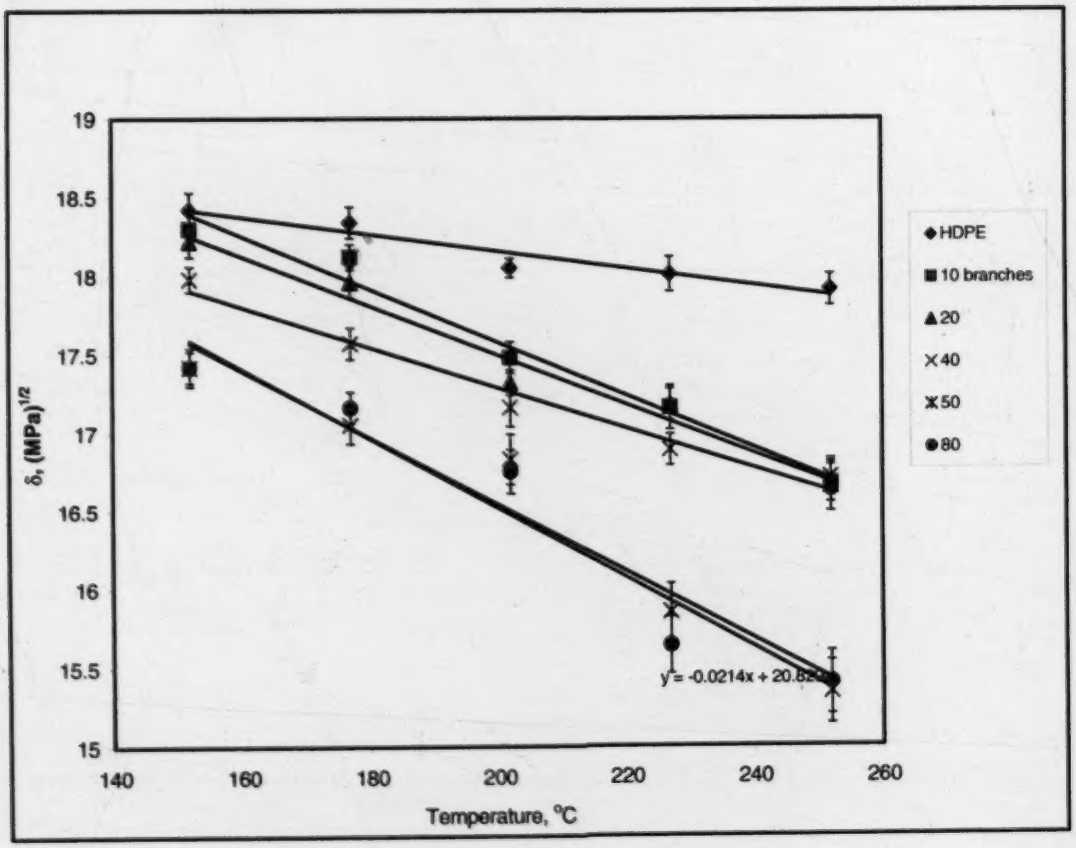

Figure 5-2 Calculated χ vs. Temperature for Blends of HDPE/BLLDPE

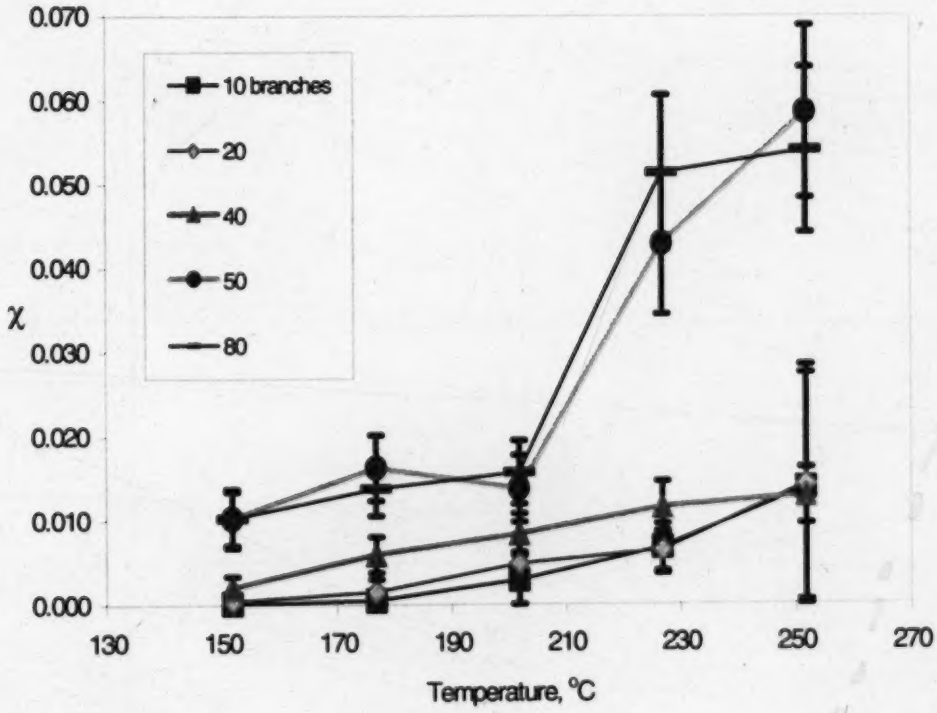

The results in Figure 5-2 show that when branch content of BLLDPE is low, χ values for the blends are rather small. Considering the ensemble fluctuation, most of χ values for low branch content of BLLDPE blends with HDPE regardless of

temperatures, are very close to zero, the critical value, $\chi_{critical}$, which implies miscibility. However, χ values become relatively large (far away from $\chi_{critical}$ even if large standard deviation is considered) when branch content of BLLDPE is high, implying less favorable blending and possible immiscibility. It can be seen in Figure 5-2 that at higher temperatures this trend becomes more prominent, especially for blends with high branch content BLLDPE. This phenomenon indicates that the blends may have a lower critical solution temperature (LCST) phase diagram, which is more frequently seen than upper critical solution temperature (UCST) behavior in polymer blends [Utracki, 1990]. Note that because the Flory-Huggins theory does not take the equation-of-state properties of the pure components into account, it cannot predict the LCST phase behavior, which is the major drawback of the theory. However, LCST behavior was observed in my simulations because I used Equation (3-13) to obtain χ values.

It should be pointed out that the true phase behavior is also dependent on the blend composition which is another important factor determining the type and shape of the phase diagram for polyethylene blend systems. Unfortunately, such a factor cannot be studied practically by the MD approach in that only individual solubility parameters of the pure components are concerned regardless of the information for the blends.

When the computed χ is plotted against the branch content (Figure 5-3), an abrupt elevation of χ can be spotted between 40 and 50 branches per 1,000 main chain carbons at higher temperatures (say, 227 °C). The results show that when branch content is high, say above 40-50, relatively large χ values are obtained,

indicating that HDPE and BLLDPE phase-separate at high temperatures (say, above 227 °C). This "cut-off " value (40-50 branches/1,000 main chain carbons) is in agreement with other researchers' findings [Alamo et al., 1997; Hill and Barharm, 1993; Morgan et al., 1997]. Experimentally, small angle neutron scattering (SANS) technique was employed in the Alamo et al. study, while indirect methods such as TEM and DSC were utilized in the Hill et al. research. It is understandable that the so-called "cut-off " value should be in a range instead of an absolute value. Also the cut-off value is suspected to be technique-sensitive according to the literature as reviewed in Chapter two.

According to above results and discussion, it can be concluded that the miscibility of HDPE/BLLDPE polyethylene blends can be characterized in terms of branch content of BLLDPE molecules. Due to the existence of branches on the main chains of BLLDPE molecules, there are more chain ends that can move more easily, which is clearly observed in the MD simulations. And also there are more CH and CH_3 groups which lead to more non-CH_2 interactions. Therefore, the molecular interactions of HDPE and BLLDPE molecules differ bigger and bigger when branch content of BLLDPE becomes larger and larger. Thus, it is characteristics of the molecular interactions of CH_2 and non-CH_2 groups that cause the phase separation of HDPE/BLLDPE blends. These results indicate that the branch content of BLLDPE may be crucial in determining the phase behavior of the blends.

Figure 5-3 Calculated χ vs. Branch Content of BLLDPE

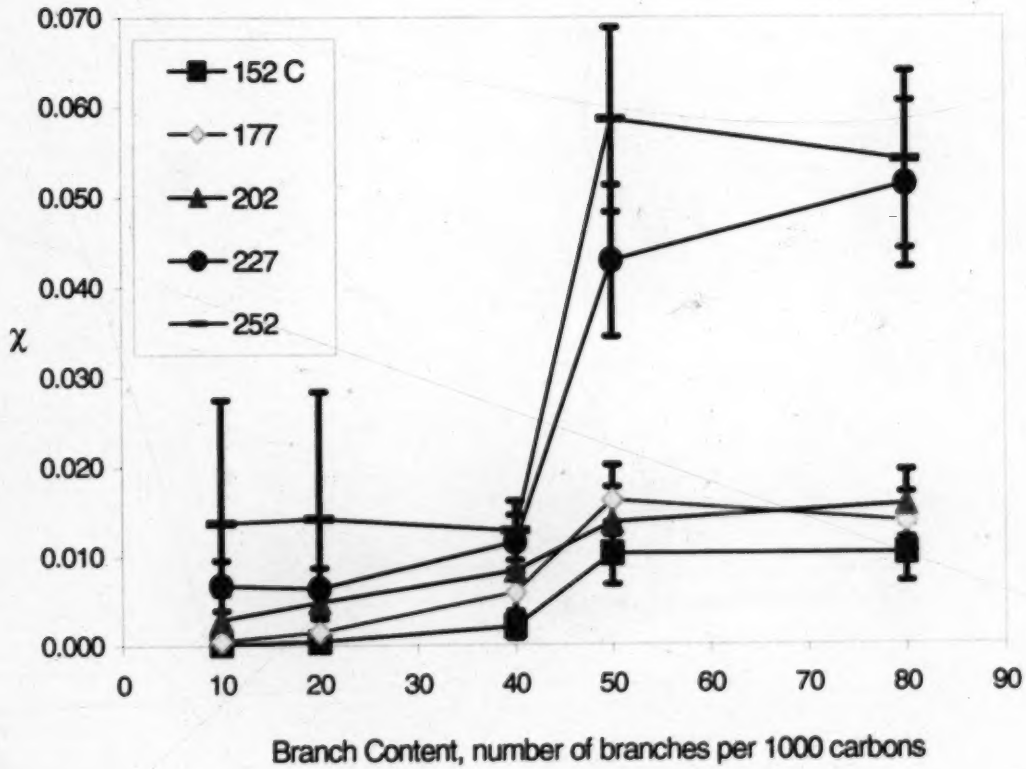

It is encouraging that the trend of branch content effect found by experimental techniques of other researchers was also captured by the MD simulation methodology, although a very simple model (the combination of Hildebrand solubility parameter approach and Flory-Huggins interaction parameter approach) and

the simplest molecular interaction potential form and parameters (DREIDING force-field) were adopted.

5.2.1.3 Standard Deviation

From the MD simulation results, we can see that the standard deviation of computed δ values is rather small and basically less than 1% from the average value. This implies that the natural fluctuation of the ensembles chosen in the MD simulations is reasonable and satisfactory. However, the standard deviation of χ is rather high. In order to justify these results, let's look at Equation 3-13 again, which can be rewritten as following:

$$\chi = K(\Delta\delta)^2 \qquad (5\text{-}2)$$

where $\Delta\delta=\delta_1-\delta_2$ and $K=V_s/RT$. Let's differentiate Equation (5-2) with respect to (Δδ) and the following expression is obtained:

$$d\chi = 2K(\Delta\delta)d(\Delta\delta) \qquad (5\text{-}3)$$

From Equation (5-3), it can be concluded that the function (5-2) has a built-in drawback when error analysis is carried out using Equation (5-2). The fractional variation of χ, $d\chi/\chi$, will be enlarged twice that of Δδ $[d(\Delta\delta)/(\Delta\delta)]$. The deviation introduced in using Equation 5-2 has nothing to do with the techniques used to determine χ. This explains why such a large standard deviation is obtained when χ is calculated based on the computed δ as shown in the previous section. Thus, it is inevitable to find large standard deviation of χ as long as equation (5-2) is utilized no matter what techniques are used to evaluate δ experimentally or theoretically.

5.2.1.4 Trans/Gauche Ratio

Torsional angle analysis in my study was made based on the trajectories obtained through MD simulations. The statistical calculations of interdependent RIS states are described in the reference [Flory, 1969; 1974]]. The frequencies of trans and gauche conformations in the MD simulations were recorded in the dihedral distribution profiles (see Figure 5-3A). Therefore, the trans/gauche ratios can be calculated by the ratios of frequencies of trans and gauche conformations. The MD simulation results for trans/gauche ratios of HDPE and BLLDPE are shown in Table 5-4 and Figure 5-4. The model code in Table5-4 bears the same meaning as it was explained before.

Table 5-4 Simulated Trans/Gauche Ratios for HDPE and BLLDPE

model code	T=425 K	450	475	500	525
	T=152 °C	177	202	227	252
0	6.2	5.5	5.2	4.5	4.2
BLLDPE					
1	5.5	5.3	5.0	4.7	4.1
2	5.1	5.2	4.8	4.4	3.7
3	3.5	3.6	3.7	3.2	3.2
4	3.5	3.5	3.3	3.0	2.7
5	2.2	2.3	2.1	2.4	2.0

Figure 5-3A, A Dihedral Distribution Profile for an HLLDPE Simulation Run

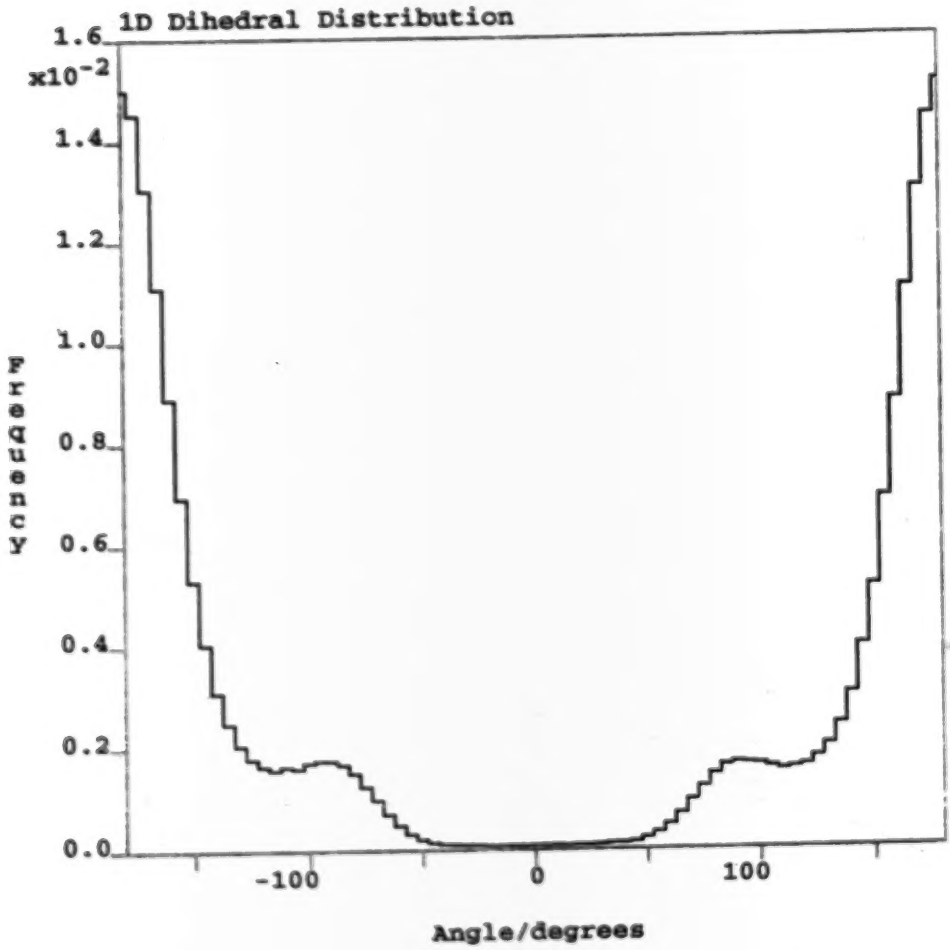

Figure 5-4 Trans/Gauche Ratio vs. Branch Content for BLLDPE

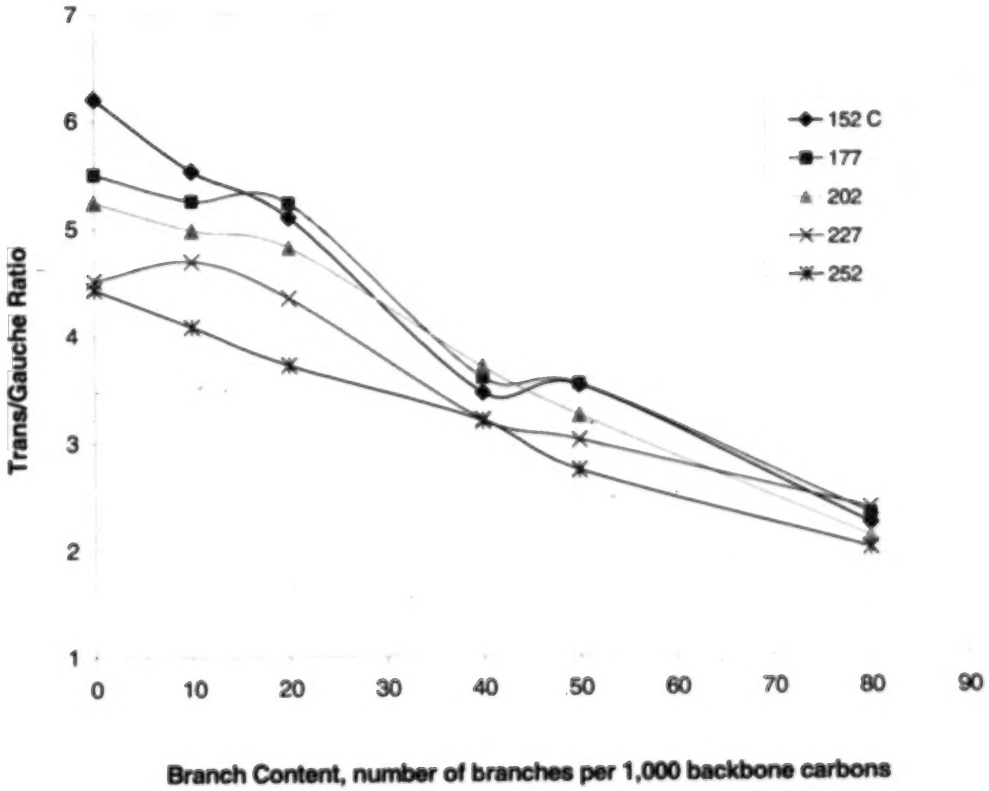

From the Table 5-4 and Figure 5-4, it can be seen that the trans/gauche ratio essentially decreases with increasing temperature for both HDPE and BLLDPE regardless of branch content as expected. It can be understood that due to Brownian motion, molecules at higher temperatures carry more energy resulting in more gauche isomeric states and less trans. It can also be spotted that the ratio decreases with

increasing branch content as well. Because of the existence of branches, the trans state conformations are perturbed the most. Therefore, the ratio drops with increasing branch content. The smooth connection lines in Figure 5-4 are given only for guiding the reader's eye.

It is worth mentioning that the HDPE trans/gauche ratio computed in the MD simulations at high temperatures (say above 227 °C) is close to the data from Raman spectroscopic experimental work [Wunder and Merajver, 1986] which indicated that ultrahigh-molecular-weight polyethylene (UHMWPE, a form of HDPE) melt had about 80% trans conformations (t/g=4) at the temperatures between 135-208 °C. However, the ratio at lower temperatures from the MD work deviated from the Raman experimental work. This may be due to the insufficient molecular thermal energy to overcome the potential barrier in my MD simulations at lower temperatures.

5.2.1.5 Pressure

As shown in Chapter 4, pressure is another important thermodynamic property that can be used to monitor the MD simulation progress like the Hamiltonian of the system. In a satisfactory MD simulation run, both Hamiltonian and pressure should reach their steady state values around the ensemble means when equilibrium is obtained although natural fluctuations are still allowed. While the Hamiltonian is the central theme for an MD simulation run, pressure can be used to check the consistency of the potential expression and parameters as discussed in Chapter four.

The pressure values in my MD simulations for HDPE/BLLDPE are listed in Table 5-5. The model code numbers bear the same meanings as before and the unit of pressure values is in MPa in the table.

Table 5-5 Pressures Simulated on HDPE/BLLDPE Systems, (MPa)

Model Code	T=425K	450	475	500	525
0	-196±31	-154±30	-136±29	-128±30	-121±27
BLLDPE					
1	-175±27	-167±29	-164±29	-152±30	-131±31
2	-178±30	-140±28	-160±29	-136±27	-107±24
3	-76±21	-154±36	-126±30	-133±29	-106±29
4	-81±20	-139±28	-153±26	-125±31	-100±31
5	-79±20	-156±28	-128±26	-104±24	-100±25

In Table 5-5, most of the pressure values for BLLDPE in MD simulations are about 700-1600 bars (70-160 MPa) off from the atmosphere (0.1 MPa) at which experimental densities of polyethylene molecules were measured [Rudin et al., 1970]. Recall that I have discussed the pressure issue in Chapter 4 about the large deviation of pressure in MD simulations and all the pressure deviations in the MD simulation fell in the normal range reported in the literature. See the references quoted in Chapter 4 for details. In fact, all the pressure values in my MD simulations including HDPE/LLDPE and HDPE/LDPE systems fell in this range and will not be shown or discussed again in the following sections. The negative sign of pressure means that the pressure pushes the simulated system inwardly, based on the convention of

Cerius2 MD simulation engine. As shown in Chapter 4, I had performed some MD simulations using COMPASS force-field and compared the computed solubility parameters with those using DREIDING2.21 that has been utilized throughout my MD studies in this thesis work. The pressures for the MD simulations using COMPASS are presented here in Table 5-6, compared with Table 5-5, the pressure values computed using Dreiding, on page 94.

Table 5-6 Pressures Simulated Using COMPASS, (MPa)

Temperature, K	HDPE	BLLDPE	HLLDPE
425	10 ± 56	-138 ± 81	-146 ± 99
525	40 ± 54	-107 ± 83	-74 ± 80

In the table, BLLDPE represents the butene-based LLDPE model with 50 branches/1,000 backbone carbons and HLLDPE the hexene-based LLDPE with 50 branches/1,000 backbone carbons. From Table 5-6, it can be seen that the pressures in the MD simulations by COMPASS seems improved to some extent as explained in Chapter four, but they are essentially in the same range for LLDPE as those shown in Table 5-5. I would like to address once again that MD simulations for polymer melts are sensitive to the densities specified in NVT ensemble simulations but not sensitive to pressures imposed by density constraint. Large pressure deviation causes only small density deviation. Thus, it is believed that my MD simulation results are satisfactory and efficient for the purpose of computing the difference of Hildebrand solubility parameters, $\Delta\delta$.

5.2.2 HDPE with Hexene-Based and Octene-Based LLDPE Blend Systems

Encouraged by the promising results for the HDPE/butene-based LLDPE blends, I decided to extend this study to the systems containing hexene- and octene-based LLDPE. However, in order to reduce the computation effort, I tried to study models with branch content less than 50 branches per 1,000 backbone carbon atoms. This is still useful for simulating commercial products of LLDPE, most of whose the branch content is rarely higher than 50 branches per 1,000 backbone carbons. Therefore, models with branch contents ranging from 10 to 50 per 1,000 backbone carbons should be sufficient to represent most of the commercial LLDPEs (excluding variations of molecular weight and distribution, branch length distribution, etc.). In the following sections, model description, MD simulation results and discussion for this work will be presented.

5.2.2.1 Molecular Models

In this particular work, ten LLDPE molecular models were created (in addition to the same HDPE model used in the previous work) and studied by MD simulations. The characteristics of the models are shown in Table 5-7. Model 0 is the HDPE as before. Models 1-5 represent molecules of hexene-based LLDPE (HLLDPE) with 5 different branch contents, and models 6-10 are representatives of octene-based LLDPE (OLLDPE) molecules with the same 5 different branch contents. The backbone structure for each LLDPE model in this study was the same as the one used in butene-based LLDPE, i.e. 1,000 carbons in the main chain with a specific number of short branches. The branch contents in this work were chosen at

10, 20, 30, 40 and 50 branches per 1,000 linear main chain carbon atoms. The simulation temperatures were the same as before (i.e., 425, 450, 475, 500 and 525 K). The densities for these models were the same as those of BLLDPE models according to the temperature dependence correlation mentioned before [Rudin et al., 1970]. The same MD simulation methodology and procedure were used in this work.

Table 5-7 Characteristics of the Models Used in this study

Model	Molar mass, g/mol	Branch content, number of branches per 1000 main chain carbons
0	14029	none
HLLDPE		
1	14590	10
2	15151	20
3	15712	30
4	16274	40
5	16835	50
OLLDPE		
6	14871	10
7	15712	20
8	16554	30
9	17396	40
10	18238	50

5.2.2.2 Results and Discussion

The computed Hildebrand solubility parameters of the HLLDPE and OLLDPE models are given in Table 5-8. Similar to the findings for the BLLDPE models, the computed δ values decrease with increasing temperature as well as with branch content for both HLLDPE and OLLDPE models. This trend has already been explained in a previous Results and Discussion section (5.2.1.2) on the HDPE/BLLDPE blends. However, the computed δ values for HLLDPE and OLLDPE

models are greater than those for BLLDPE (see table 5-3) at identical conditions (temperature and branch content). Therefore, the resulting χs between HDPE and HLLDPE and OLLDPE are smaller than those between HDPE and BLLDPE, indicating that blends of HDPE/HLLDPE and HDPE/OLLDPE are more miscible than blends of HDPE/BLLDPE. This conclusion is in good agreement with that of TEM and DSC experiments done by other researchers [Hill and Barham, 1993]. In their study, they found that the closed-loop region in the phase diagram they developed shrank but did not change the shape essentially for blends of HDPE with octene-based LLDPE in comparison with blends of HDPE with butene-based LLDPE, indicating that OLLDPE is more miscible with HDPE than is BLLDPE.

When the δ values were used to calculate χ and the resulting χ was plotted against temperature and branch content, the temperature and branch content dependence obtained for both HDPE/HLLDPE and HDPE/OLLDPE blends were similar to those as for the HDPE/BLLDPE blends shown in Figure 5-5 to Figure 5-8. The rapid jump occurs above 40 branches per 1,000 main chain carbons for both HDPE/HLLDPE and HDPE/OLLDPE blends at most of the temperatures studied. Note that the magnitude of χ in Figure 5-5 to Figure 5-8 is about half that in the figures for HDPE/BLLDPE blend studies (See Figures 5-2 and 5-3).

From the results shown in Figure 5-5 to Figure 5-8, we can see that the length of short branches in LLDPEs seems not to affect the cut-off value for HDPE/LLDPE blends. However, LLDPEs with four or six carbon short branches seem to be more miscible with HDPE than those with two carbon short branches. Thus, it can be concluded that the branch content of LLDPE is the dominant factor in determining

the phase behavior of HDPE/LLDPE blends. However, the length of short branches of LLDPE also affects the miscibility between HDPE and LLDPE components. These results are consistent with Hill and Barham's experimental observations [Hill and Barham, 1993].

It is worth pointing out that, as mentioned in Chapter four, the computed δ values using DREIDING force-field match with those from the P-V-T experimental measurements well [Han et al., 1999] (see also Table 5-8A).

Table 5-8 Computed Hildebrand Solubility Parameters, δ, of the Models, $(MPa)^{1/2}$

Model Code	Simulation Temperature, °C				
	152	177	202	227	252
0	18.4±0.1	18.3±0.1	18.1±0.1	18.0±0.1	17.9±0.1
HLLDPE					
1	18.4±0.1	18.1±0.1	17.8±0.1	17.5±0.1	17.3±0.1
2	18.3±0.1	18.2±0.1	17.8±0.1	17.6±0.1	17.3±0.1
3	18.2±0.1	18.1±0.1	17.9±0.1	17.3±0.2	17.2±0.1
4	18.1±0.1	18.1±0.1	17.6±0.1	17.3±0.1	17.0±0.1
5	17.8±0.1	17.7±0.1	17.1±0.1	16.6±0.1	16.2±0.1
OLLDPE					
6	18.3±0.1	18.4±0.1	18.0±0.1	17.4±0.1	17.1±0.1
7	18.1±0.1	18.0±0.1	17.9±0.1	17.5±0.1	17.3±0.1
8	18.1±0.1	17.8±0.1	17.5±0.1	17.3±0.1	17.0±0.1
9	18.0±0.1	17.8±0.1	17.7±0.1	17.3±0.1	16.8±0.1
10	17.6±0.1	17.2±0.1	17.0±0.1	17.0±0.1	16.7±0.10

Table 5-8A The Comparison of δ Values of Polyethylene Melts at 166 °C, Measured by P-V-T Method and Computed by MD Simulations, $(MPa)^{1/2}$

	HDPE	BLLDPE*	OLLDPE**
P-V-T Method	17.8 ± 0.1	17.8 ± 0.1	17.5 ± 0.1
MD Simulation***	18.3 ± 0.1	17.3 ± 0.1	17.9 ± 0.1

* The average branch content of BLLDPE is 46.5 branches per 1,000 backbone carbons in P-V-T measurements and 50 in MD simulations.

** The average branch content of OLLDPE is 38.0 branches per 1,000 backbone carbons in P-V-T measurements and 40 in MD simulations.

*** The δ values from MD simulations at 166 °C were obtained by using linear regression.

Figure 5-5 Temperature Dependence of χ for Blends of HDPE/HLLDPE

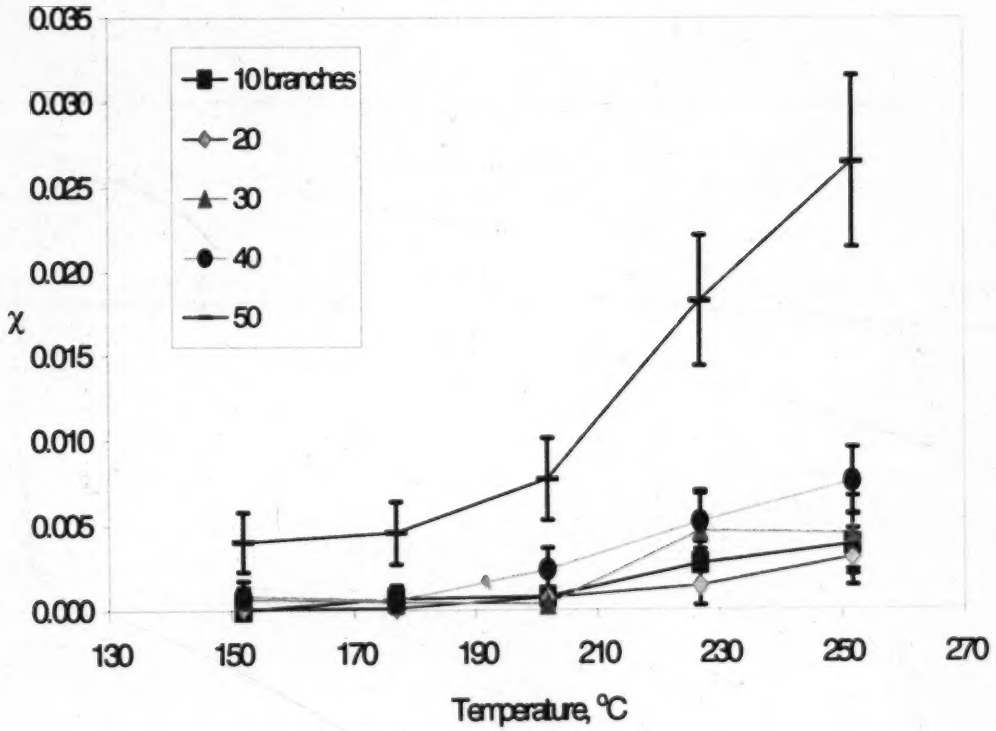

Figure 5-6 Branch Content Dependence of χ for Blends of HDPE/HLLDPE

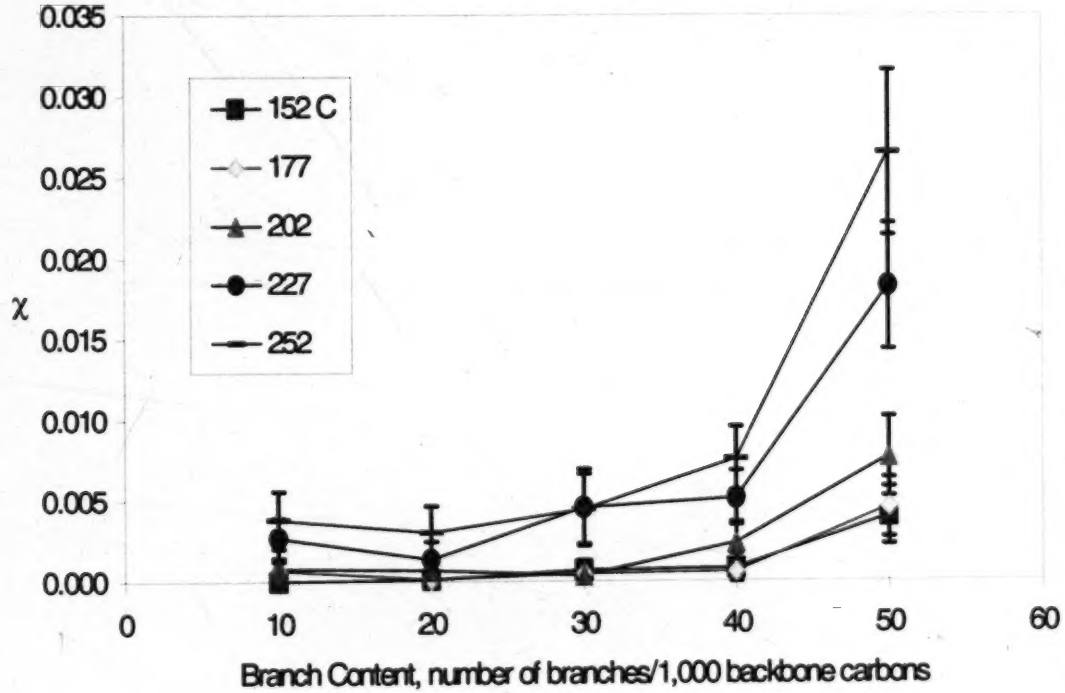

Figure 5-7 Temperature Dependence of χ for Blends of HDPE/OLLDPE

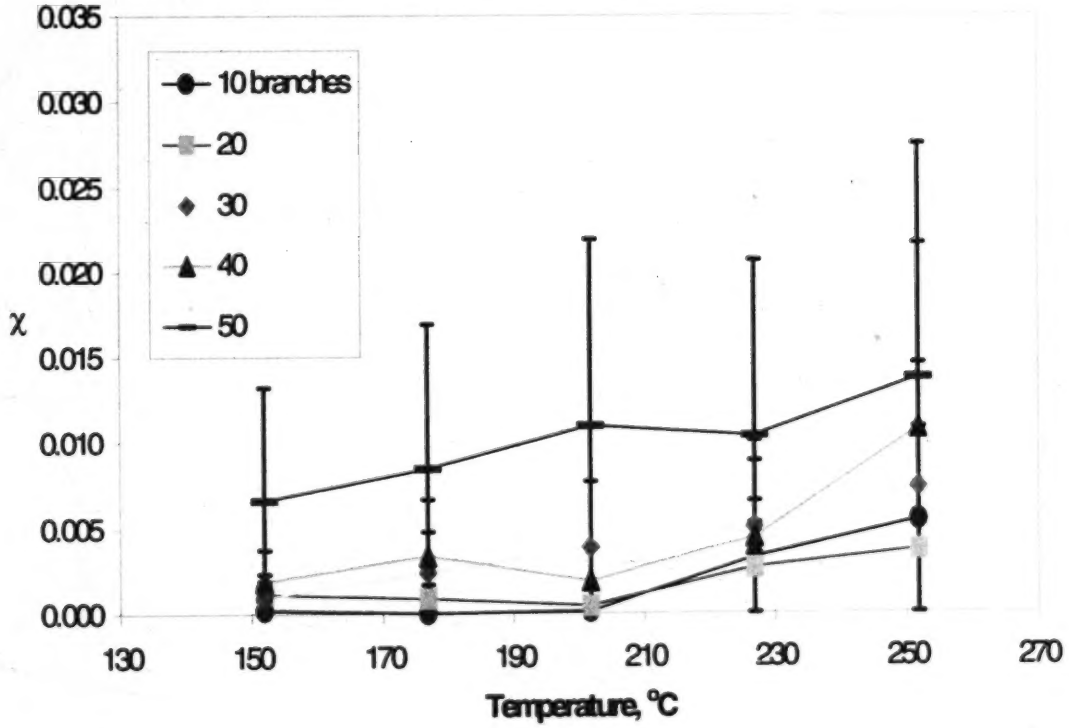

Figure 5-8 Branch Content Dependence of χ for Blends of HDPE/OLLDPE

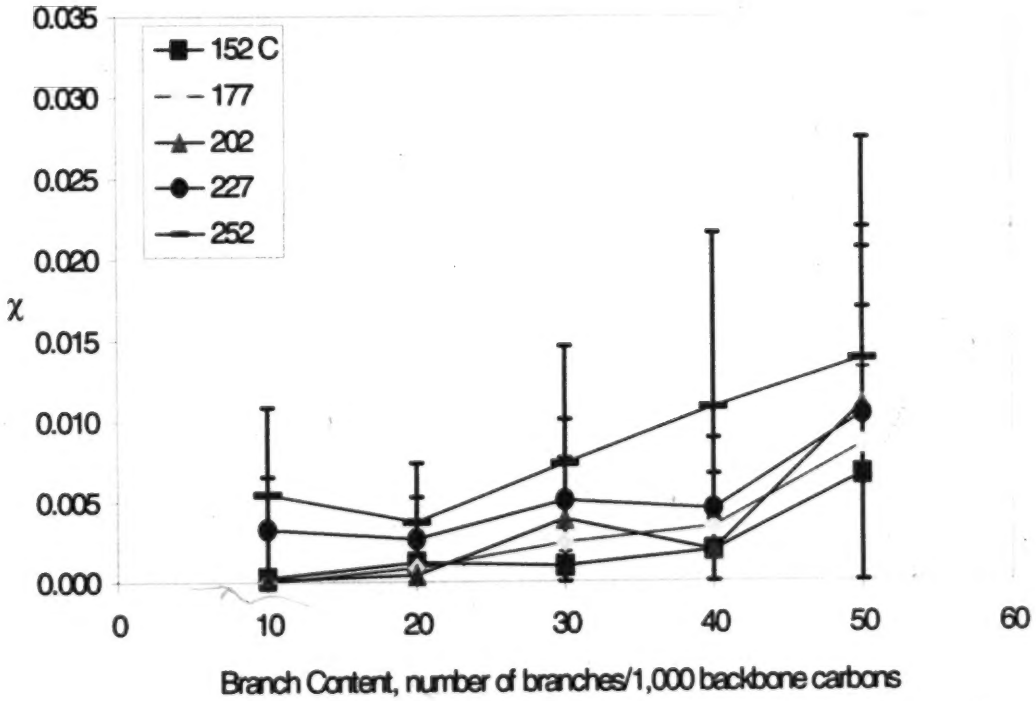

5.2.2.3 Trans/Gauche Ratio

The computed trans/gauche ratios of the backbones of the hexene-based LLDPE and octene-based LLDPE models are presented in Table 5-9, Figure 5-9 and Figure 5-10.

The trends of dependence on the temperature and branch content for both HLLDPE and OLLDPE are similar to those of BLLDPE (see Figure 5-9, Figure 5-10 and Figure 5-4).

Table 5-9 Simulated Trans/Gauche Ratios for HDPE, HLLDPE and OLLDPE

Model Code	T=425 K	450	475	500	525
0	6.2	5.5	5.2	4.5	4.2
HLLDPE					
1	4.7	4.7	4.4	4.1	3.7
2	4.2	4.0	4.0	3.6	3.6
3	4.1	3.6	3.6	3.5	3.1
4	3.9	3.5	3.4	3.2	2.8
5	3.1	3.1	3.1	2.9	2.5
OLLDPE					
6	4.7	4.6	4.2	3.9	3.8
7	4.4	4.2	4.1	3.6	3.4
8	3.9	4.0	3.6	3.3	3.2
9	3.7	3.6	3.4	3.2	2.8
10	3.1	3.0	3.0	3.1	2.4

Figure 5-9 Trans/Gauche Ratios for HLLDPE at the Simulation Temperatures

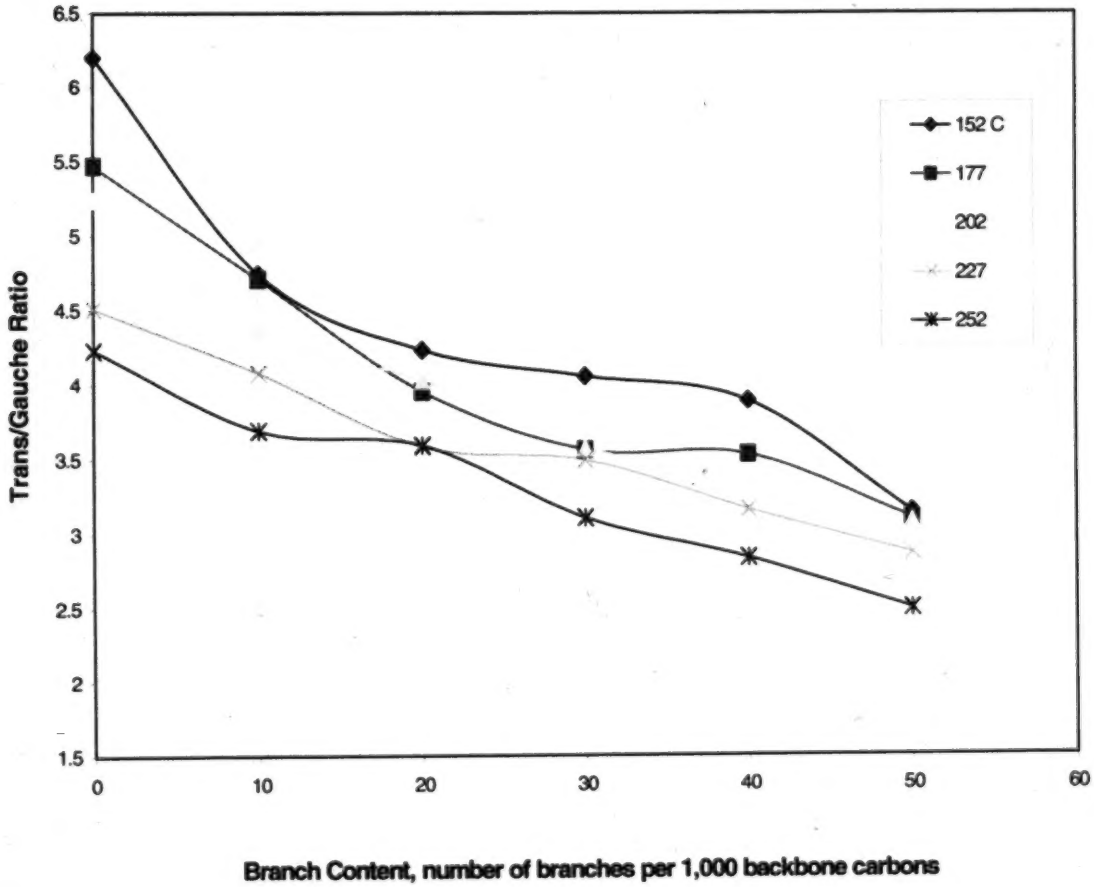

Note: Lines in the graph are drawn to guide the eye.

Figure 5-10 Trans/Gauche Ratios for OLLDPE at the Simulation Temperatures

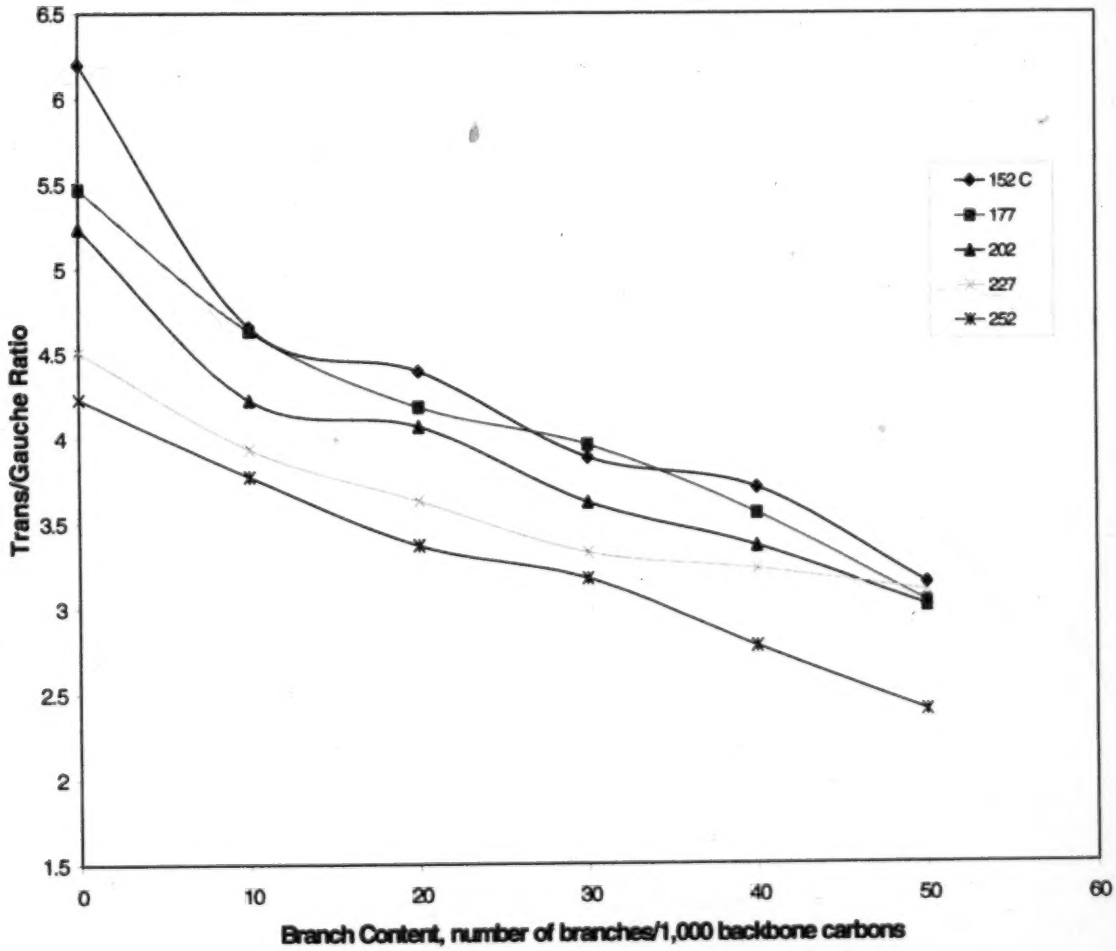

5.3 HDPE/LDPE Blends

5.3.1 Introduction

The melt miscibility issue of HDPE/LDPE blends has been quite controversial for the last decade, as discussed in Chapter 2. Views from complete homogeneity to liquid-liquid phase-separation have been expressed in the literature [Hill et al., 1993; Alamo et al., 1997; Barham et al., 1996; Hill, 1994; Alamo et al. 1994; Agamalian et al., 1999; Hill and Puig, 1997].

The branch content effect was also explored experimentally by indirect methods [Martínez-Salazar et al., 1991; Plans et al., 1991]. However, the effect of branch content of LDPE molecules was completely ignored in the work of Hill et al. and Alamo et al. Although the branch content of LDPE used in the studies of these researchers had significant differences (see Chapter 2 for reference), it did not draw the attention of either group of researchers in the debate. Unlike LLDPE molecules that can be prepared using hydrogenated polybutadiene (HPB) showing controlled number of branches and branch distribution with narrow molecular weight distribution, it is impossible to control the number of branches and branch distribution in LDPE polymerization due to the high-pressure free-radical polymerization process.

Surprisingly, the level of branch content for LDPE above which the blends are immiscible and segregate in the melt was found in this study to be around 25-30 branches/1,000 long chain carbons at the chosen simulation temperatures. This value is significantly lower than that of HDPE/LLDPE blends. The major difference between LLDPE and LDPE models is that each modeled LDPE molecule has three long chains while each modeled LLDPE molecule has only one long chain. The

present results together with those of the HDPE/LLDPE blends suggest that the long chain branching may have significant influence on the miscibility of polyethylene blends.

5.3.2 Molecular Models

In this particular study, seven models for LDPE molecules were constructed besides the HDPE model used before. The characteristics of the models are shown in Table 5-10.

Table 5-10. Characteristics of the Models Used in the Simulations

Model Code	Molar mass, g/mol	Branch content, number of branches per 1000 long chain carbons
0	14029	none
LDPE		
1	14534	10
2	15151	20
3	15263	22
4	15376	25
5	15489	27
6	15656	30
7	16273	40

In the table, model 0 is an HDPE without any branches; models 1 to 7 are LDPE with different branch contents. The HDPE molecule was modeled as a linear chain with 1,000 carbons as the same as before. Each LDPE molecule was modeled with three long chains and a specific number of short branches. The three long chains consisted of 500, 300 and 200 carbons, respectively. Therefore, the total number of carbons contained in the three long chains for each LDPE model was 1,000 so that the molecular weight for each of LDPE model can be compared with corresponding LLDPE model with same number of short-branches. The two long chains with 200 and 300 carbons were attached arbitrarily on the eighty-sixth carbon and the three-hundred-and-fiftieth carbon of the longest chain with 500 hundred carbons, respectively. Because of the back-biting effect during the high-pressure free-radical polymerization process, four-carbon short branches are predominant in LDPE molecules. Therefore, all short branches for each LDPE model in my simulations were chosen to contain 4 carbons and were randomly assigned to the three long chains. The branch contents for LDPE models were chosen with 10, 20, 22, 25, 27, 30 and 40 branches (including long and short branches) per 1,000 long chain carbons. For example, the model with 10 branches here had 4 long chain ends and 6 short branches; the model with 20 branches had 4 long chain ends and 16 short branches and so on. Note that most of the commercial LDPE products bear 15-30 branches/1,000 carbons.

5.3.3 Results and Discussion

The computed Hildebrand solubility parameters of the LDPE models are presented in Table 5-11. In this table, the model number bears the same meanings as in the previous convention.

As shown once again, the computed δ values decrease with increasing temperature as well as with branch content generally, as expected. The reason for this phenomenon has been explained before. We can see that HDPE has a weaker temperature dependence of Hildebrand solubility parameters than LDPE does. The difference of the temperature dependence of δ between HDPE and LDPE becomes more pronounced at higher temperatures.

When the δ values were used to calculate χ and such data are plotted against temperature (Figure 5-11), it is observed that when branch content is low, there is weak temperature dependence of χ and χ values are low ($\chi<0.01$). However, when the branch content is high (above 30 branches per 1,000 long-chain carbons), the χ versus temperature curve goes through a maximum at around 230 ^{o}C and the maximum is quite high ($\chi\equiv0.025$) as shown in Figure 5-11, indicating that the blends may have a closed-loop phase diagram. Nonetheless, it is not surprising that none of the curves show an inverse temperature dependence of χ because the χ computed based on δ does not follow the inverse temperature dependence as explained before. This observation is in agreement with recent IGC experimental findings [Zhao and Choi, 2000], in which a closed-loop phase diagram of the blends was suggested. However, in my simulation results, the temperature range of the peak positions is located at a higher temperature region than found by Zhao and Choi. This may be due

to the differences in molecular structures and distributions of the polyethylenes used in MD simulations and inverse gas chromatography (IGC) experiments.

Table 5-11 Computed Hildebrand Solubility Parameters, δ, $(MPa)^{1/2}$

For HDPE/LDPE Model Systems

Model Code	Simulation Temperature, °C				
	152	177	202	227	252
0	18.4±0.1	18.3±0.1	18.1±0.1	18.0±0.1	17.9±0.1
LDPE					
1	18.5±0.2	17.9±0.1	17.5±0.1	17.4±0.2	16.4±0.2
2	18.7±0.2	17.8±0.1	17.5±0.1	17.0±0.2	16.9±0.2
3	18.6±0.1	18.0±0.1	17.4±0.1	17.1±0.1	17.0±0.1
4	18.2±0.1	18.0±0.1	17.3±0.1	17.2±0.2	17.0±0.1
5	18.2±0.1	18.0±0.2	17.2±0.1	17.1±0.2	16.9±0.2
6	17.7±0.2	17.7±0.2	17.2±0.2	16.3±0.1	16.4±0.2
7	17.8±0.1	17.8±0.2	17.0±0.12	16.3±0.1	16.4±0.2

Figure 5-11 Temperature Dependence of χ for HDPE/LDPE Blends

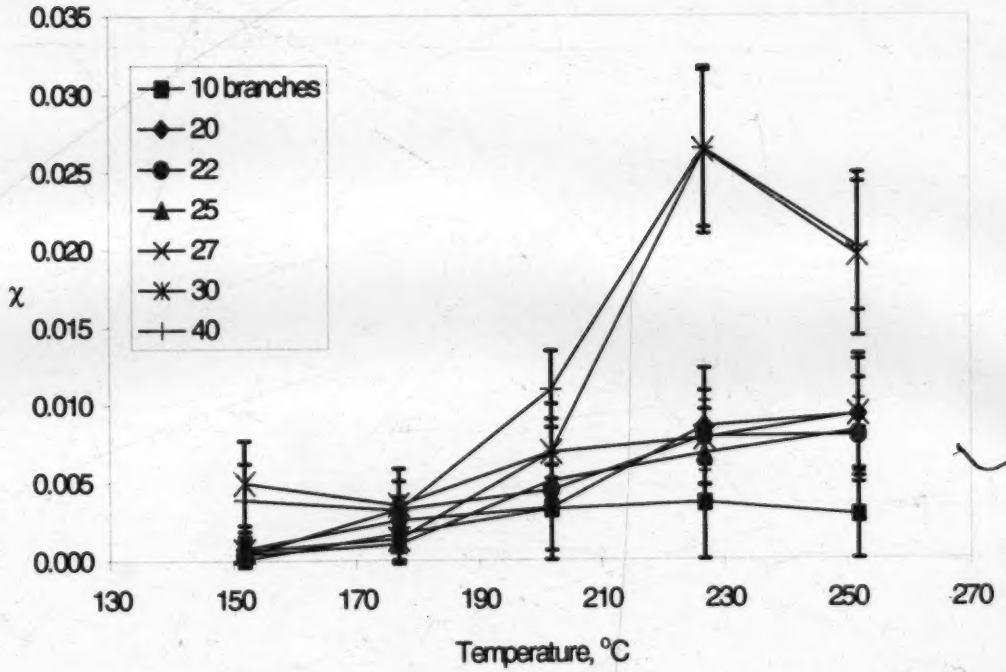

When the computed χ is plotted against the branch content (Figure 5-12), two significant jumps can be spotted for the computed χ values. The lower one occurs around 20 and the upper one around 30 branches per 1,000 long chain carbons, depending on temperature, with more prominent changes at higher temperatures (say, above 227 °C). This means that when branch content of LDPE is higher than 30, HDPE/LDPE will phase-separate. Once again, such phase-separation behavior will be more pronounced at high temperatures (above 227 °C). This cut-off value of branch content of LDPE (30 branches/1,000 long chain carbons) is in good agreement with Martínez-Slazar et al.'s findings [Martínez-Slazar et al., 1991; Plans et al., 1991], in which they found that the cut-off value should be in the range from 20 to 30 based on melting point depression measurements.

Comparing with my previous MD studies on HDPE and LLDPE blends, for which the cut-off value of the LLDPE branch content was found to be around 40-50 branches per 1,000 backbone carbons (see previous sections on HDPE/LLDPE blends), the present value is significantly lower. Since the major difference between LDPE and LLDPE models is the long chain branches, it is suggested that in addition to the branch content, long chain branching also plays an important role in controlling the melt phase behavior of polyethylene blends.

Figure 5-12 Computed χ vs. Branch Content of LDPE for HDPE/LDPE Blends

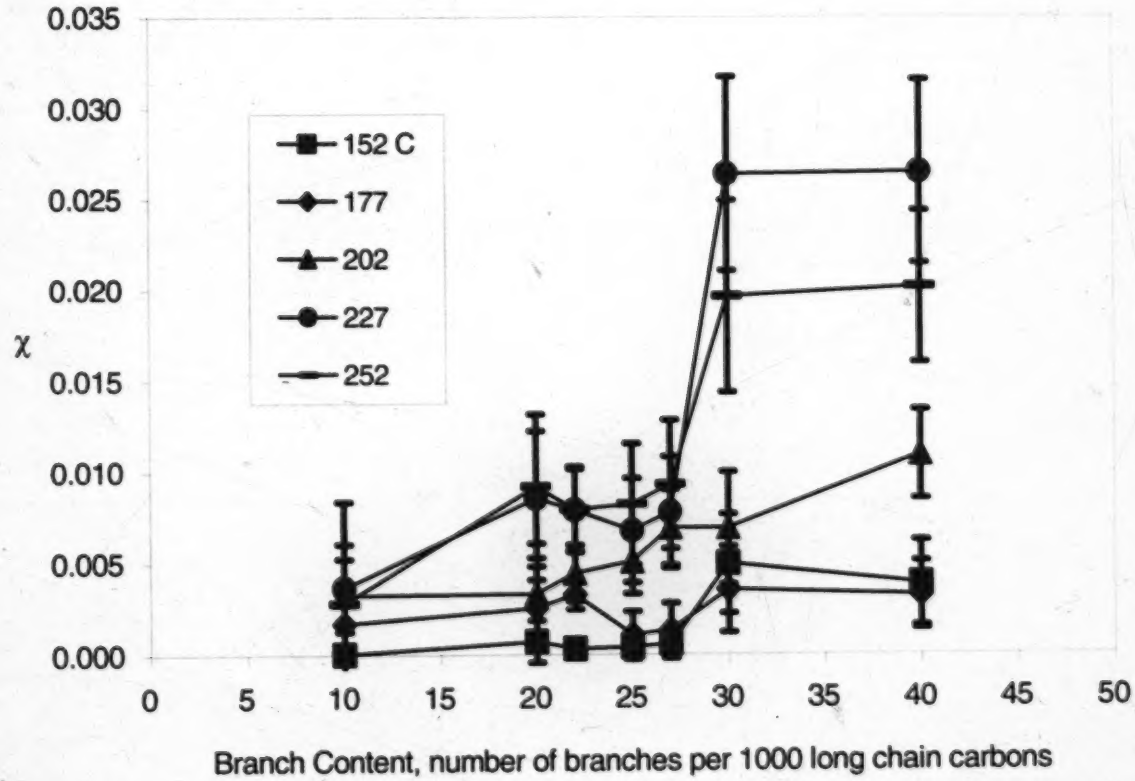

Based on my MD simulation results, I would suggest that conclusions of Hill et al. [Barham et al., 1988; Hill et al., 1991; 1992; 1993; 1994] and Alamo et al. [Alamo et al., 1994 and 1997; Londono et al., 1995; Agamalian et al., 1999] on the phase behavior of HDPE/LDPE blends are correct. Note that the LDPE polymers used in the former group of researchers had a branch content of 26 per 1,000 carbon atoms that should be in similar range of branch content cut-off value according to my MD findings. Although I have proposed the cut-off value around 30, the polymers used by Hill et al. may have had a much more complicated molecular weight distribution and branch length distribution than my models. Furthermore, the composition effect could not be studied by my approach. The LDPE polymers used in the latter group of researchers had only 14 to 19 branches per 1,000 carbon atoms that is below the cut-off value of branch content of LDPE proposed based on my MD simulation results. In conclusion, the issue of miscibility of HDPE/LDPE is not a simple one since branch content of LDPE and long chain branching characteristics must be taken into account.

5.3.4 Trans/Gauche Ratio

The trans/gauche ratios and pressures simulated for HDPE and LDPE systems are just reported in Table 5-12 and Table 5-13.

Table 5-12 Simulated Trans/Gauche Ratios for HDPE and LDPE

Model Code	T=425 K	450	475	500	525
0	6.2	5.5	5.2	4.5	4.2
LDPE					
1	5.2	5.2	4.7	4.6	4.0
2	4.8	4.5	4.5	3.8	3.7
3	4.7	4.5	4.4	3.8	3.7
4	4.6	4.3	4.0	3.6	3.6
5	4.4	4.3	3.8	3.6	3.5
6	4.4	4.0	3.7	3.5	3.4
7	3.8	3.4	3.7	3.4	3.0

Table 5-13 Pressures Simulated on HDPE and LDPE Systems, (MPa)

Model Code	T=425K	450	475	500	525
0	-196±31	-154±30	-136±29	-128±30	-121±27
LDPE					
1	-83±22	-81±22	-81±22	-74±28	-70±21
2	-76±21	-77±20	-71±20	-75±21	-62±62
3	-37±28	-78±20	-73±20	-65±19	-63±20
4	-78±21	-84±21	-83±19	-71±19	-59±19
5	-79±22	-80±19	-68±19	-68±18	-69±19
6	-79±21	-84±21	-74±20	-74±19	-70±19
7	-87±19	-72±19	-66±20	-64±18	-61±19

5.4 LDPE/LLDPE Blends

5.4.1 Introduction

The melt miscibility issue of LDPE/LLDPE blend systems is the most complicated one due to the complexity of the variable branch contents and the wide range of distribution of variable short-branch lengths for both components. However, LDPE/LLDPE systems have become more and more important in polyethylene industry nowadays, because such blends retain both good mechanical properties from LLDPE and easier processibility from LDPE [Utracki, 1989]. While blending LDPE into LLDPE can enhance transparency and melt strength, blending LLDPE into LDPE can improve melt rheological properties and toughness of the final polymer products.

Since the branch content of branched polyethylenes plays a very important role in determining the phase behavior of HDPE/LLDPE and HDPE/LDPE blends, I believe that branch content will also impose an effect on the miscibility of LDPE/LLDPE blends. Accordingly, I have paid attention to the branch content effect when the phase behavior of the LDPE/LLDPE blend systems was studied based on my MD simulations. Because the δ values of LDPE and LLDPE are available from the previous calculation, I therefore calculated the χ values of the LDPE/LLDPE systems.

5.4.2 Results and Discussion

Flory-Huggins interaction parameters between LDPE and LLDPE with various branch content levels for both components at all simulation temperatures

were calculated for most of the LDPE and LLDPE modeling pairs based on the computed Hildebrand solubility parameters of LLDPE and LDPE models obtained previously. Then χ was plotted against temperature and branch content of LDPE. Because there are too many plots, not all the results are shown here. Only a few representative plots will be presented here. These plots can be classified into two categories. One category is plots for LLDPE and LDPE blends with lower branch contents of LDPE, say below 25. The other category is plots for the same blends but with higher branch contents of LDPE, say above 30 branches per 1,000 long chain carbons.

Figure 5-13 to Figure 5-20 belong to the first category and are plots of χ versus T and χ versus LLDPE branch for both LDPE/HLLDPE and LDPE/OLLDPE blends with LDPE branch contents of 10 branches (Figure 5-13 to Figure 5-16), and 20 branches/1,000 long chain carbons of LDPE (Figure 5-17 to Figure 5-20). From these figures, we can see that except for only a few points, most of the χ values between LLDPE and LDPE are rather small, implying miscibility. In fact, for blends of LDPE/HLLDPE and LDPE/OLLDPE with LDPE branch content up to 27, the χ vs. T and χ vs. branch content of LDPE plots are more or less the same, i.e, small χ values are obtained. Note that I used the same scale for the plots here for the purpose of comparison.

Figure 5-13 χ vs. T for Blends of HLLDPE/LDPE-with-10-branches

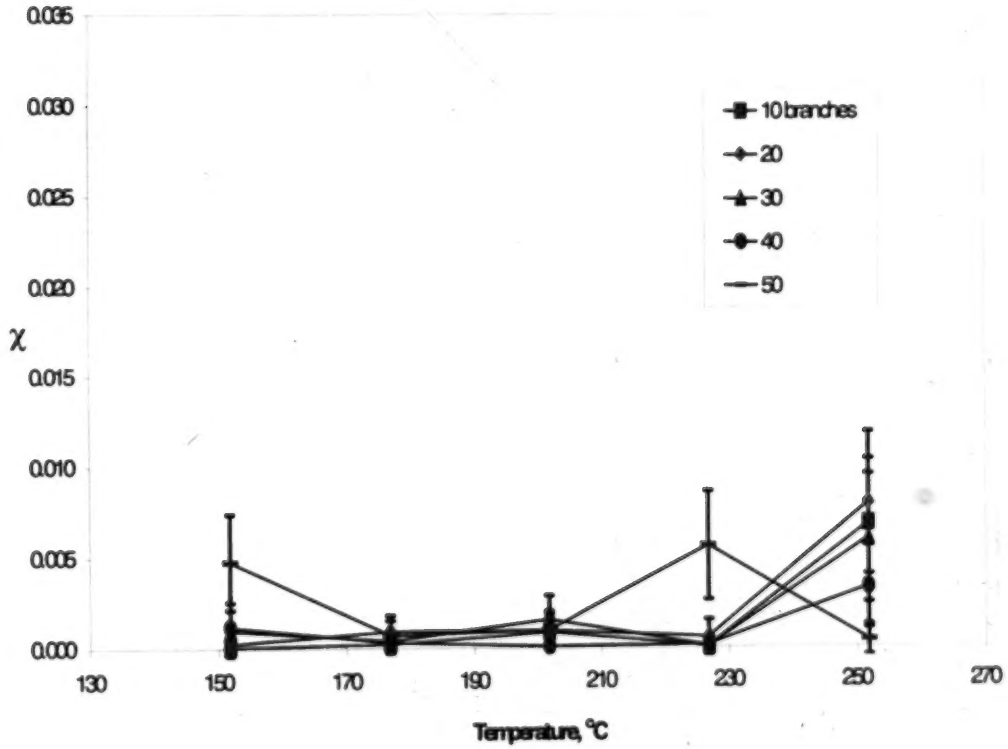

Figure 5-14 χ vs. HLLDPE Branch Content for HLLDPE/LDPE-with-10-branches

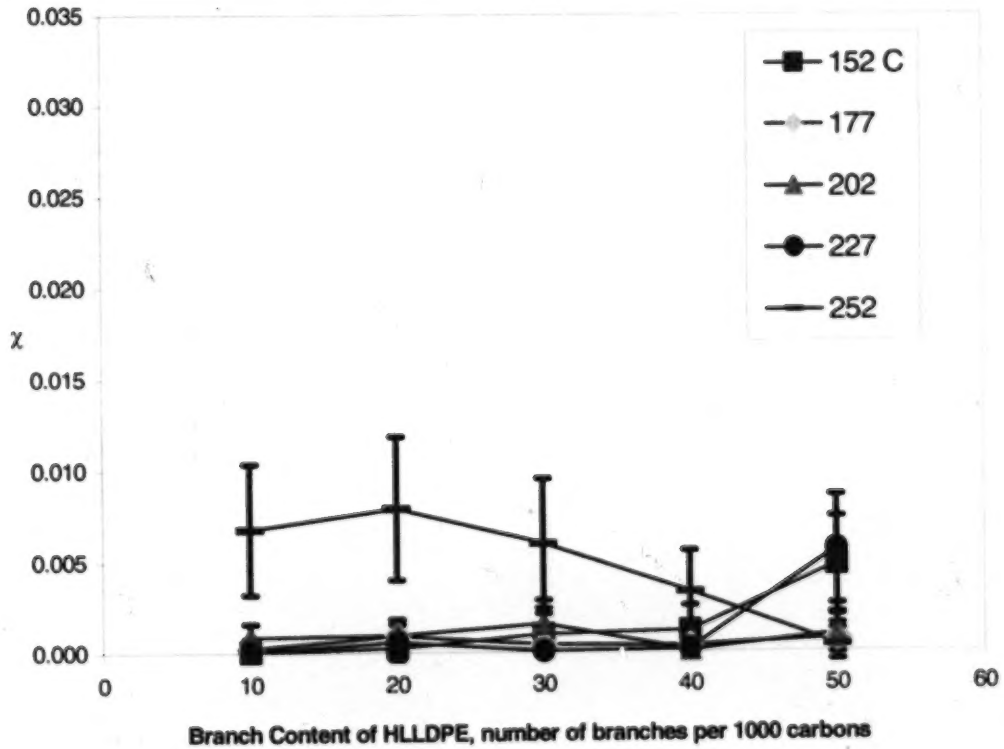

Figure 5-15 χ vs. T for Blends of OLLDPE/LDPE-with-10-branches

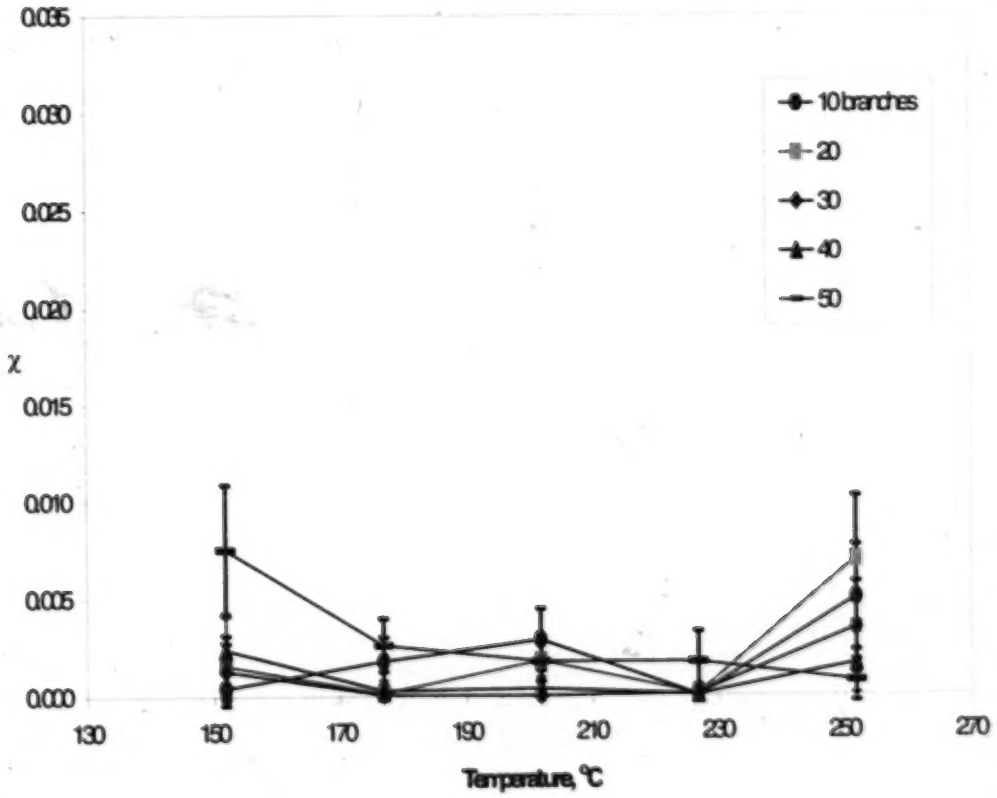

Figure 5-16 χ vs. OLLDPE Branch Content for OLLDPE/LDPE-with-10-branches

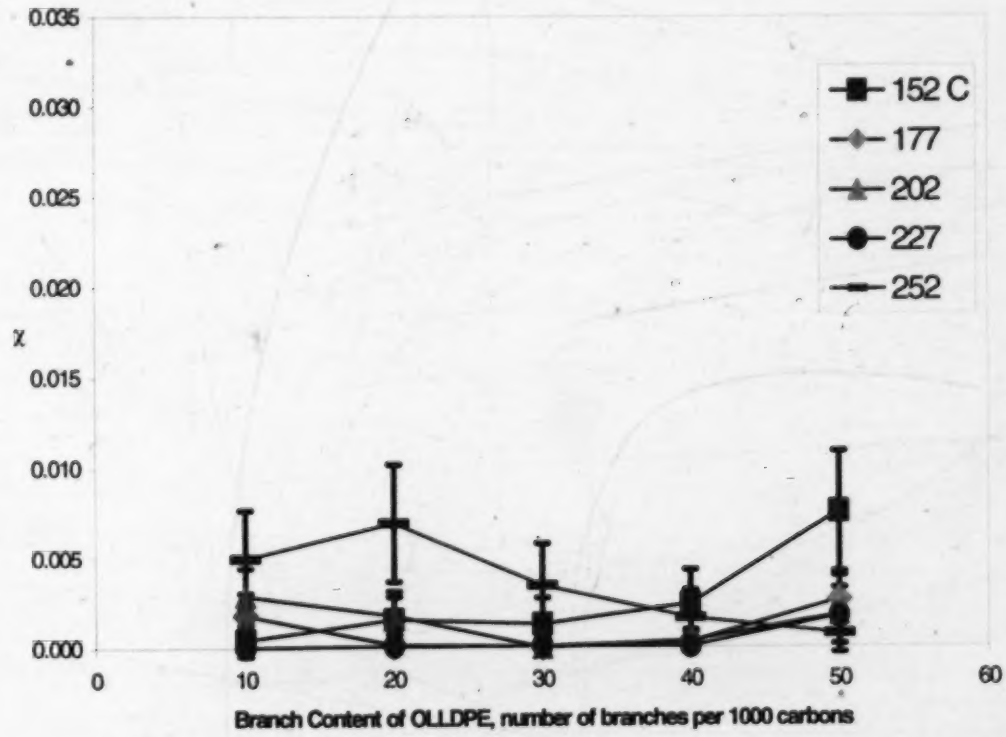

Figure 5-17 χ vs. T for Blends of HLLDPE/LDPE-with-20-branches

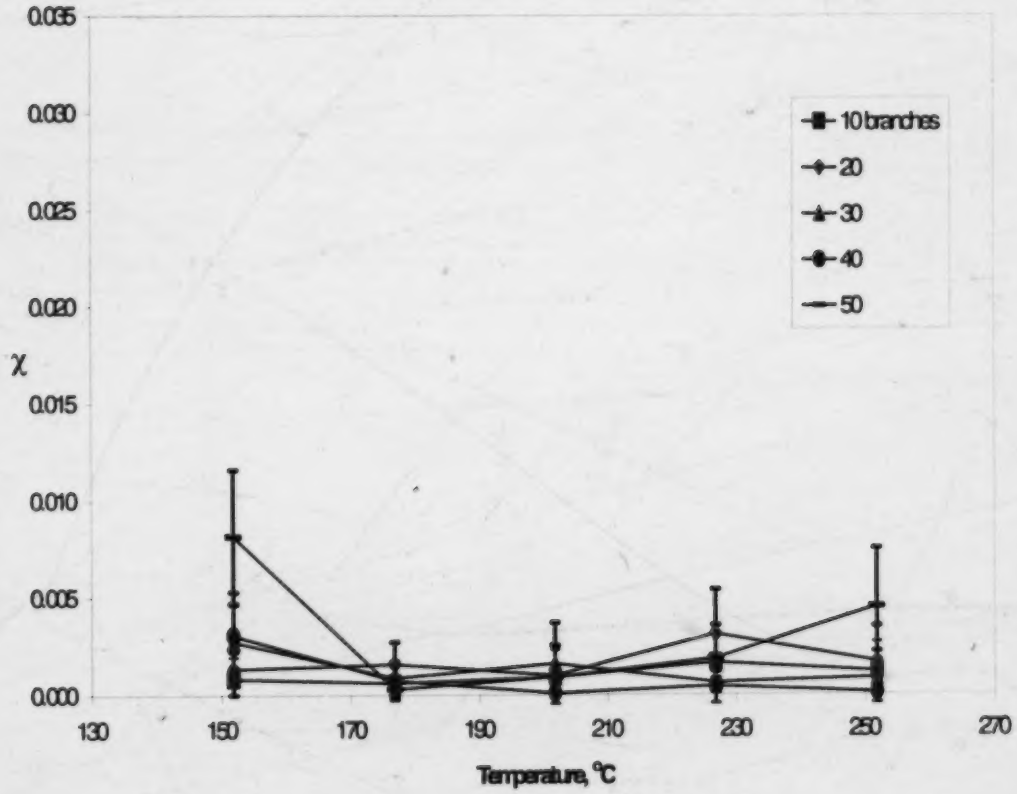

Figure 5-18 χ vs. HLLDPE Branch Content for HLLDPE/LDPE-with-20-branches

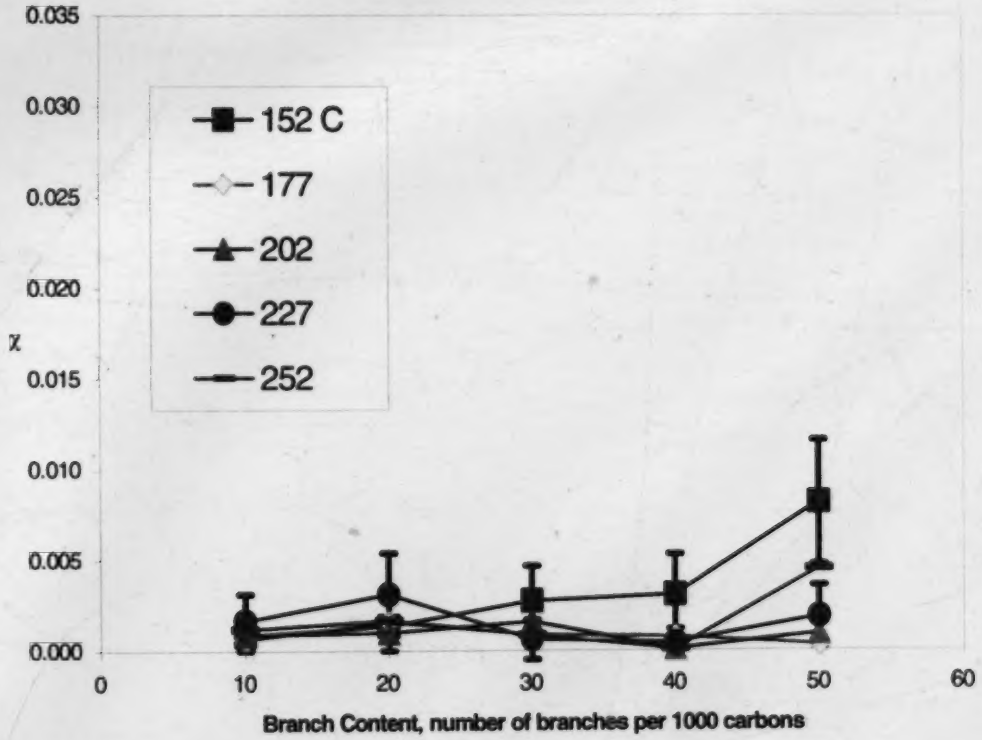

Figure 5-19 χ vs. T for Blends of OLLDPE/LDPE-with-20-branches

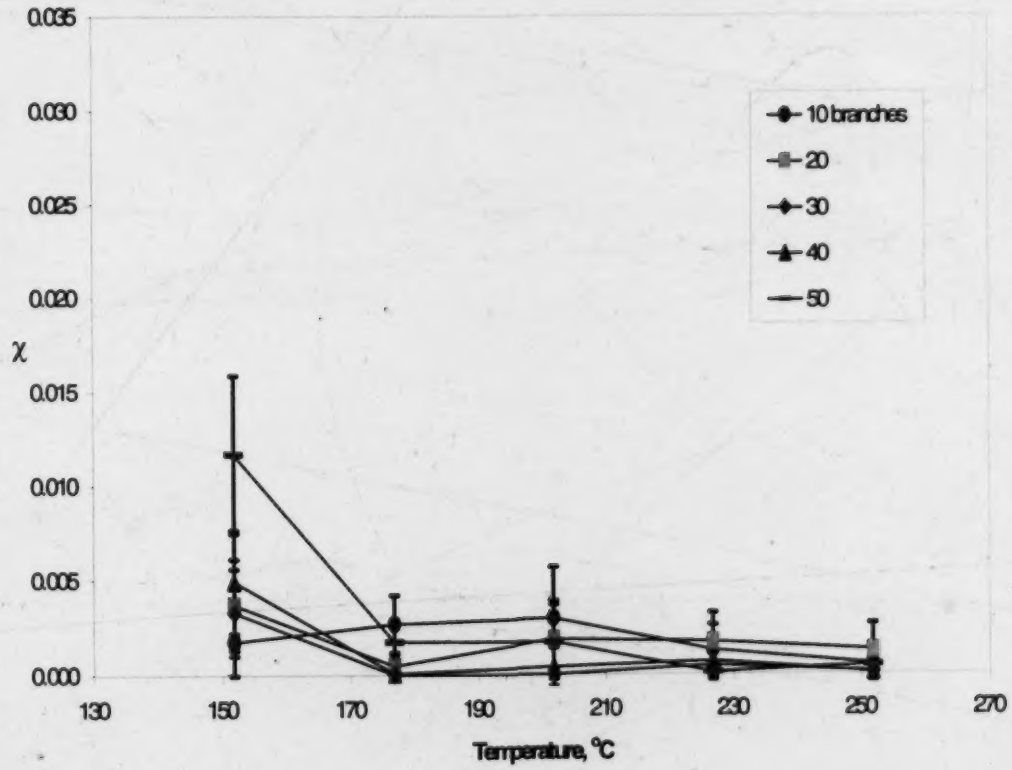

Figure 5-20 χ vs. OLLDPE Branch Content for OLLDPE/LDPE-with-20-branches

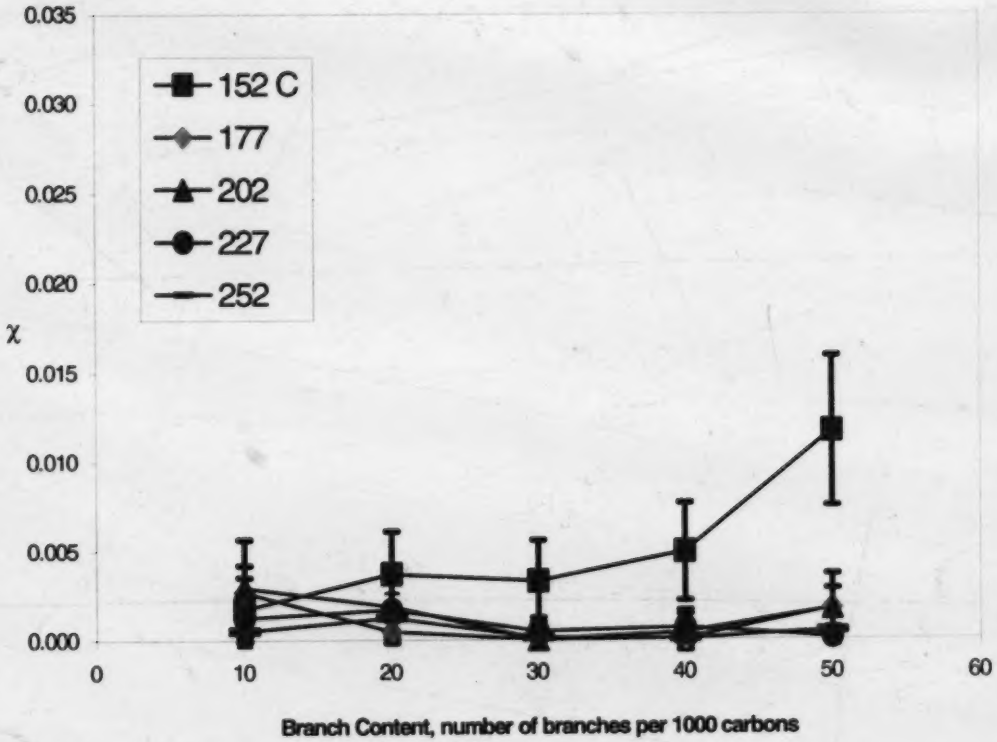

However, a different picture caught my eye when plots of the other category were viewed carefully. Figure 5-21 to Figure 5-28 are plots of χ versus T and χ versus branch content of LDPE for both LDPE/HLLDPE and LDPE/OLLDPE blends with LDPE branch content of 30 (Figure 5-21 to Figure 5-24) and 40 (Figure 5-25 to Figure 5-28). From χ versus branch content of LDPE plots, it can be seen when branch content of LDPE is above 30, some relatively large χ values were obtained at low LLDPE branch content side, indicating immiscibility. Figures 5-22, 5-24, 5-26 and 5-28 depict this picture. Thus, it could be concluded that the branch content of LDPE might be deterministic on the phase behavior of these blends. When branch content of LDPE exceeds 30 branches per 1,000 long chain carbons, blends of LDPE/LLDPE may phase-separate. It is interesting that even both components bear the same branch content (above 30), the LDPE/LLDPE blends may still phase-separate (due to relatively large χ values), indicating that the branch content may not be the only factor that dominates the phase behavior of the blends. Therefore, it is advised that LDPE at low branch content level (below 30) is preferred when LDPE/LLDPE blends are being made provided that thermodynamic stability of the blends is desired.

When the plots of χ versus temperature of LDPE/LLDPE blends for high LDPE branch contents (above 30) are being examined, a maximum at around 227 ^{o} C can be spotted immediately for all of the curves on these plots irrespective of the branch content of LLDPE. Figures 5-21, 5-23, 5-25 and 5-27 describe this observation. This implies that LDPE/LLDPE blends with high LDPE branch contents seem to have a closed-loop phase diagram. This phenomenon has already been

observed for HDPE/LDPE blends as discussed before, suggesting that the characteristics of LDPE play a major role in determining the shape or type of the phase diagram of the blends when LDPE gets involved with any other type of polyethylene.

Figure 5-21 χ vs. T for Blends of HLLDPE/LDPE-with-30-branches

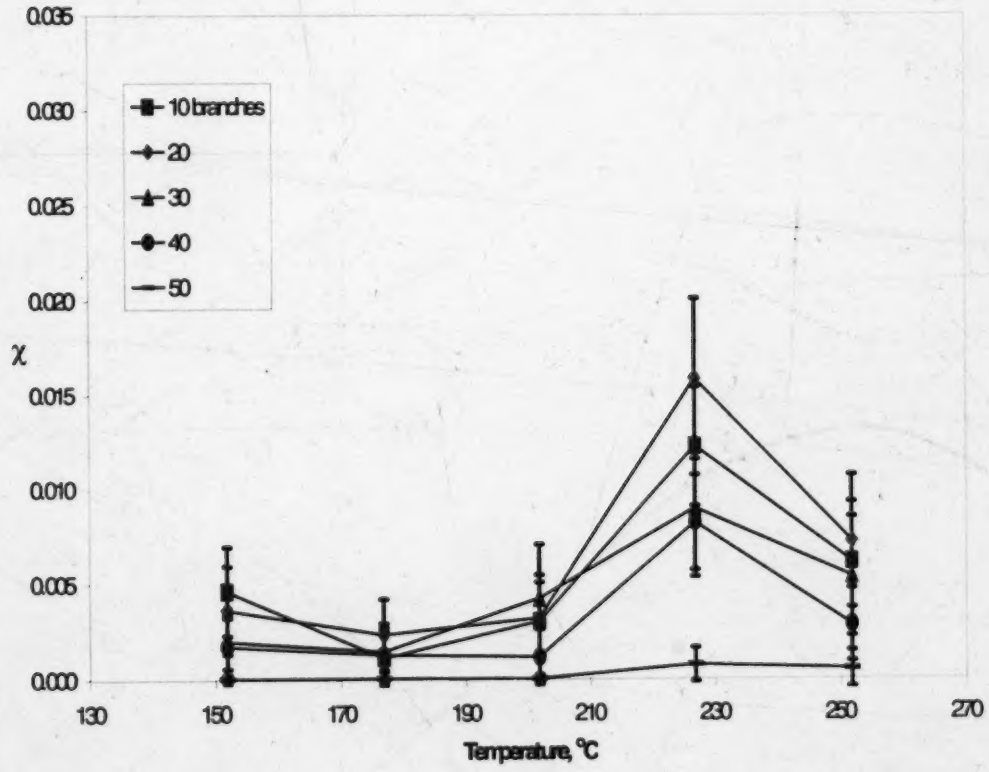

Figure 5-22 χ vs. HLLDPE Branch Content for HLLDPE/LDPE-with-30-branches

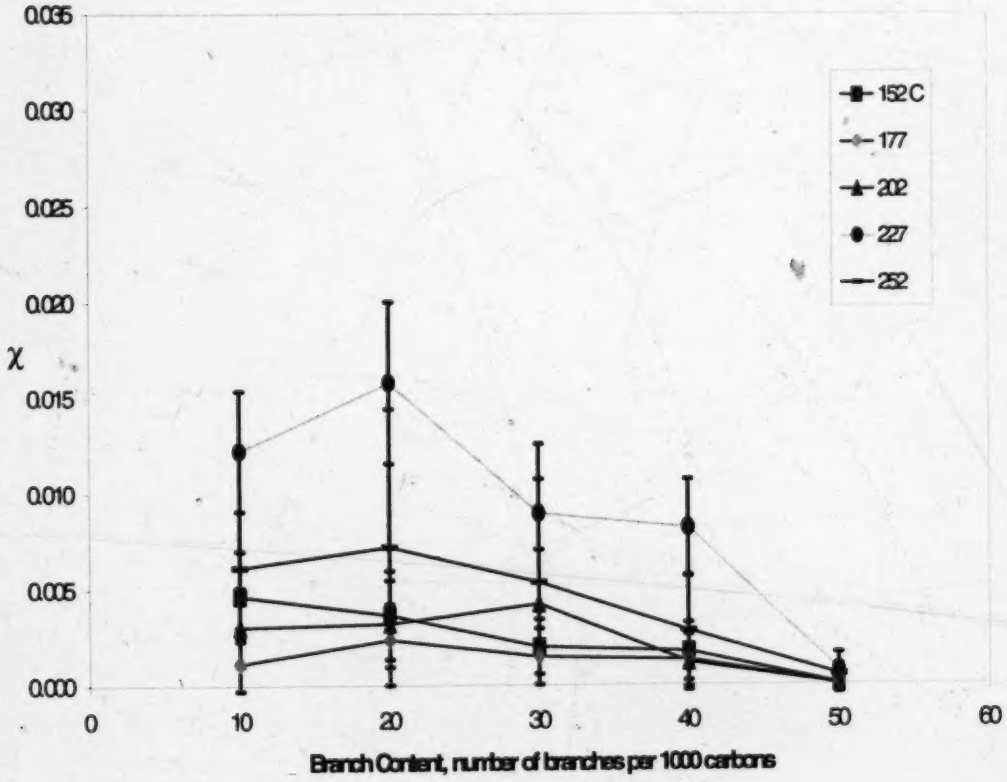

Figure 5-23 χ vs. T for Blends of OLLDPE/LDPE-with-30-branches

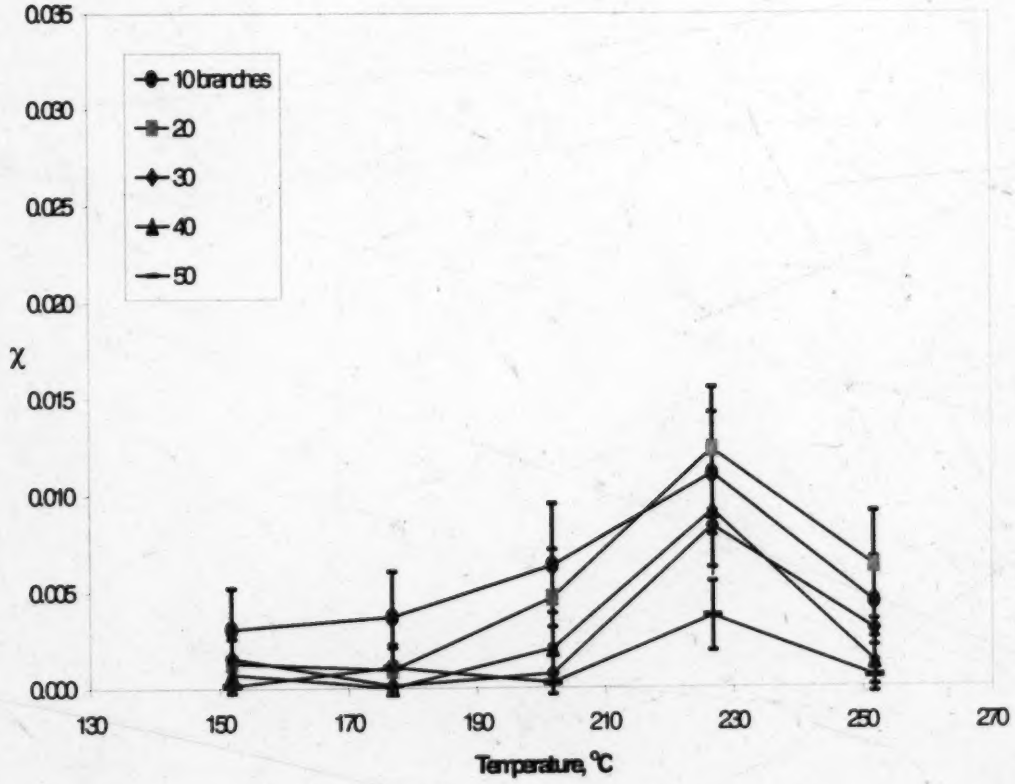

Figure 5-24 χ vs. OLLDPE Branch Content for OLLDPE/LDPE-with-30-branches

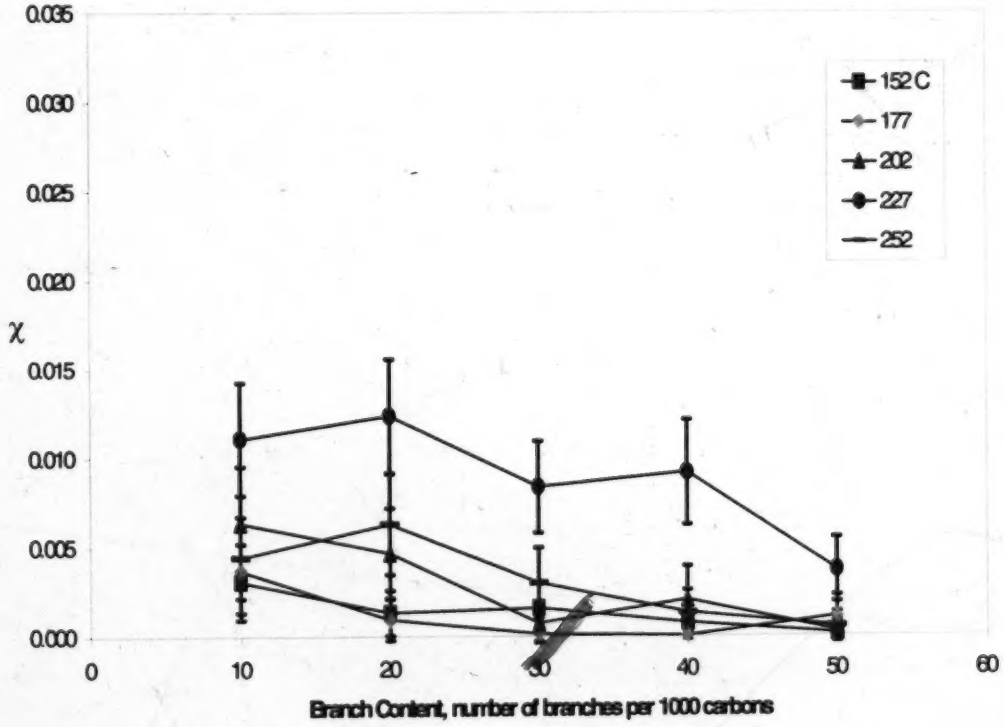

Figure 5-25 χ vs. T for Blends of HLLDPE/LDPE-with-40-branches

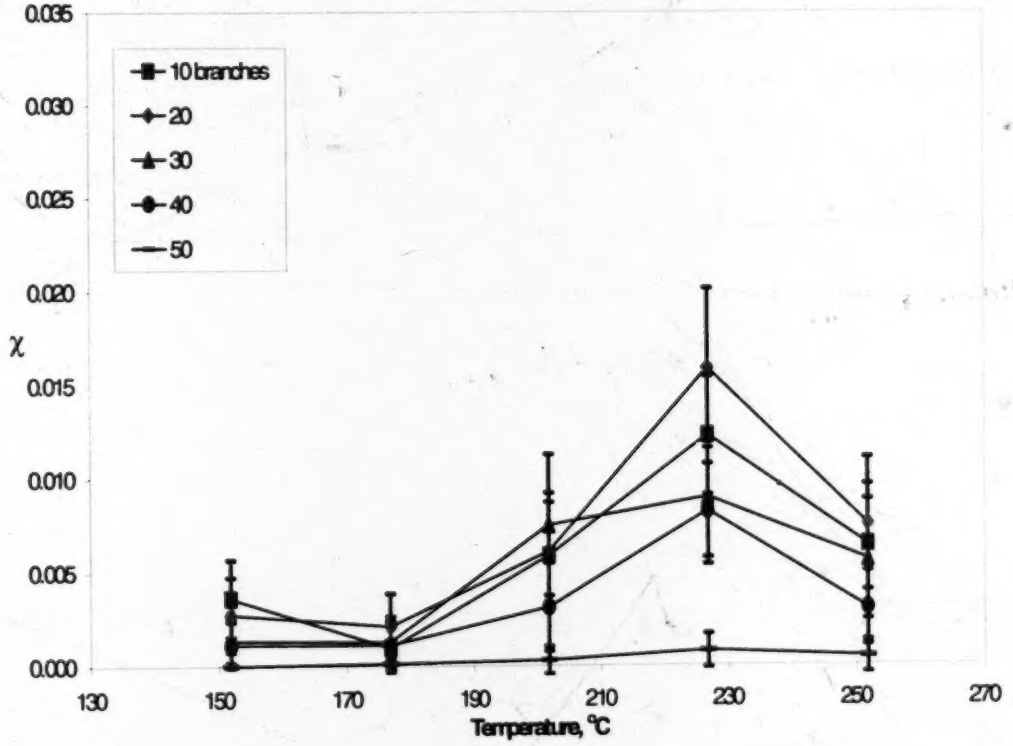

Figure 5-26 χ vs. HLLDPE Branch Content for HLLDPE/LDPE-with-40-branches

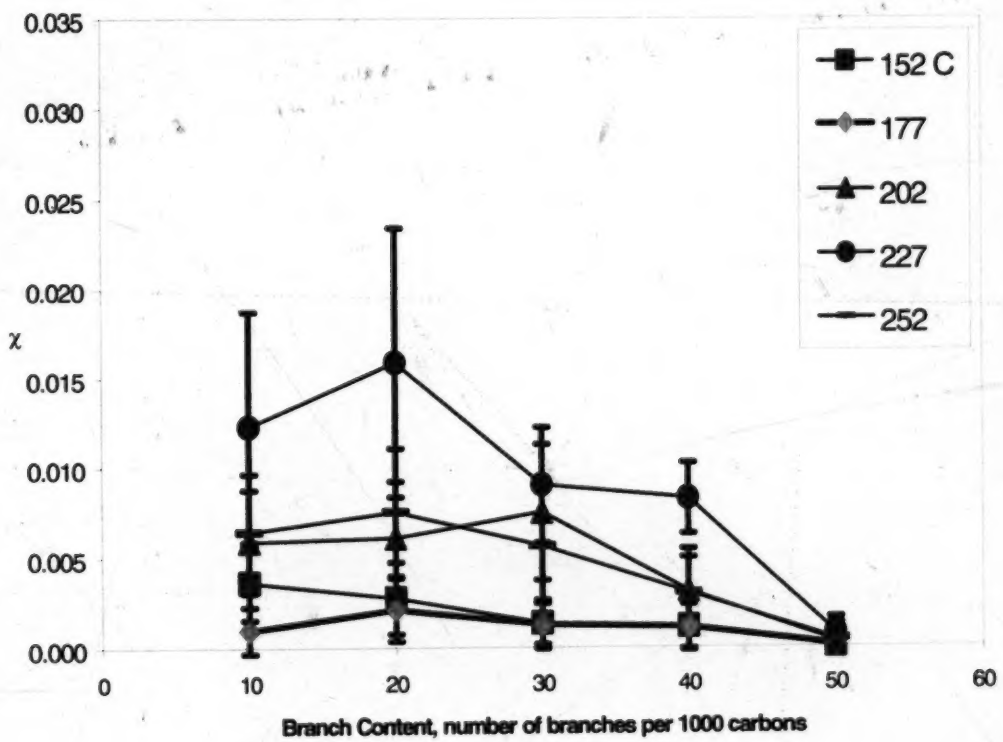

Figure 5-27 χ vs. T for Blends of OLLDPE/LDPE-with-40-branches

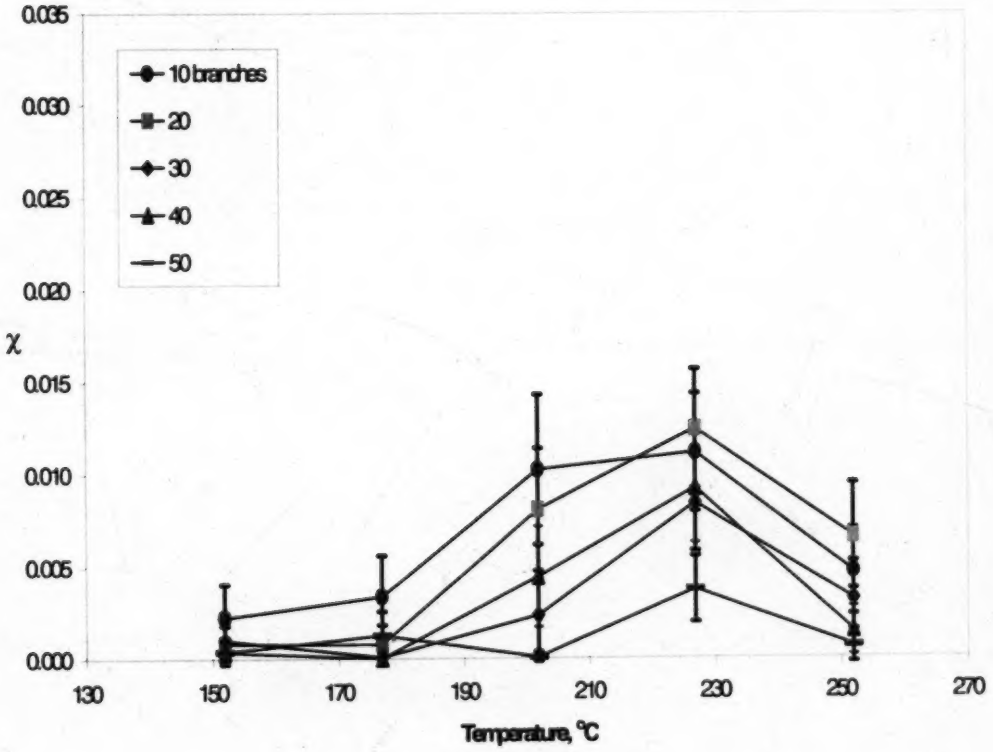

Figure 5-28 χ vs. OLLDPE Branch Content for OLLDPE/LDPE-with-40-branches

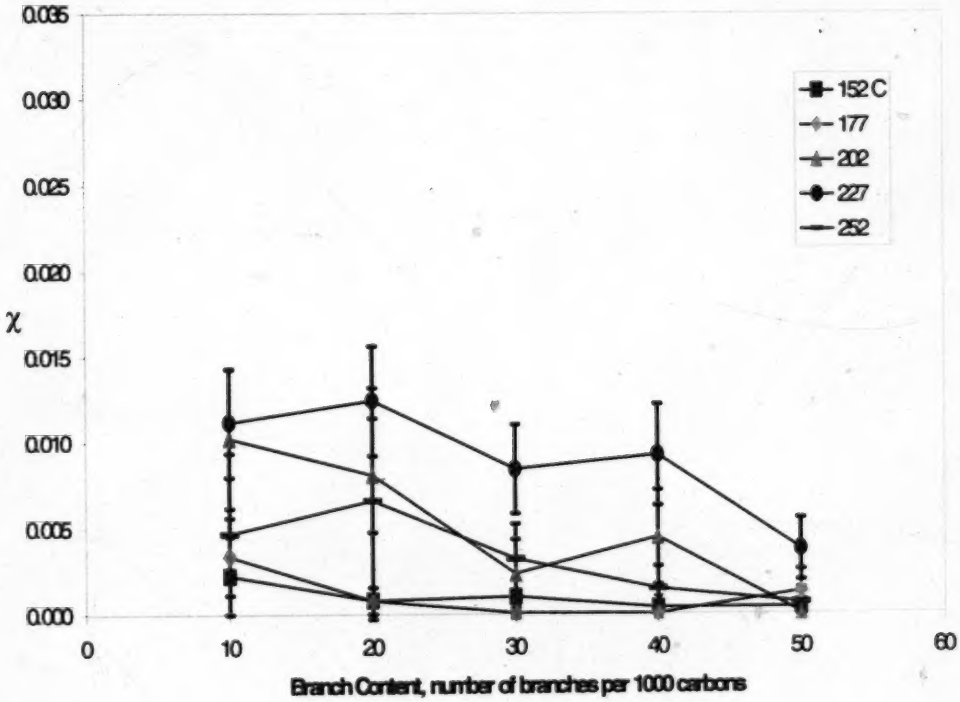

It is worth pointing out that the values of χ calculated for both HDPE/LLDPE and HDPE/LDPE blends are higher than those for LDPE/LLDPE blends even at high LDPE branch contents (pay attention to the scale of these plots). This indicates that LDPE/LLDPE blends are more miscible than HDPE/LLDPE and HDPE/LDPE blends. This is somewhat expected because both LLDPE and LDPE carry some kind of branching characteristics so that they have similar molecular interaction (CH_2 or non-CH_2 groups) energies.

These calculation results are essentially in agreement with Hill and Puig's TEM and DSC experimental results on the samples quenched from the melt. In their study, the branch content of LLDPE (octene-based) was reported to be 15 branches per 1,000 backbone carbons while the branch content of LDPE was reported to be 26 branches per 1,000 backbone carbons with 10 long branches and 16 short branches [Hill and Puig, 1997]. At first sight, it seems that the branch content level of LDPE used in their study is below the critical value that I have suggested, around 30. However, the polymers used in their study must have much more complicated molecular weight distribution as well as branch distributions than my simple models. Nonetheless, they carried out their experiments within the temperature range from 110 to 190 °C while my studies range from 152 to 252 °C. The phase-separated temperature range suggested from their phase diagram seems lower than what I suggest here. This also may be attributed to the molecular structure differences between the polymers used in their and the models used in my studies.

Chapter 6

Scanning Electron Microscopy

6.1 Introduction

Under the pressure to expedite development of modern technology, morphological or structural observations of materials at the micron (μm) or submicron level have been greatly needed for the last few decades. Therefore, advanced microscopy techniques have been developed for these needs. The scanning electron microscopy technique is one of the powerful tools developed for these purposes.

A description of a scanning electron microscope (SEM) appeared in the literature in the late 1930's but such a microscope was not commercially available until 1965, offered by the Cambridge Scientific Instruments (Mark I Instrument). The SEM and the electron probe microanalyzer (EPMA) are two powerful tools that can be used to observe and characterize heterogeneities of organic and inorganic materials on such a micron scale. The main interest in SEM examination is the signals of secondary and backscattered electrons in that these signals change due to the differences in surface topography when the electron beam is swept across the specimen. However, in EPMA, the major analysis of radiation is the characteristic x-rays that are emitted due to the electron bombardment. Therefore, EPMA can provide both qualitative and quantitative compositional information of the specimen at the micron level.

The SEM is one of the most versatile instruments used for the examination and analysis of the microstructural characteristics of solids. Examinations of micro-features with high-resolution at the order of 5 nm can be achieved by SEM. Another important advantage of the SEM is its large depth of field, as a result, producing the three-dimensional appearance of the specimen image. This gives users much information about the specimen and distinguishes SEM from other microscopy techniques. In contrast, the transmission electron microscope (TEM) can provide very detailed information for very thin samples but it will be tedious to use TEM to reconstruct the three-dimensional surface images easily obtained by SEM.

The EPMA is considered to be one of the most powerful instruments for the microanalysis of inorganic and organic materials. It is useful because compositional information can be obtained from the specimen using characteristic x-ray lines with a spatial resolution of the order of 1 μm. Nowadays, advanced SEM instruments are usually equipped with this x-ray analyzer, so that EPMA comes along with the whole SEM package.

In the late 1960's or early 1970's, reports on its applications to polymer field, mainly adhesives and coatings, were seen in the literature [Princen, 1971].

6.2 The Working Principle of SEM

The working principle of SEM is comparable to common optical microscopy instruments. In the latter, an image is produced by the interaction between a light beam and the specimen while in the SEM it is created by the interaction between an electron beam and the specimen. In fact, both electron and light beam could be

considered as particles or as propagating waves in space. The primary feature of the SEM is that the SEM image is formed point by point by scanning an electron beam (probe) across the specimen.

The SEM consists of electron gun (equivalent to light source in an ordinary optical microscope) and magnetic lenses (equivalent to lenses in an ordinary optical microscope). Resolution and contrast are two key parameters in microscopy studies. Resolution is the minimum distance between two object features at which they can still be seen as two distinct features while the contrast of a feature is the fractional change in image brightness.

While the contrast of features in an ordinary optical microscope comes from the differences of refractive index of the components composing the specimen, showing light and dark image regions, the contrast in the SEM comes from the differences of the surface topography and/or chemical composition (elements), showing bright and dark regions. It is known that hydrocarbon polymers show little compositional contrast in SEM because of the low atomic numbers of the elements they contain. Thus, the SEM is not generally useful in the studies of polyolefin blends unless the composition contrast can be enhanced in certain ways (for example, putting tracer particles in one of the blend components in this thesis work). The compositional contrast feature in the SEM is mainly used in studies of metallurgic materials for element mapping, and the topographic contrast feature of the SEM is widely used in the morphological investigations of polymer mixtures.

It is obvious that examinations of mixtures containing components with similar refractive index like polyethylene blends in melt state cannot be done by using

ordinary microscopy techniques. However, with appropriate preparation of PE blend samples, the SEM should be able to draw information of the phase behavior of the blends by carefully observing the morphology of the fracture surface features of samples of a bulk material. If the sample is biphasic in nature, the interfacial features (for example, weak adhesion) of the sample should appear on the surfaces of the broken sample of the bulk materials, and the SEM is able to detect these surface feature differences.

Imaging signals in the SEM are coming from both the backscattered and secondary electrons. Backscattered electron image (BEI) has compositional contrast with low resolution about 1 μm and it is a powerful tool to determine the chemical composition of a material by use of x-ray microanalysis. However, secondary electrons are emitted from the specimen with low energy so that they come from the top few nanometers of the material [Goldstein et al., 1992]. Thus, in the polymer field, high-resolution topographic SEM images are primarily produced by secondary electron scattering. Early SEM applications in the polymer field were reviewed by White and Thomas [1984].

6.3 Introduction to Morphological Studies of Polyolefin Blends via SEM

In general, microscopic investigation is preferred to determine the phase behavior of polymer blends by morphological observations. Optical microscopy of polymer morphology is easy and inexpensive. There are many reports of using this technique in polyethylene blend studies (mainly in the studies of crystalline characteristics) but it is limited by its low magnification and resolution, especially for

weak phase contrast polymer blends in the liquid state. Microscopic investigation of polyethylene blends in the melt is very difficult to carry out or give an unambiguous view because of the small difference between the two refractive indices and the similar chemical compositions of the components.

The specimen preparation for scanning electron microscopic experiment is rather simple and the data interpretation is straightforward. Therefore, the SEM technique has been widely used in polymer morphology studies in the last few decades. However, the SEM studies were mainly restricted to the observations of morphologies of materials in solid state. The miscibility studies of polymer blends in the melt state by SEM have to be inferred by examining the solid state morphology of samples quenched from the melt.

Gupta et al. [1992] studied the tensile and flexural properties and the morphology after tensile fracture of solid-state HDPE/LLDPE blends. The HDPE used in their study had a density of 0.952 g/cm^3 while the LLDPE had a density of 0.924 g/cm^3. The LLDPE was a copolymer of 1-octene and ethylene, but the branch content of LLDPE (1-octene percentage) was not reported. The authors found that the composition of blends played a role in determining these properties. It was reported that in the middle range of compositions, i.e., 40-60% LLDPE, the blends showed an increase of ultimate tensile strength and tensile modulus with increasing the proportion of LLDPE. This phenomenon was attributed to the involvement of the LLDPE component in co-crystallization with HDPE. The SEM pictures showed that there were some obvious transverse connections between the fibrils that were argued

due to the intercrystalline LLDPE phase. Gupta et al. suggested that LLDPE would play a role in reducing the weakness in the transverse direction through fibrillation.

In the polyethylene industry, films are produced in large amount with LLDPE as reviewed in Chapter two. In general, the LLDPE with higher density produces stiffer films but the dart impact resistance is reduced. Therefore, studies on increasing the properties (say, stiffness and/or dart impact resistance) of films by blending polystyrene into LLDPE were reported in the literature with investigations of both mechanical property and morphology of the blends. Sato et al. [1994] studied the blends of LLDPE with high impact polystyrene (HIPS). They found that the stiffness would increase with increasing the amount of HIPS while the dart impact and machine direction tear resistance decreased not very much. It was attributed to the presence of a rubber in HIPS which was believed to behave as a compatibilizer. The SEM pictures showed that the HIPS phase was imbedded as spheres in the LLDPE matrix for compression-molded samples but for a blown film it looked fibril-like in the machine direction and stick-like in the transverse direction. After the styrene phase was etched out, the stick-like features disappeared and, instead, hole-like features were left on the SEM micrographs, confirming that the stick-like features were HIPS.

It is known that most polymer blends are immiscible or incompatible and thus bear poor mechanical properties due to the weak adhesion between phases. Usually, the phase morphology created during the processing stage has a strong influence on the performance of the blends. For example, the impact properties of films are controlled by the droplet size and shape of the dispersed phases [Wu, 1985; Hobb,

1986]. Therefore, it is important to know how morphologies develop during processing. Yang et al. [1994] studied blends of LLDPE and polystyrene mainly for the purpose of investigating the morphological developments during compatibilized and noncompatibilized blending of these components, and the effects of processing conditions, composition, and compatibilizers upon the size and distribution of the dispersed phase. They concluded by examinations of the SEM micrographs that adding compatibilizers (block copolymers) to the blends reduces the interfacial tension between the immiscible components, resulting in smaller average size of the dispersed droplets. However, the characteristic morphologies for both compatibilized and noncompatibilized blending of the components were quite similar. They also indicated that the viscosity ratio would have no significant effect on the size of the dispersed particles for lower polystyrene content blends (20% polystyrene). However, blends with viscosity ratio far away from unity would result in a broader size distribution for the dispersed phase.

Bourry and Favis [1998] studied the morphology development of HDPE and polystyrene blends by SEM during twin-screw extrusion and found that the size and size distribution of the dispersed phase were independent of the mixing procedure in terms of the different methodologies of the addition of the polystyrene component. Based on the results, they suggested that the final blend morphology would not depend on the melting or softening step, but would be determined in the melt state. It was explained that the morphology of the dispersed phase was developed so rapidly in the melt so that it was essentially the last flow environment experienced by the blend that would determine its final morphology. This is in contrast with the conclusions

that the most significant morphology development of a polymer blend occurs during the first few minutes of mixing, when melting and softening of the materials are also occurring [Han, 1973]. This indicates that the mechanism of morphology development during mixing needs further investigations.

Guo et al. [1998] investigated the effect of compatibilizers (di- or tri-block copolymers of ethylene and styrene) on the LDPE/PS blends using SEM and mechanical measurements. They found that the coalescence rate of the dispersed phase in the blend during annealing could be very fast but a suitable block copolymer compatibilizer could significantly reduce the coalescence rate or even effectively suppress coalescence and thus stabilize the morphology of the blend. The phenomenon was attributed to the smaller interfacial tension between the components due to the presence of the compatibilizer and to the steric interactions of the copolymer chains at the interface, i.e. entangling with the chains of both components.

Mekhilef and Verhoogt [1996] studied several polymer blend systems involving polyethylenes by SEM to investigate the phase inversion and dual-phase continuity phenomena. They indicated that co-continuity would usually be achieved at the phase inversion point for a two-phase polymer blend but the mechanical properties might not be the simple additive contributions of the components due to the weak interfacial interactions. However, if suitable interfacial modifiers (compatibilizers) were introduced to the blend system, co-continuous structures and improved mechanical properties could be achieved simultaneously. The SEM micrographs showing the continuous change of morphology for two-phase polymer blends were quite clear and convincing.

Wang et al. [1998] developed a new method to stabilize the LDPE and PS blends system by a two-step cross-linking process. In their approach, the LDPE was first cross-linked partially and then was melt-blended with PS. A styrene-butadiene-styrene block copolymer (SBS) was finally added to the melt and mixed and they referred to the process as the two-step cross-linking process. They indicated that at the final mixing stage, the residual free radicals in the LDPE would react with SBS, resulting in significant improvement of the impact strength, tensile modulus and elongation-at-break. Based on the observations of the SEM examinations, they contended that the interfacial adhesion increased significantly although the domain sizes did not differ significantly from with the non-cross-linked system.

Rana et al. [1998] studied blend systems of HDPE with metallocene LLDPE polyethylene (MCPE) and HDPE with polypropylene (PP) by thermal, mechanical and morphological examinations. Based on their results, they indicated that the morphology of HDPE/MCPE blends at whole composition range was more homogeneous than that of HDPE/PP systems. The morphology of HDPE/MCPE would become more heterogeneous when the proportion of MCPE was increased from about 30% MCPE. They concluded that both HDPE/MCPE and HDPE/PP systems would be thermodynamically immiscible but HDPE was more compatible with MCPE than with PP.

From the above studies, it can be seen that the morphologies of immiscible blend systems can be characterized by the SEM technique efficiently because interfacial characteristics (weak adhesion) of the immiscible blends will be reflected

in the fracture surfaces, resulting in characteristic topography which can then be detected by the SEM technique. In Chapter 2, the possibility of inferring the melt state miscibility from solid state morphology by a quenching approach was reviewed and discussed in considerable detail. Therefore, it was reasoned that if polyethylene blend systems are biphasic in nature in the melt state, the SEM technique might be able to detect the phase behavior of the blends from the quenched samples regardless of the refractive index similarity of the components. Based on this consideration, I carried out SEM exploration of the melt miscibility of polyethylene blends, which has been rarely seen in the literature.

6.4 The Procedure of SEM Examinations in the Thesis Work

6.4.1 Melt-blending

All samples for SEM examinations were melt-blended using a Haake Rheocord 90 mixer with two counter-rotating blades. Selection of the blending conditions is essentially based on a two-level four-variable fractional factorial experimental design for a previous study of LLDPE and LDPE blends [Hussein et al., 1997]. The blending temperature was chosen at 190 and 230 °C depending on the research interests while blending time was chosen to be 10 minutes. The melt-blended samples were removed from the mixer and allowed to be cooled down to room temperature naturally. To remove the thermal and mechanical history experienced in the mixer, all samples were held in an oven for annealing at 160 °C for one hour before the final specimens for SEM examinations were made. Then the samples were quenched into liquid nitrogen for about 5 minutes immediately after being removed

from the oven. However, in one case, a specimen was made by turning off the oven with the samples held at 160 °C in the oven and letting the samples cool down with the oven temperature decreasing itself, to examine the cooling procedure effect.

6.4.2 The SEM Examinations

All SEM observations were carried out on a HITACHI S-2700 Scanning Electron Microscope equipped with a Link eXL, Energy Dispersion X-ray Analysis System (EDX), i.e., the EPMA system as described before, operated by Tina Barker. The SEM specimens were made by annealing the blend samples in an oven at 160 °C for one hour and then quenched in liquid nitrogen immediately after being withdrawn from the oven. The fracture surfaces were created by breaking the liquid-nitrogen-cooled samples with a hammer. In order to make them conductive, the fracture surfaces of the specimens were coated with carbon and then examined in the SEM. Both backscattered electron and secondary electron imaging methods were employed. The electron beam voltage used throughout our SEM experiments was chosen at 10 and sometimes 20 kv.

Chapter 7

SEM Observations of Polyethylene Blends

7.1 Composition Effect on the Morphology of HDPE/LDPE, HDPE/LLDPE and LLDPE/LDPE Blends

7.1.1 Materials and Experiments

Both HDPE/LDPE and HDPE/LLDPE blend samples with HDPE composition (Φ) of 0, 25, 50, 75 and 100% were made to study the composition effects on the morphology of these blends. LDPE/LLDPE blend samples with LLDPE composition of 0, 25, 50, 75, 100% were also studied. The characteristics of the polymers used in this study are listed in Table 7-1 while the blend sample annotation is shown in Table 7-2.

Table 7-1 Characteristics of PE Samples from Nova Chemicals

Polymer	M_w	M_w/M_n	Branches/1000 C
LDPE	99 K	5.8	22
HDPE	137 K	4.89	~0
LLDPE*	105 K	3.57	N/A

*Copolymer of 1-butene and ethylene.

Table 7-2 The Annotation of Blend Samples

Sample	Description
1	0 % HDPE in HDPE/LDPE blend (pure LDPE)
2	25 % HDPE in HDPE/LDPE blend
3	50 % HDPE in HDPE/LDPE blend
4	75 % HDPE in HDPE/LDPE blend
5	100% HDPE in HDPE/LDPE blend (pure HDPE)
6	0 % HDPE in HDPE/LLDPE blend (pure LLDPE)
7	25 % HDPE in HDPE/LLDPE blend
8	50 % HDPE in HDPE/LLDPE blend
9	75 % HDPE in HDPE/LLDPE blend
10	25% LLDPE in LLDPE/LDPE blend
11	50% LLDPE in LLDPE/LDPE blend
12	75% LLDPE in LLDPE/LDPE blend

The blend samples were prepared by melt blending using a Haake Rheocord 90 mixer with two counter-rotating blades. No extra antioxidant was added during mixing. The blending conditions were chosen at: a temperature of 190 °C; a speed of counter-rotating blades at 50 rpm and a blending time of ten minutes. The selection of the blending conditions was essentially based on a two-level four-variable fractional factorial experimental design for a previous study of LLDPE and LDPE blends [Hussein et al., 1997]. See Chapter 6 for the SEM specimen preparation procedure.

7.1.2 Results and Discussion

Figure 7-1 to Figure 7-5 are SEM pictures of samples 1-5, HDPE/LDPE blends prepared with the blending conditions as described above. From the pictures, it seems that there is a continuous change of morphologies with increasing HDPE content. The morphologies of the two pure components, i.e. LDPE (Figure 7-1) and HDPE (Figure 7-5), are very much different. There are some fiber-like features in the SEM micrographs of LDPE. In contrast, the morphology of HDPE is more flat. It can be seen that from 50-100 % HDPE content, the morphologies of the binary blends are more or less similar to that of pure HDPE. However, it is difficult to infer the melt miscibility between the components from these pictures. The morphology of these blends is obviously different from that of the typical immiscible blend, near-spheres of the minor phase dispersed in the matrix of the major phase. Therefore, at this resolvable domain size scale, it can be reasoned that no phase separation could be detected for the blends studied. These results are in agreement with those predicted from my MD simulations. The LDPE used in this study has a branch content of 22 that is below the cut-off value of branch content of LDPE, around 25-30, for the blends of HDPE/LDPE to phase-separate, found by MD simulations as presented in Chapter 5, previously.

Figure 7-6 to Figure 7-9 are SEM pictures of samples 6 to 9, HDPE/LLDPE blends with HDPE composition at 0, 25, 50 and 75 percent, (see also Figure 7-5 for 100% HDPE). There is also a continuous change of morphology with increasing the content of HDPE. LLDPE displays an inherent particulate nature, probably because of its two-component nature (linear and branched molecules together) [Hill and Puig,

1997; Wardhaugh and Williams, 1995; Mirabella et al., 1988; Channell et al., 1994;]—see Figure 7-6. Thus, the complexities of the morphologies of the PE blend with LLDPE involved might be an indication of co-existing multiple phases.

It is worth mentioning that it seems that the morphology of HDPE does not change significantly with changing the molecular weights of HDPE in the study.

Next, it is natural to wonder whether the type of branching (LDPE vs. LLDPE) influences the morphology in HDPE. It is easiest to consider the two 50% blends described by Figure 7-3 (HDPE/LDPE) and Figure 7-8 (HDPE/LLDPE). It can be seen that the morphology of the blends of HDPE/LDPE is much different from that of HDPE/LLDPE, indicating that the microstructure (i.e., the branch type) of branched polyethylene molecules (including LDPE and LLDPE) affects the morphology of their blends with HDPE significantly. However, simple conclusions can not be drawn regarding the miscibility between the components based only on the SEM studies because the morphologies of these blends are much different from that of typical immiscible blends such as polyethylene-polystyrene [Wu, 1985; Hobb, 1986; Bourry and Favis 1998; see also Figure 7-17 and Figure 7-18].

Figure 7-10 to Figure 7-12 are SEM pictures of samples 9 to 12. From these pictures, we can see that the morphologies of these blends are quite fiber-like, which is different from the morphologies of HDPE/LDPE blends and close to the morphologies of HDPE/LLDPE blends.

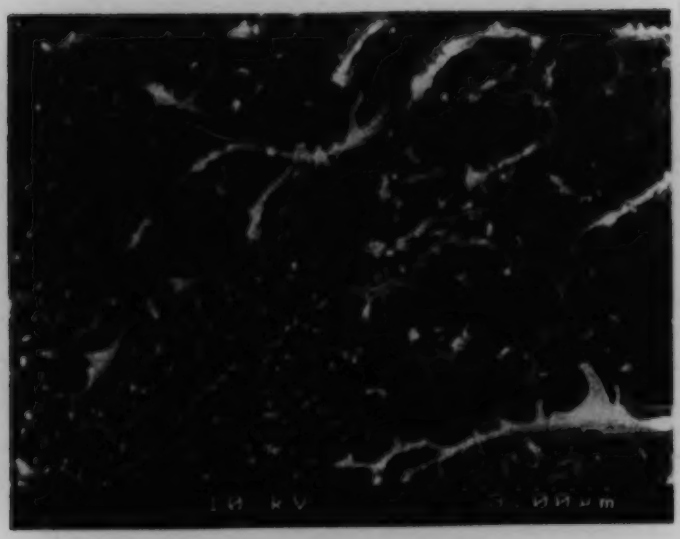

Figure 7-1, SEM Picture of Pure LDPE, Sample 1

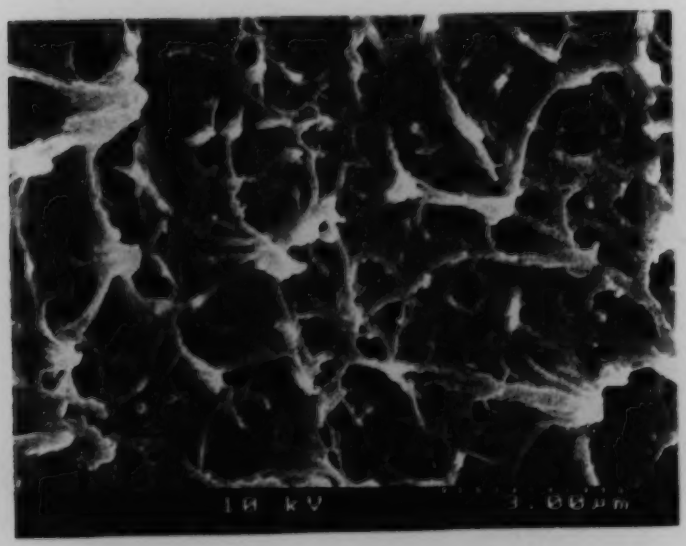

Figure 7-2, 25% HDPE in LDPE, Sample 2

Figure 7-3, 50% HDPE in LDPE, Sample 3

Figure 7-4, 75% HDPE in LDPE, Sample 4

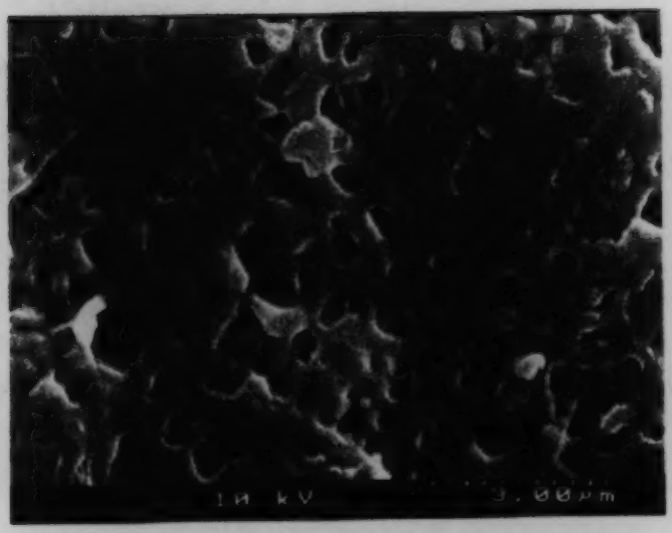

Figure 7-5, Pure HDPE, Sample 5

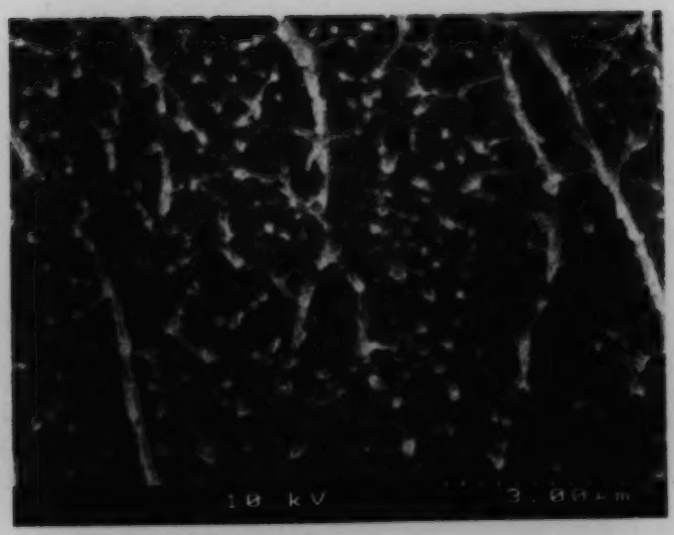

Figure 7-6, Pure LLDPE, Sample 6

Figure 7-7, 25% HDPE in LLDPE, Sample 7

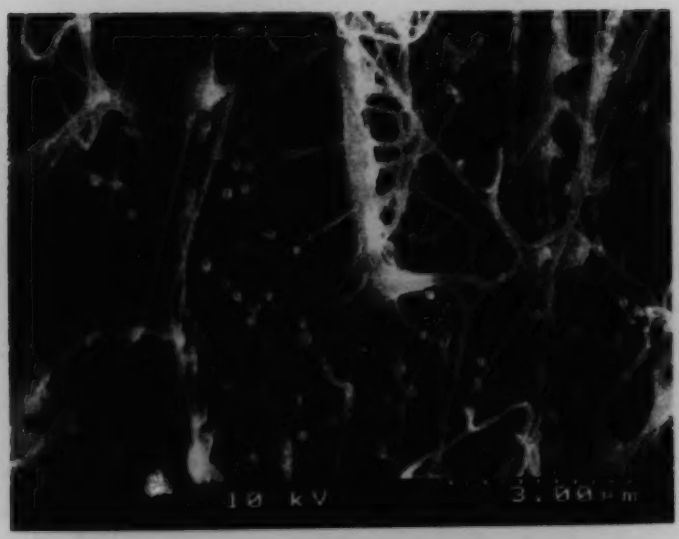

Figure 7-8, 50% HDPE in LLDPE, Sample 8

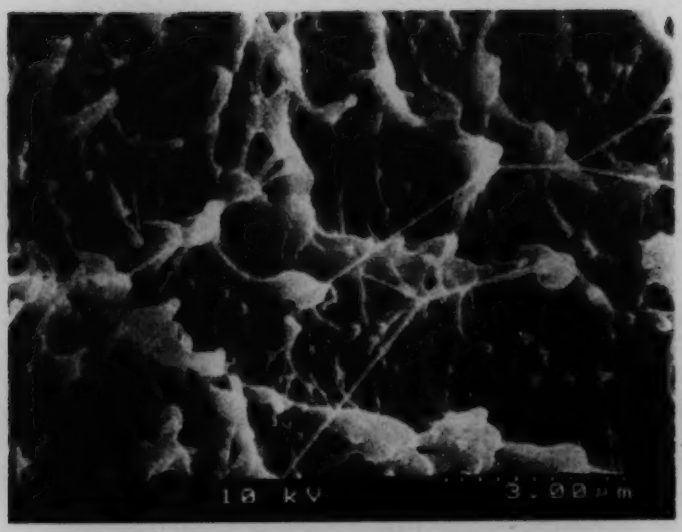

Figure 7-9, 75% HDPE in LLDPE, Sample 9

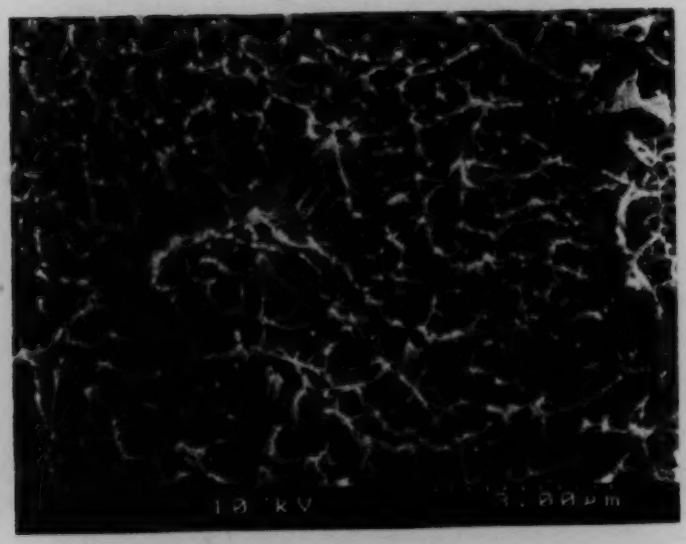

Figure 7-10, 25% LLDPE in LDPE, Sample 10

Figure 7-11, 50% LLDPE in LDPE, Sample 11

Figure 7-12, 75% LLDPE in LDPE, Sample 12

7.2 Tracer Studies on the Phase Behavior of Polyethylene Blends

7.2.1 HDPE/LDPE Blends-A Special Case

In order to enhance the compositional contrast in SEM observations, tracers were added into polyethylene blends through different approaches. In one case, for a blend of LDPE with a special type of HDPE produced by Nova Chemicals Corp. and hereafter denoted HDPE^{+}, a surprising morphology of the tracer distribution in the blend was found. The tracer particles were found unevenly distributed in the blends, indicating a two-phase PE blend (as is shown below). The observed morphology for this special case is unexplainable so far. I was not able to produce this result by using other kinds of HDPE resins. However, I believe that it is worth reporting this observation.

7.2.1.1 Materials

The characteristics of the samples used in this study are shown in Table 7-3. The tracer used in this study, powders of barium sulfate ($BaSO_4$), is a SIGMA commercial product, B-3758, Lot 94H0251 and was used as received. Barium sulfate was used because it is inexpensive and the atomic number of barium is much larger than that of carbon and/or hydrogen, which is easily seen in a PE material and enhances the polyethylene phase contrast provided that the tracer particles reside only in either phase.

Table 7-3. Characteristics of PE Samples From Nova Chemicals

Sample	M_w *	M_w/M_n*	Branches/1000 C
HDPE+	291K	4.4	0
LDPE	99K	5.8	22

* Molecular Weights were measured by GPC calibrated with HDPE standards obtained from NIST.

7.2.1.2 Variations in Sample Preparation Methods

Blend samples were made by melt blending using a Haake Rheocord 90 mixer as before. The blending conditions were: temperature at 190 °C for most samples and 230 °C in one case; a speed of counter-rotating blades at 50 rpm and a blending time of ten minutes. All blend samples were prepared at the above conditions and cooled to room temperature in air after they were removed from the mixer. Then the specimens for SEM examinations were prepared by holding the samples (prepared based on the above conditions) in an oven at 160 °C for one hour and then cooled from the melt by either quenching or slow cooling as explained below. Refer to Table 7-4.

Sample A is the HDPE+ mixed with 10% $BaSO_4$ at 190 °C for 10 minutes. It was cooled by quenching the sample into liquid nitrogen immediately after being removed from the oven at 160 °C. Sample B is a blend of 20% A and 80% LDPE blended at 190 °C for 10 minutes. It was cooled by shutting down the oven kept at

160 °C and letting the sample cool to room temperature within the oven (slow cooling method). Sample C was basically the same as sample B but it was cooled by quenching the same as sample A. Sample D was a blend of 20% A and 80% $HDPE^+$ (without $BaSO_4$ in it) blended at 190 °C for 10 minutes. It was cooled by quenching the sample into liquid nitrogen immediately after being removed from the oven at 160 °C. Sample E was a blend of 20% A and 80% LDPE blended at 230 °C for 10 minutes. It was quenched using the same way as in the preparation of samples A, B and D.

Table 7-4. Sample annotation *

Sample	Conditions of sample preparation
A	$HDPE^+$ with 10% $BaSO_4$ mixed at 190 °C, 50 rpm for 10 minutes (quenched, see text)
B	20% A and 80% LDPE (slowly cooled, see text)
C	Same blend as sample B (quenched, see text)
D	20% A and 80% $HDPE^+$ (without BaSO4), blended at 190 °C, 50 rpm for 10 minutes (quenched, see text)
E	20% A and 80% LDPE, blended at 230 °C, 50 rpm for 10 minutes (quenched, see text)

* NOTE: All the percentages shown in the table are by weight.

The SEM investigations were carried out using the same equipment, with a specimen preparation procedure similar to that detailed in the last section. The tracer composition was confirmed using EDX and the particle sizes were roughly measured with the SEM. Both backscattered electron and secondary electron imaging methods were employed. The micrographs are following, Figure 7-13 through Figure 7-17.

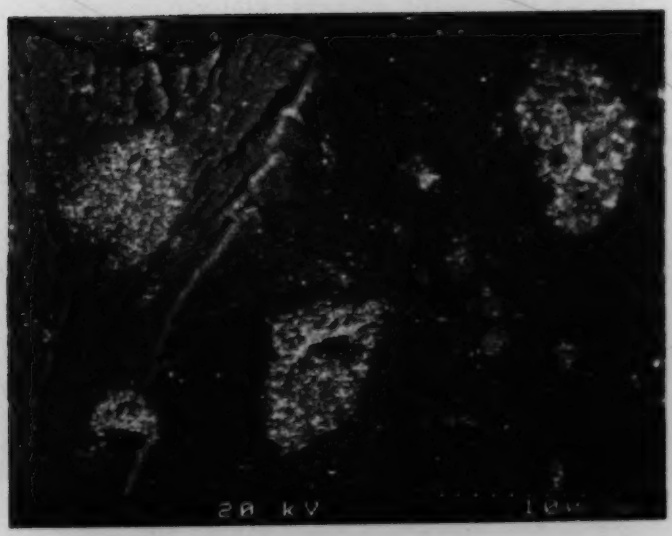

Figure 7-13 SEM Picture of Sample B

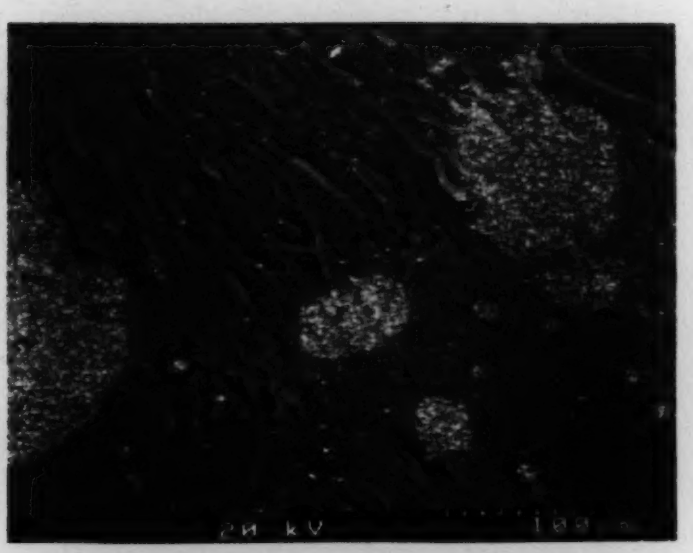

Figure 7-14 SEM Picture of Sample C

Figure 7-15 SEM Picture of Sample A

Figure 7-16 SEM Picture of Sample D

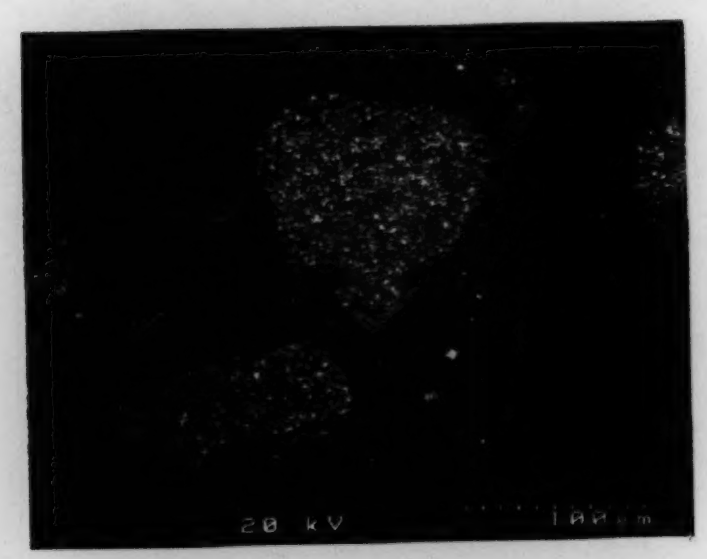

Figure 7-17 SEM Picture of Sample E

7.2.1.3 Results and Discussion

Figure 7-13 is the SEM picture of sample B. In Figure 7-13, $BaSO_4$ is dispersed in the blend as clusters. The average size of clusters is around 50 μm. Sample B is basically a 20% $HDPE^+$ and 80% LDPE blend but 10% $BaSO_4$ was mixed in the $HDPE^+$ component previously as a tracer. The rationale of using a tracer is that if HDPE and LDPE blends are phase-separated, the tracer might stay in the HDPE phase (or HDPE-rich phase if partial miscibility is the case when the two components are blended together). In fact, this hypothesis is in good agreement with the experiment results in Figure 7-13. The proportion of the areas concentrated with $BaSO_4$ takes a view which is roughly consistent with the $HDPE^+$ content in the blend. Therefore, it is reasonable to assume that the clusters are the $HDPE^+$ phase (or $HDPE^+$-rich phase if partial miscibility is applicable) while the continuous phase is LDPE. If the $BaSO_4$ were uniformly distributed in Figure 7-13, one could reason that the PE components were miscible and formed a single liquid phase.

Figure 7-14 is the SEM micrograph of the quenched sample, sample C (see text and Table 7-4 for reference). It shows a view similar to that of Figure 7-13 except that the clustering size is even a bit larger. This result conflicts with conventional thinking. Usually, for rapidly cooled samples, single-phase or smaller domain size morphology would be expected to be seen if a single phase melt is the case. [Hu et al.; Kyu et al, 1987]. The explanation of the result could be that the melt itself is phase-separated. When the melt is cooled down rapidly, the liquid state morphology is preserved and the tracer particles cannot get out of the $HDPE^+$ or $HDPE^+$-rich phase easily. For slowly cooled samples, there is more time for the tracer particles to

migrate from the $HDPE^+$ phase because of the concentration gradient of the tracer particles, so the sizes of the clusters can be smaller than those of the quenched samples. This result implies that the blend may be biphasic in liquid state as well as in solid states. This is in good agreement with Hill et al. 's study [1993-1999] except that the domain size is much larger than that of their reports, in which micron level domain sizes were reported, which cannot be explained.

In order to know if a phase-separation is caused by the tracer itself, sample D (20% A and 80% $HDPE^+$ without tracer) was prepared and examined by SEM. Figure 7-15 is the SEM micrograph of sample A that is the $HDPE^+$ mixed with 10% $BaSO_4$. From the picture, we can see that $BaSO_4$ particles are evenly distributed in the $HDPE^+$ matrix. Clusters of tracer particles were only found in the binary blends of $HDPE^+$ and LDPE. This could be an indication of phase separation of the components in the blend. In contrast, Figure 7-16 depicts an electron micrograph of sample D and uniform distribution of $BaSO_4$ particles in the whole $HDPE^+$ matrix is seen in the figure. The above results indicated that $BaSO_4$ would not contribute to the $HDPE^+$ and LDPE blend phase segregation; otherwise we could have seen clusters of HDPE/tracer in the SEM micrograph of sample D.

In addition, the effect of blending temperature on the phase behavior of $HDPE^+$ and LDPE blends has been investigated. 20% $HDPE^+$ with $BaSO_4$ was blended with 80% LDPE at 230 °C, 50 rpm for ten minutes. Figure 7-17 shows the micrograph of sample E. The picture is essentially the same as those of samples blended at 190 °C. The result indicates that the blending temperature under

investigation does not change the phase behavior of binary blends of $HDPE^{+}$/LDPE significantly.

7.2.2 Tracer Studies of Blends of Polystyrene and LDPE

In order to study the phenomenon of tracer particles clustered in local areas in previous binary blends of $HDPE^{+}$/LDPE, I compared my results of HDPE/LDPE blends with those of blends of polystyrene (PS) and LDPE that are well-known to be immiscible blends [Sato et al. 1994; Wu, 1985; Hobb, 1986; Bourry and Favis 1998].

The LDPE sample was the same as the one used in the previous study while the PS sample was a commercial product from Dow Chemicals, with molecular weight (number average), M_n of 200, 000.

Figure 7-18 and Figure 7-19 are SEM micrographs of binary blends of PS (20% by weight) and LDPE (80% by weight). The blending temperature was at 190 °C for 10 minutes. The sample in Figure 7-18 was made by immersing the blend into liquid nitrogen immediately after being drawn from the blender chamber while the sample in Figure 7-19 was made by annealing the blend in an oven at 160 °C for one hour and then quenched in liquid nitrogen. The micrographs (no tracer was needed) of these two samples show morphologies typical of immiscible polymer blends (minor phase in form of spheres) and the PS spheres in Figure 7-19 are bigger than those in Figure 7-18, indicating Ostwald ripening behavior.

Figure 7-20 and Figure 7-21 are SEM micrographs of blends of 20%PS and 80%LDPE, too. However, Figure 7-20 depicts a picture of a blend in which the tracer ($BaSO_4$) was mixed with PS (10% by weight) before PS was blended with LDPE,

while Figure 7-21 describes the scene of a blend in which the tracer was mixed with LDPE (10% by weight) before PS was blended with LDPE. From Figure 7-20 and Figure 7-21, we can see that the tracer particles were always trapped in the continuous LDPE phase regardless of the mixing procedures, indicating that the tracer has a tendency to stay in or migrate to a certain polymer phase, in this case LDPE rather than PS. This finding supports my previous conclusion that the tracer particle was trapped in the $HDPE^+$ or $HDPE^+$-rich phase in the $HDPE^+$/LDPE blend.

From the difference of the SEM pictures of the above HDPE/LDPE and PS/LDPE blends, we can see that PS/LDPE blends always show spheres in matrix which is typical of immiscible blends. Therefore, we could also reason that the inter-phase of HDPE/LDPE is not as sharp as that of PS/LDPE and partial miscibility may apply to the HDPE/LDPE blend, which is reasonably expected because of the closer similarity of chemical structure between HDPE and LDPE molecules than that between PS and LDPE molecules.

Figure 7-18, 20% PS in LDPE, quenched into liquid nitrogen immediately after blending

Figure 7-19, 20% PS in LDPE, quenched into liquid nitrogen after annealing at 160 °C for one hour

Figure 7-20, 20% PS in LDPE with PS initially mixed with 10% tracer

Figure 7-21, 20% PS in LDPE with LDPE initially mixed with 10% tracer

7.2.3 Concluding Remarks on Tracer Studies

Based on the above results, some conclusions could be drawn. The binary blends of linear ($HDPE^+$) and branched polyethylene (LDPE) under study seem to be biphasic both in solid and in liquid states. As shown before, the clusterings of the tracer particles might be the $HDPE^+$ phase (or $HDPE^+$-rich phase if partial miscibility is applicable). The phase domain size is rather large, around 50 μm on average. This domain size has not been reported so far and could not be explained so far. The tracer, $BaSO_4$, seems not to affect the phase behavior of binary blends of linear and branched polyethylene as demonstrated in this work. There are no significant effects of blending temperature on the phase behavior of the blends.

Some comments must be given in regard to this special case. Firstly, it is worth mentioning that the above results were well-reproduced by using the SEM equipment in the laboratory at NOVA Chemicals (Calgary, AB) with this special blend. Secondly, as indicated previously, I tried various other types of HDPE but I was not able to reproduce the above results. Therefore, the above conclusions can only be applied to the blend with the specific $HDPE^+$ that was made by NOVA Chemicals researchers at laboratory scale. Nonetheless, the domain size seems too large and the possibility of the artifact of SEM pictures could not be eliminated. No explanations can be given at this time for this special case but I believe that it is worth reporting this surprising phenomenon here for other researchers' reference.

7.3 More Words on SEM Studies of the Morphology of Polyethylene Blends

From the above results and discussion, it can be seen that SEM technique can be used for investigating the morphological characteristics of polymer blends but it is more useful in characterizing more obviously immiscible blends at about the micron level of domain sizes. When the miscibility/immiscibility issue of polymer blends is unknown, for example, blends of polyethylene with different polyethylenes, the SEM technique may not be able to detect the immiscibility between the components. In fact, in my SEM explorations of the morphology of polyethylene blends, more experiments such as those investigating the effects of blending time, cooling rate, etc. were carried out. However, no more clear or conclusive results were generated based on these experiments. Therefore, according to these studies, the SEM technique is not recommended for the melt miscibility/immiscibility studies of polyethylene blends.

Chapter 8

Final Words

8.1 Summary and Comments

8.1.1 Theoretical Work

Literature regarding the miscibility of various polyethylene blends was extensively reviewed and the findings and contradictions were pointed out. Thermodynamics and statistical thermodynamics of polymer mixtures were discussed as the introduction to the background of the application of the molecular dynamics simulation techniques to the studies of the issue of the melt miscibility of polyethylene blends.

Strategies based on MD simulation were developed for predicting melt miscibility of polyethylene blends. The MD involves computing the individual Hildebrand solubility parameters of various kinds of polyethylene models, including linear polyethylene (HDPE) and branched polyethylene (LDPE and LLDPE) with different levels of branch contents over a wide range of temperatures at which polyethylenes are usually blended or processed in polyethylene industry. In many cases, my MD simulation results are supported by experimental observations of other researchers. Thus, I am convinced that the adoption of DREIDING force-field and united-atom models in my MD simulations is valid for the purpose of computing the Hildebrand solubility parameter differences between different types of polyethylene molecules in order to predict the phase behavior of polyethylene blends.

The miscibility of different polyethylene blends is characterized by Flory-Huggins interaction parameters calculated from the individual solubility parameters of pure components. Extensive information on Hildebrand solubility parameters of models of individual polyethylene molecules computed from MD simulations was obtained from this thesis work. Simulations of each PE model were carried out at five different temperatures, 425 (152), 450 (177), 475 (202), 500 (227) and 525 (252) K (°C). HDPE was modeled with a 1,000 united-carbon main chain while LDPE molecules were modeled by a 500 carbon long chain attached with 2 long branches with 300 and 200 carbons, plus different levels of branch contents of short branches with 4 carbons. The branch contents of LDPE were chosen at 10, 20, 22, 25, 27, 30 and 40 branches as total per 1,000 long chain carbons. LLDPE molecules were modeled with a 1,000 carbon backbone chain with different levels of short branches with 2, 4 and 6 carbons, presenting corresponding Ziegler-Natta type of copolymers of ethylene with 1-butene, 1-hexene and 1-octene co-monomers. The branch contents of LLDPE were chosen at 10, 20, 30, 40 and 50 branches per 1,000 main chain carbons for most of the models. Every effort has been made to make all models in my MD simulations as close as possible to the representatives of corresponding commercial products.

The blends studied by MD simulations in this thesis work included HDPE/LLDPE, HDPE/LDPE and LDPE/LLDPE (molecular weights of each pair are comparable). The simulation results for polyethylene blends and comments on them are summarized as follows:

1. HDPE/LLDPE:

The blends may phase-separate when branch content of LLDPE exceeds a certain critical value. The cut-off value of branch content was found to be around 40-50 branches per 1,000 backbone carbon atoms of LLDPE, above which the blends are immiscible. The branch content of LLDPE is the controlling factor on the phase behavior of HDPE/LLDPE blends. The results also suggest that the blends may have a LCST type of phase diagram. The length of short branches seems not as important as branch content. However, some effect of branch length was found. The MD simulation results showed that the Flory-Huggins interaction parameters are smaller for the longer-branched LLDPE when blended with the same HDPE; that is, χ is larger for HDPE/BLLDPE blends than that for HDPE/HLLDPE blends and χ for HDPE/HLLDPE blends is larger than that for HDPE/OLLDPE blends. In another word, blends of HDPE and LLDPE with longer branches seem more miscible than blends of HDPE and LLDPE with shorter branches when branch content of LLDPE is kept the same. However, the results would not affect the cut-off value for HDPE/LLDPE blends. The results of this study suggest that the molecular interactions of non-CH_2 groups would be the major reason that leads to phase separation of the blends.

2. HDPE/LDPE:

Similarly, the blends may phase-separate at high branch content of LDPE. The cut-off value was found to be around 25-30 branches per 1,000 long chain carbons of LDPE, which is significantly lower than that of the HDPE/LLDPE blends. It seems

that the blends may have a closed-loop phase diagram. The major difference of models of LLDPE and LDPE molecules is that each LDPE model has three long chains while only one in each LLDPE model. Therefore, it can be concluded that long chain branching also plays an important role in determining the phase behavior of polyethylene blends other than simply contributing to the total branch content of branched polyethylenes.

3. LDPE/LLDPE:

For this family of blends, the Flory-Huggins interaction parameters of the blends are rather small when LDPE branch content is below 30, indicating that LDPE seems to be miscible with LLDPE at all simulation temperatures studied. In contrast, when branch content of LDPE exceeds 30, phase separation may occur in the blends of both LDPE/HLLDPE and LDPE/OLLDPE. Thus, LDPE with low branch content is suggested when LDPE/LLDPE blends are being made, provided that thermodynamic stability is desired. The closed-loop phase diagram was implied for LDPE/LLDPE blends when LDPE branch content is above 30. It was also found that LDPE/LLDPE blends seem more miscible (having lower χ) than HDPE/LLDPE and HDPE/LDPE blends. It is not surprising that the latter result was obtained considering the microstructure difference between linear and branched polyethylenes.

However, some factors were not incorporated in my MD simulation studies. It is known that miscibility of polymer blends is affected by molecular weight as indicated in Flory-Huggins theory. However, as demonstrated in Chapter 4, δ is not

sensitive to molecular weight in my MD simulations. Thus, the effect of molecular weight and molecular weight distribution on the miscibility between different polyethylene components according to χ calculated based on δ computed by MD simulations could not be studied by my simulation work. Besides, in real LDPE molecules, the short branches are not uniform in length along main chains, i.e., a distribution of short branches with different length exists. However, the investigation of the effect of the above factors is not feasible due to the limitations of computation resources at the moment. Since only δ of pure components was computed in my MD simulation work (and then χ was calculated using the computed δ of pure components), the effect of blend composition on the miscibility of the blend components could not be studied. These factors may also affect the phase behavior of polyethylene blends. Therefore, one must be very cautious when drawing conclusions based only on MD simulations, although most of my MD results are supported by others' experimental observations. However, MD simulations can provide a good insight and reasonable predictions of the melt miscibility of polyethylene blends as my work has shown.

8.1.2 Experimental Work

The application of SEM technique to characterize the phase behavior of polyethylene blends was explored in the thesis. All HDPE/LDPE, HDPE/LLDPE and LDPE/LLDPE blends were studied using SEM, and here the variable of composition was included in the study. Although much effort has been made, it is difficult to draw a conclusion on the phase behavior of polyethylene blends only based on SEM

analysis of fractured samples. However, in one case by using a tracer technique, for a blend of LDPE with a special type of HDPE, a surprising morphology of the tracer distribution in the blend was found. The tracer particles were found unevenly distributed in the blends, indicating a two-phase blend. The observed morphology for this special case is unexplainable so far. Although the result could not be produced by using other kinds of HDPE resins, this interesting phenomenon has been reported in the thesis in detail.

In fact, applications of many other microscopy techniques have been explored in the thesis work. Ordinary light microscopy technique was used to observe the weld line of different polyethylene mixtures. In the experiments, two pieces of different polyethylenes were put together on the slides and pressed under a cover slide in the oven above their melting temperatures. Then the weld line between the different polyethylene pieces was observed with an Olympus BH-2 microscope equipped with a programmed temperature-control hotstage. For certain pairs of polyethylene samples, the weld line was found to be retained even the samples were held at temperatures which were well above their melting temperatures. This might suggest immiscibility, since if the pair was miscible they would interdiffuse and the weld line would vanish (as some other pairs of polyethylene samples did). However, due to the weak contrast, it was difficult to capture the picture with a camera directed perpendicular to the slide, despite the fact that it could be detected by the naked eye from certain observation angles. Other microscopy techniques such as polarized light, infrared and Raman microscopy [Ward and Mi, 1999] were also tried but most of them were not encouraging so far.

In conclusion, the above microscopy techniques used in the thesis work were found not to be promising in determining the phase behavior of polyethylene blends.

8.2 Future Work

As shown in this thesis, the application of MD simulations of the melt miscibility studies on polyethylene blends is quite successful and encouraging. A great deal of information has been drawn from this thesis work. Most of the MD simulation results on δ and χ are supported by experimental observations of others. However, due to the limitation of computation resources, some factors were not studied or explored to the full extent. More extensive work is required to reveal the above effects.

First, the MD simulation technique can be applied to study blends of the metallocene type of LLDPE (which have uniform branch distribution) with other types of PE, for example, HDPE, LDPE or Ziegler-Natta type of LLDPE (which have random branch distribution) because applications of metallocene type of LLDPE have become exceedingly important.

In fact, some work of MD simulations on the miscibility of blends of HDPE with metallocene type of LLDPE has been done during the thesis work. The results are quite different from those of the blends of HDPE with Ziegler-Natta type of LLDPE, indicating that the distribution of short-chain-branching is also an important factor in determining the melt miscibility of HDPE/LLDPE blends in addition to the branch content. Experimentally, Zhang et al. [2001] found that the distribution of short-chain-branching has more significant effect on melting and crystallization

behaviors of LLDPE than the average short-chain-branch content. However, melt miscibility issue of blends of HDPE with metallocene type of LLDPE has not been seen in the literature. Thus, more extensive work on metallocene type of LLDPE is required to reveal the short-chain-branching distribution effect on the melt miscibility of HDPE/LLDPE blends.

Secondly, because the actual polyethylene molecules are much more complicated, my simple models for representing the actual one may not be able to detect some minute information. Therefore, more precise models for polyethylene molecules are preferred. For example, variation of the length of short-chain branch and its distribution on LDPE, and variation of the number of long-chain branches in the models of LDPE molecules, etc. can be taken into account.

References:

Agamalian M., R.G Alamo, M.H. Kim, J.D. Londono, L. Mandelkern and G.D. Wignall, "Phase behavior of blends of linear and branched polyethylenes on micron length scales via ultra-small-angle neutron scattering", *Macromolecules*, **32**, 3093-3096, 1999

Alamo R.G., J.D. Londono, L. Mandelkern, F.C. Stehling and G.D. Wignall, "Phase behavior of blends of linear and branched polyethylenes in the molten and solid states by small-angle neutron scattering", *Macromolecules*, **27**, 411-417, 1994

Alamo R.G., W.W. Graessley, R Krishnamoorti, D.J. Lohse, J.D. Londono, L. Mandelkern, F.C. Stehling and G.D. Wignall, "Small angle nertron scattering investigations of melt miscibility and phase segregation in blends of linear and branched polyethylenes as a function of the branch content", *Macromolecules*, **30**, 561-566, 1997

Alizadeh A., A. Muñoz-Escalona, B. Vallejo and J. Martínez-Salazar, "Structure and melting of blends of linear and branched polyethylenes crystallized at high undercooling", *Polymer*, **38**, 1207-1214, 1997

Allen M.P. and D.J. Tildesley, *Computer Simulation of Liquids*, Oxford University Press: Oxford, 1987

Allinger N.L., "Conformational analysis. 130. MM2. A hydrocarbon force field utilizing V_1 and V_2 torsional terms", *J. Am. Chem. Soc.*, **99**, 8127-8134, 1977

Barham P.J and M.J. Hill, A. Keller and C.C.A. Rosney, "Phase separation in polyethylene melts" *J. Materials Sci. letters*, **7**, 1271-1275, 1988

Barham P.J., M.J. Hill and G. Goldbeck-Wood, "A qualitative scheme for the liquid phase separation in blends of homopolymers with their branched copolymers", *Polymer*, **34**, 2981-2988, 1993

Bassett D.C. and A. M. Hodge, "On lamellar organization in certain polyethylene spherulites", *Proc, Roy. Soc, Lond. A*, **359**, 121-132, 1978

Berendsen H.J.C., J.P.M. Postma, W.F. van Gunsteren, A. DiNola and J.R. Jaak, "Molecular dynamics with coupling to an external bath", *J. Chem. Phys.*, **81**, 3684-3690, 1984

Bohn L., "Incompatibility and phase formation in solid polymer mixtures and graft and block copolymers" *Rubber Chem. Technol.*, **41**, 495-513, 1968

Bourry D. and B.D. Favis, "Morphology development in a polyethylene/polystyrene binary blend during twin-screw extrusion", *Polymer*, **39**, 1851-1856, 1998

Brooks B.R., R.E. Bruccoleri, B.D. Olafson, D.J. States, S. Swaminathan and M Karplus, "CHARM: A program for macromolecular energy, minimization, and dynamics calculations", *J. comp. Chem.*, **4**, 187-217, 1983

Brown D. and J.H.R Clark, "A comparison of constant energy, constant temperature and constant pressure ensembles in molecular dynamics simulations of atomic liquids", *Molecular Physics*, **51**, 1243-1252, 1984

Burkert U. and N.L. Allinger, "Molecular mechnics" *in ACS Monograph 177, ACS*: Washington, D.C., 1982

Channell A.D., E.Q. Clutton and G. Capaccio, "Phase segregation and impact toughness in linear low density polyethylene", *Polymer*, **35**, 3893-3898, 1994

Cheam T.C. and S. Krimm, "Mixed-crystal infrared studies of chain-folding in polyethylene single crystals: low-temperature and molecular weight studies", *J. Polymer Science, Polymer Physics*, **19**, 423-447, 1981

Choi P., "Molecular dynamics studies of the thermodynamics of HDPE/butene-based LLDPE blends", *Polymer*, **41**, 8741-8747, 2000

Choi P., "Three-dimensional solubility and interaction parameters: inverse gas chromatograph and molecular dynamics studies", *Ph.D. thesis*, University of Waterloo, 1995

Colbourn E.A., *Computer Simulation of Polymers*, Longman Group UK Limited, England, 1994

Cornell W.D., P. Cieplak, C.I. Bayly, I.R. Gould, K.M. Merz, D.M. Ferguson, D.C. Spellmeyer, T. Fox, J.W. Caldwell and P.A. Kollman, (1) "A second generation force field fro the simulation of proteins, nucleic acids, and organic molecules", *J. Am. Chem. Soc.*, **117**, 5179-5197, 1995

Cornell W.D., P. Cieplak, C.I. Bayly, I.R. Gould, K.M. Merz, D.M. Ferguson, D.C. Spellmeyer, T. Fox, J.W. Caldwell and P.A. Kollman, (2) "Book reviews", *J. Am. Chem. Soc.*, **118**, 2309-2310, 1996

Crist B. and M.J. Hill, "Recent developments in phase separation of polyolefin melt blends", *J. Polym. Sci. B, Polym. Phys.*, **35**, 2329-2353, 1997

Datta N.L. and A.W. Birley, "Thermal analysis of polyethylene blends", *Plast. Rubber Process. and Appl.*, **2**, 237-245, 1982

de Pablo J. J., M. Laso and U. W. Suter, "Simulation of polyethylene above and below the melting point", *J. Chemical Physics*, **96**, 2395-2403, 1992

Dudowicz J. and K.F. Freed, "Influence of monomer structure and interaction asymmetries on the miscibility and interfacial properties of polyolefin blends" *Macromolecles*, **29**, 8960-8972, 1996

Dumoulin M.M. et al., *Progress in Polym. Process.*, **Chapter 7**, 186, 1989

Fan Z., I. A. Hussein, P. Choi and M.C. Williams, "D.S.C. study of the miscibility of LDPE/LLDPE blends", *47th CSCHE Conference*, Edmonton, Oct., 1997

Flory P.J., *Principles of Polymer Chemistry*, Cornell University Press: Ithaca, New York, 1953

Flory P.J., "Thermodynamics of high polymer solutions", *J. Chem. Phys.*, **9**, 660-661, 1941

Flory P.J., "Thermodynamics of high polymer solutions", *J. Chem. Phys.*, **10**, 51-61, 1942

Flory P.J., "Foundations of rotational isomeric state theory and general methods for generating configurational averages", *Macromolecules*, **7**, 381-392, 1974

Flory P.J., *Statistical Mechanics of Chain Molecules*, **Chapter 3**, 55-66, John Wiley & Sons, New York, 1969

Foreman K.W. and K.F. Freed, "Influence of stiffness, monomer structure, and energetic asymmetries on polymer blend miscibilities: applications to polyolefins", *Macromolecules*, **30**, 7279-7295, 1997

Foreman K.W. and K.F. Freed, "Microscopic parameters influencing the phase separation in compressible binary blends of linear semiflexible polymers", *J. Chem. Phys.* **106**, 7422-743, 1997

Freed K. F. and J. Dudowicz, "Lattice cluster theory for pedestrians: the incompressible limit and the miscibility of polyolefin blends", *Macromolecules*, **31**, 6681-6690, 1998

Freeman P.I., and J.S. Rowlinson, "Lower critical points in polymer solutions", *Polymer*, **1**, 20-26, 1960

Geil P.H., "Morpology of amorphous polymers", *Ind. Eng. Chem., Prod. Res. Dev.* **14**, 59-71, 1975

Goldstein J.I., A.D. Romig, D.E. Newbury, C.E. Lyman, P. Echlin, C. Fiori, D.C. Joy and E. Lifshin, *Scanning Electron Microscopy and X-ray Microanalysis*, Plenum, New York, 1992

Graessley W.W., R. Krishnamoorti, N.P. Balsara, R.J. Butera, L.J. Fetters, D.J. Lohse, D.N. Schulz and J.A. Sissano, "Thermodynamics of mixing for blends of model ethylene-butene copolymers", *Macromolecules*, **27**, 3896-3901, 1994

Graessley W.W., R. Krishnamoorti, G.C. Reichart, N.P. Balsara, L.J. Fetters and D.J. Lohse, "Regular and irregular mixing in blends of saturated hydrocarbon polymers", *Macromolecules*, **28**, 1260-1270, 1995

Guo H.F., S. Packirisamy, R.S. Mani, C.L. Aronson, N.V. Gvozdic and D.J. Meier, "Compatibilizing effects of block copolymers in low-density polyethylene and polystyrene blends" , *polymer*, **39**, 2495-2505, 1998

Gupta A.K., S.K. Rana and B.L. Deopura, "Mechanical properties and morphology of high-density polyethylene/linear low-density polyethylene blend", *J. of Appl. Polym. Sci*, **46**, 99-108, 1992

Halgren T.A. (1), "Merck molecular force field. I. Basis, form, scope, parameterization, and performance of MMFF94", *J. Comput. Chem.* **17**, 490-519, 1996

Halgren T.A (2), "Merck molecular force field. II. MMFF94 van der Waals and electrostatic parameters for intermolecular interactions", *J. Comput. Chem.* **17**, 520-552, 1996

Halgren T.A and R.B. Nachbar, "Merck molecular force field. IV. Conformational energies and geometries for MMFF94" *J. Comput. Chem.* **17**, 587-615, 1996

Han C.D., "A study of bicomponent coextrusion of molten polymers", *J. Appl. Polym. Sci.*, **17**, 12891303, 1973

Han S.J., D.J. Lohse, P.D. Condo and L.H. Sperling, "Pressure-volume-temperature properties of polyolefin liquids and their melt miscibility", *J. Polym. Sci., Polym. Phys.*, **37**, 2835-2844, 1999

Hansen C.M., "The three dimensional solubility parameter – key to paint component affinities: I. solvent, plasticizers, polymers, and resins", *J. Paint Technol.*, **39**,104-117, 1967

Hildebrand J.H. and R.L. Scott, "*The solubility of Non-Electrolytes*", Dover, New York, 1964

Hill M.J., "Liquid-liquid phase separation in binary blends of a branched polyethylene with linear polyethylenes of differing molecular weight", *Polymer*, **35**, 1991-1993, 1994

Hill M.J. and P.J. Barham, "Liquid-liquid phase separation in blends containing copolymers produced using metallocene catalysts", *Polymer*, **38**, 5595-5601, 1997

Hill M.J., P.J. Barham, A. Keller and C.C.A. Rosney, "Phase segregation in melts of blends of linear and branched polyethylene", *Polymer*, **32**, 1384-1393, 1991

Hill M.J., P.J. Barham and A. Keller, "Phase segregation in blends of linear with branched polyethylene: the effect of varying the molecular weight of the linear polymer", *Polymer*, **33**, 2530-2541, 1992

Hill M.J. and P.J. Barham, "Liquid-liquid phase separation in melts of blends of linear with branched polyethylenes: morphological exploration of the phase diagram", *Polymer*, **33**, 4099-4107, 1992

Hill M.J. and P.J. Barham, "Diffusion effects in blends of linear with branched polyethylenes", *Polymer*, **33**, 4891-4897, 1992

Hill M.J., P.J. Barham and J. van Ruiten, "Liquid-liquid phase segregation in blends of a linear polyethylene with a series of octene copolymers of differing branch content", *Polymer*, **34**, 2975-2980, 1993

Hill M.J. and P.J. Barham, "Interpretation of phase behaviour of blends containing linear low-density polyethylenes using a ternary phase diagram", *Polymer*, **34**, 1802-1808, 1994

Hill M.J. and P.J. Barham, "Absence of phase separation effects in blends of linear polyethylene fractions of differing molecular weight", *Polymer*, **36**, 1523-1530, 1995

Hill M.J. and C.C. Puig, "Liquid-liquid phase separation in blends of a linear low-density polyethylene with a low-density polyethylene", *J. Appl. Polym. Sci.*, **65**, 1921-1931, 1997

Hill M.J.R.L. Morgan and P.J. Barham, "Minimum branch content for detection of liquid-liquid phase separation, using indirect techniques, in blends of polyethylene with ethylene-octene and ethylene-butene copolymers", *Polymer*, **38**, 3003-3009, 1997

Hill M.J., L. Oiarzabal and J.S. Higgins, "Preliminary studies of polypropylene/linear low density polyethylene blends by transmission electron microscopy", *Polymer*, **35**, 3332-3337, 1994

Hobb S., "The effect of rubber particle size on the impact properties of high impact polystyrene (HIPS) blends", *Polym. Eng. Sci.*, **26**, 74-81, 1986

Hoover W.G., "Canonical dynamics: Equilibrium phase-space distributions", *Am. Phys. Soc.*, **31**, 1695-1697, 1985

Hosier I.L., D.C. Bassett and I.T. Moneva, "On the morphology of polyethylene crystallized from a sheared melt", *Polymer*, **36**, 4197-4202,1995

Hu S., T. Kyu and R.S. Stein, "Characterization and properties of polyethylene blends I. Linear low-density polyethylene with high-density polyethylene", *J.Polym. Sci. Polym. Phys.*, **25**, 71-87, 1987

Huggins M.L., "Solutions of long chain compounds", *J. Chem. Phys.*, **9**, 440, 1941

Huggins M.L., "Thermodynamic properties of solutions of long-chain compounds", *Ann. N.Y. Acad. Sci.*, **43**, 1-32, 1942

Hussein I.A., Z. Fan, P. Choi and M.C. Williams, "Phase behavior of LDPE/LLDPE blends prepared at optimum blending conditions", *47th CSCHE Conference*, Edmonton, Oct., 1997

Hwang M.J., T.P. Stockfisch and A.T. Hagler, "Derivation of class II force fields. 2. Derivation and characterization of a class ii force field, CFF93, for the alkyl functional group and alkane molecules", *J. Am. Chem. Soc.*, **116**, 2515-2525, 1994

Jorgensen W.L., D.S. Maxwell and J. Tirado-Rives, "Development and testing of the OPLS all-atom force field on conformational energetics and properties of organic liquids", *J. Am. Chem. Soc.*, **118**, 11225-11236, 1996

Kanig V.G., "Ein neues Kontrastierverfahren für die elektronenmikroskopische Untersuchung von Polyäthylen", *Kolloid Z. Z. Polym.*, **251**, 782-783, 1973

Kanig G., "Neue elektronenmikroskopische Untersuchungen über die morphologie von polyäthylenen", *Prog. Colloid Poly. Sci.*, **57**, 176-191, 1975

Karol F.J., "The polyethylene revolution", *Chem. Tech.*, **13**, 222-228, 1983

Kavassalis T.A., P. Choi and A. Rudin, "Molecular models and three dimensional solubility parameters of nonionic surfactants" In: Gubbins KE, Quirke N, Editors. *Molecular Simulation and Industrial Applications – Methods, Examples and Prospects*, 315-329, Gordon and Breach Science Publishers, Amsterdam, 1996

Kern R.J., "Component effects in phase separation of polymer-polymer-solvent systems", *J. Polym. Sci.*, **21**, 19-25, 1956

Krishnamoorti R., W.W. Graessley, L.J. Fetters, R.T. Garner and D.J. Lohse, "Anomalous mixing behavior of polyisobutylene with other polyolefins", *Macromolecules*, **28**: 1252-1259, 1995

Krishnamoorti R., W.W. Graessley, G.T. Dee, D.J. Walsh, L.J. Fetters and D.J. Lohse, "Pure component properties and mixing behavior in polyolefin blends", *Macormolecules*, **29**, 367-376, 1996

Kyu T., S. Hu and R. Stein, "Characterization and properties of polyethylene blends II. Linear low-density with conventional low-density polyethylene", *J.Polym. Sci. Polym. Phys.*, **25**, 89-103, 1987

Laso M., J. J. de Pablo and U. W. Suter, "Simulation of phase equilibria for chain molecules", *J. Chemical Physics*, **97**, 2817-2819, 1992

Londono J.D., J.K. Maranas, M. Mondello, A. Habenschuss, G.S. Grest, P.G. Debenedetti, W.W. Graessley, and S.K. Kumar, "Chain-packing effects in the thermodynamics of polymers", *J. of Polymer Sci, Polym. Phys.*, **36**, 3001-3005, 1998

Londono J.D., G.D. Wignall, R.G. Alamo, L. Mandelkern and J.S. Lin, "The morphology of blends of linear and branched polyethylenes by small-angle neutron and X-ray scattering", *Mat. Res. Soc. Symp. Proc.*, **376**, 281-290, 1995

Lucas K., *Applied Statistical Thermodynamics*, Spring-Verlag, Berlin, Heidelberg, 1991

Luettmer-Strthmann J. and J.E.G. Lipson, "Miscibility of polyolefin blends" *Macromolecules*, **32**, 1093-1102, 1999

Mackerell A.D., J. Wiórkiewicz-Kuczera and M. Karplus, "An all-atom empirical energy function for the simulation of nucleic acids", *J. Am. Chem. Soc.*, **117**, 11946-11975, 1995

Maple J.R., M.J. Hwang, T.P. Stockfisch, U. Dinur, M. Waldman, C.S. Ewig and A.T. Hagler, "Derivation of class II force fields. I. Methodology and quantum force field for the alkyl functional group and alkane molecules", *J. Comput. Chem.* **15**, 162-182, 1994

Maranas J.K., M. Mondello, G.S. Grest, S. Kumar, P.G. Debenedetti and W.W. Graessley, "A molecular dynamics study of intermolecular structure, thermodynamics and miscibility in hydrocarbon polymers", *Computers Chem. Eng.*, **22**, Suppl., S19-S26, 1998

Maranas J.K., M. Mondello, G.S. Grest, S. Kumar, P.G. Debenedetti and W.W. Graessley, "Liquid structure, thermodynamics, and mixing behavior of saturated hydrocarbon polymers. 1. Cohesive energy density and internal pressure", *Macromolecules*, **31**, 6991-6997, 1998

Mark H.F., N.M. Bikales, C.G Overberger and G. Menges, editor in chief: J.I. Kroschwitz, "Ethylene polymers", *Encyclopedia of Polymer Science and Engineering*, 2nd edition, **6**, 383-494, 1985

Mark J., *Handbook of Polymer Properties*, American Institute of Physics Press, Woodbury, NY, 257, 1996

Martínez-Salazar J., M. Sanchez Cuesta and J Plans, "On phase separation in high- and low-density polyethylene blends: 1. Melting-point depression analysis", *Polymer*, **32**, 2984-2988, 1991

Mayo S.L., B.D. Olafson and W.A. Goddard, "DREIDING: a generic force field for molecular simulations", *J. Phys. Chem.*, **94**, 8897-8909, 1990

McQurrie D.A., *Statistical Mechanics*, Harper and Row, New York, 1976

Mekhilef N. and H. Verhoogt, "Phase inversion and dual-phase continuity in polymer blends: theoretical predictions and experimental results", *Polymer*, **37**, 4069-4077, 1996

Mirabella F.M. JR, S.P. Westphal, P.L. Fernando, E.A. Ford and J.G. Williams, "Morphological explanation of the extraordinary fracture toughness of linear low density polyethylenes", *J. Polym. Sci., Polym. Phys.*, **26**, 1995-2005, 1988

Mirabella F.M. and J.S. Barley, "Ostwald ripening in an immiscible hydrogenated polybutadiene and high-density polyethylene blend" *J. Polym. Sci., Polym. Phys.*, **32**, 2187-2195, 1994

Morgan R.L., M.J. Hill, P.J. Barham and C.J. Frye, "Liquid-liquid phase separation in ternary blends of linear polyethylene with two ethylene-butene copolymers", *Polymer*, **38**, 1903-1909, 1997

Morgan R.L., M.J. Hill and P.J. Barham, "Morphology, melting behaviour and co-crystallization in polyethylene blends: the effect of cooling rate on two homogeneously mixed blends", *Polymer*, **40**, 337-348, 1999

MSI, *Forcefield-Based Simulations*, Molecular Simulation Manual, Molecular Simulation Incorporated, 1997

Müller A.J., V. Balsamo and C.M. Rosales, "On the miscibility and mechanical compatibility of low density and linear low density polyethylene blends", *Polym. Networks Blends*, **2**, 215-223, 1992

Müller A.J. and V. Balsamo, "Thermal characterization of low density and linear low density polyethylene blends", *Adv. Polym. Blends and Alloys Technol.*, **5**, 1-21, 1994

Nath S. K., B. J. Banaszak and J J. de Pablo, "A new united atom force field for α-olefins", *J. Chemical Physics,* **116**, 3612-3616, 2001

Nicholson J.C., T.M. Finerman and B Crist, "Thermodynamics of polyolefin blends: small-angle neutron scattering studies with partially deuterated chains", *Polymer*, **31**, 2287-2293, 1990

Nosé S., "A unified formulation of the constant temperature molecular dynamics methods", *J. Chem. Phys.*, **81**, 511-519, 1984

Nosé S., "A molecular dynamics method for simulations in the canonical ensemble", *Molecular Physics*, **52**, 255-268, 1984

Olabisi O., L.M. Robeson and M.T. Shaw, *Polymer-Polymer Miscibility*, Academic Press, New York, 1979

Olabisi O. and R. Simha, "A semiempirical equation of state for polymer melts", *J. Appl. Polym. Sci.*, **21**, 149-163, 1977

Olley R., A. Hodge, D.C. Bassett and J.J. Thomson, "A permanganic etchant for polyolefines", *J. Polym. Sci., Polym. Phys.*, **17**, 627-643, 1979

Pathria R.K., *Statistical Mechanics*, Pergamon Press, Oxford, 1972

Patrick M., V. Bennett and M.J. Hill, "A comparison of methods of specimen preparation for transmission electron microscopy of bulk polyethylene", *Polymer,* **37**, 5335-5341, 1996

Peng Z.W., C.S. Ewig, M. Hwang, M. Waldman and A.T. Hagler, "Derivation of class II force fields. 4. van der Waals parameters of alkali metal cations and halide anions" *J. Phys. Chem. A*, **101**, 7243-7252, 1997

Plans J., M. Sánchez Cuesta and J. Martínez-Salazar, "On phase separation in high- and low-density polyethylene blends: 2. A working model", *Polymer*, **32**, 2989-2991, 1991

Prigogine I., *The Molecular Theory of Solutions*, North-Holland Pub,. Amsterdam, 1957

Princen L.E. (editor), *Scanning Electron Microscopy of Polymers and Coatings*, John and Wiley & Sons, NewYork, 1971

Puig, C.C., M.J. Hill and P.J. Barham, "Liquid liquid phase separation in polypropylene homopolymer/polypropylene copolymer melts", *Polymer,* **34**, 3117-3119, 1993

Puig C.C., J.A. Odell, M.J. Hill, P.J. Barham and M.J. Folkes, "A comparison of blends of linear with branched polyethylenes prpared by melt mixing and by solution blending", *Polymer*, **35**, 2452-2457,1994

Rana D., C.H. Lee, S. Choe, K. Cho and B.H. Lee, "Thermal, mechanical and morphological behaviors of binary blends of metallocene polyethylene with high density polyethylene and polypropylene", *Korea Polymer Journal*, **6**, 158-166, 1998

Rappé A.K., C.J. Casewit, K.S. Colwell, W.A. Goddard and W.M. Skiff, "UFF, a full periodic table force field for molecular mechanics and molecular dynamics simulations", *J. Am. Chem. Soc.*, **114**, 10024-10035, 1992

Ree M., T Kyu and R.S. Stein, "Quantitative small-angle light-scattering studies of the melting and crystallization of LLDPE/LDPE blends", *J. Polymer Science, Polymer Physics*, **25**, 105-126, 1987

Rego López J.M., M.T. Conde Braña, B. Terselius and U.W. Gedde, "Crystallization of binary linear polyethylene blends", *Polymer*, **29**,1045-1051, 1988

Rego López J.M. and U.W. Gedde, "Crystallization and morphology of binary blends of linear and branched polyethylene: polarized light microscopy, small-angle light scattering and thermal analysis", *Polymer*, **30**, 22-26, 1989

Rhee J. and B. Crist, "Thermodynamics and phase separation in melt blends of polyethylene and model copolymers", *Macromolecules*, **24**, 5663-5669, 1991

Rigby D., H Sun and B.E. Eichinger, "Computer simulations of poly(ethylene oxide): force field, PVT diagram and cyclization behaviour", *Polym. Int.*, **44**, 311-330, 1997

Rudin A., *The Elements of Polymer Science and Engineering*, 2nd edition, Academic Press, New York, 1999

Rudin A., K.K. Chee and J.H. Shaw, "Specific volume and viscosity of polyolefin melts", *J. Polym. Sci.*, Part C, **30**, 415-427, 1970

Sammon C., C. Mura, P. Eaton and J. Yarwood, "Raman microscopic studies of polymer surfaces and interfaces", *Analusis*, **28**, 30-34, 2000

Sato K., R. Saetre, J. Taylor and D.L. Cooke, "Blends of LLDPE and polystyrene for film applications", *ANTEC*, 2423-2427, 1994

Schelten J., G.D. Wignall, D.G.H. Ballard and G.W. Longman, "Small-angle neutron scattering studies of molecular clustering in mixtures of polyethylene and derterated polyethylene", *Polymer*, **18**, 1111-1120, 1977

Schipp C., M.J. Hill, P.J. Barham, V.M. Cloke, J.S. Higgins and L. Oiarzabal, "Ambiguities in the interpretation of small-angle neutron scattering from blends of linear and branched polyethylene", *Polymer*, **37**, 2291-2297, 1996

Schweizer K.S and J.G. Curro, in *Advances in Chemical Physics*, **XCVIII**, New York, 65-67, 1997

Stein R.S. and Zachmann H.G., *PMSE Abstr.*, **209**, 48, 1995

Sun H., "COMPASS: an ab initio force-field optimized for condensed-phase applications-overview with details on alkane and benzene compounds", *J. Phys. Chem. B*, **102**, 7338-7364, 1998

Sun H. and Rigby D., "Polysiloxanes: ab initio force field and structural, conformational and thermophysical properties", *Spectrochimica Acta, Part A*, **53**, 1301-1323, 1998

Tashiro K., R.S. Stein and S.L. Hsu, "1. Thermal and vibrational spectroscopic study by utilizing the deuteration technique", *Macromolecules*, **25**, 1801-1808, 1992

Tashiro K., M. Izuchi, M. Kobayashi and R.S. Stein, "Cocrystallization and phase segregation of polyethylene blends between the D and H species. 3. Blend content dependence of the crystallization behavior", *Macromolecules*, **27**, 1221-1227, 1994

Utracki L.A., *Polymer Alloys and Blends-- Thermodynamics and Rheology*, Hanser Publishers, Munich, 1989

Utracki L.A. and Schlund B., "Linear low density polyethylenes and their blends: Part 2. Shear flow of LLDPE's", *Polym. Eng. Sci.*, **27**, 367-379, 1987

Utracki L.A. and B. Schlund, "Linear low density polyethylenes and their blends: part 4. Shear flow of LLDPE blends with LLDPE and LDPE", *Polym. Eng. Sci.*, **27**, 1512-1522, 1987

Verlet L., "Computer 'Experiment' on classical fluids. I. Thermodynamical properties of Lennard-Jones molecules", *Physical Review*, **159**, 98-103, 1967

Vesely D., "Microstructural characterization of polymer blends", *Polym. Eng. Sci.*, **36**, 1586-1593, 1996

Wang Z., C.M. Chan, S.H. Zhu and J. Shen, "Compatibilization of polystyrene and low density polyethylene blends by a two-step crosslinking process", *polymer*, **39**, 6801-6806, 1998

Ward Y and Y Mi, The study of miscibility and phase behaviour of phenoxy blends using Raman spectroscopy", *Polymer*, **40**, 2465-2468, 1999

Wardhaugh L.C. and M.C. Williams, "Blockiness of olefin copolymers and possible microphase separation in the melt", *Polym. Eng. Sci.*, **35**, 18-27, 1995

Weiner S.J., P.A. Kollman, D.A. Case, U.C. Singh, C. Ghio, G. Alagona, S. Profeta, Jr and P.Weiner, "A new force field for molecular mechanical simulation of nucleic acids and proteins", *J. Am. Chem. Soc.*, **106**, 765-784, 1984

White J.R. and E.L. Thomas, "Advances in SEM of polymers", *Rubber Chem. Technol.*, **57**, 457-506, 1984

Williams K.P.J. and I.C. Wilcock, "Raman spectroscopy of polymers", *Chemical Analysis*, **'97 conference, volume3, paper 4'**, 1-6, 1997

Wu S., "Phase structure and adhesion in polymer blends: A criterion for rubber toughening", *Polymer*, **26**, 1855-1863, 1985

Wunder S.L. and S.D. Merajver, "Ultrahigh-molecular-weight polyethylene: Raman spectroscopic study of melt anisotropy", *J. Polym. Sci., Polym. Phys.*, **24**, 99-110, 1986

Yang L.Y., T.G. Smith and D. Bigio, "Melt blending of linear low density polyethylene and polystyrene – Effects of processing conditions, composition, and compatibilizers upon morphology development", *ANTEC*, 2428-2432, 1994

Yoon D.Y., G.D. Smith and T. Matsuda, "A comparison of a united atom and an explicit atom model in simulations of polyethylene", *J. Chem. Phys.*, **98**, 10037-10043, 1993

Zhang M., D.T. Lynch and S.E. Wanke, "Effect of molecular structure distribution on melting and crystallization behavior of 1-butene/ethylene copolymers", *Polymer*, **42**, 3067-3075, 2001

Zhao Y., S. Liu and D. Yang, ""Crystallization behavior of blends of high-density polyethylene with novel linear low-density polyethylene", *Macromol. Chem. Phys.*, **198**, 1427-1436, 1997

Zhao L. and P. Choi, "Determination of solvent-independent polymer-polymer interaction parameter by an improved inverse gas chromatographic approach" *Polymer*, **42**, 1075-1081, 2001